The Jansky-Very Large Array Sky Survey (VLASS)

August 8, 2014

Contents

1 Executive Summary/Overview

The VLA Sky Survey (VLASS) is a modern, tiered ("wedding-cake") survey with the VLA designed to provide a broad, cohesive science program with forefront scientific impact, capable of generating unexpected scientific discoveries, generating involvement from all astronomical communities, and leaving a lasting legacy value for decades. The VLASS is structured to combine comprehensive all sky coverage ("all-sky") with sequentially deeper coverage ("wide" and "deep") in carefully identified parts of the sky, including the Galactic plane, and capable of informing time domain studies. This approach enables both focused and wide ranging scientific discovery through the coupling of deeper narrower tiers with increasing sky coverage at shallower depths, addressing key science issues and providing a statistical interpretational framework. Thus the combined sum of all tiers far outweighs that of the individual components, enabling detailed investigations for a broad range of astrophysical research topics including: Galactic H II regions and supernova remnants, radio transients, star-forming galaxies, AGN physics, galaxy formation, and the polarized sky. Such an approach provides both astronomers and the citizen scientist with information for every accessible point of the radio sky, while simultaneously addressing fundamental questions about the nature and evolution of astrophysical objects. Multi-wavelength communities studying rare objects, the Galaxy, radio transients, or galaxy evolution out to the peak of the cosmic star formation rate density will equally benefit from VLASS. Furthermore, this tiered survey structure will help guide a number of PI-led science projects that could not be properly conceived (e.g., due to insufficient statistics) without the time investment of VLASS. Finally, the VLASS was developed through unprecedented community involvement and consensus building, including a public workshop at the AAS, the submission of over 26 white papers and long competitive debate, the Survey Science Group (SSG), *along with its community working groups of more than ∼200 multi-wavelength astronomers*.

In addition to scientific and legacy considerations, the proposed VLASS definition pays close attention to what will soon be coming online via the various Square Kilometer Array (SKA) pathfinders (e.g., ASKAP/EMU, APERTIF/WODAN, MeerKAT/MIGHTEE, LOFAR) and the SKA itself. In doing so, VLASS showcases the strengths and unique capabilities of the VLA, namely high resolution full stokes parameter imaging and exquisite point-source sensitivity for going deep, free from the effects of source confusion, which are critical for source identification. For the next $\gtrsim$10 yr (i.e., until an SKA$_1$; $\gg$ 2020), the VLA will provide the combination of the highest resolution and point-source sensitivity of any GHz radio interferometer in the world. This has led to the choice of S-band (2–4 GHz) and a combination of A- and B-configurations as the frequency and resolution choices for the entire survey. Considerations for polarization studies also leads to the S-band as a natural choice, since depolarization will be lower than at L-band.

1.1 Survey Definition Components

ALL-SKY (Tier 1): The entire sky visible to the VLA (i.e., $\delta > -40°$; 82% of the celestial sphere—same as the NVSS footprint) will be covered to a depth of at least 100 μJy/beam (1σ) in the S-band (2–4 GHz) with a resolution of $\lesssim 2\farcs1$. In doing this, the survey will achieve FIRST-like depth over the entire VLA-visible sky with better than a factor of two improvement in angular resolution (critical for source identification), providing sufficient bandwidth coverage for determination of spectral indices and Faraday rotation measures for strong sources. This survey will provide an indispensable resource for the entire astronomical community to systematically study classes of objects as well as to identify and study radio counterparts to their own multi-wavelength observations.

The ALL-SKY component will enable the discovery and study of rare classes of objects in the radio, such as the radio counterparts to $z > 6$ quasars. Coverage over the entire VLA-visible sky

will also allow the broader astronomical community to determine the radio emitting properties of rare classes of objects that are identified at other wavelengths (e.g., brown dwarfs, supernova remnants, or objects from future surveys such as LSST). The radio flux densities from VLASS will be used, in combination with data from surveys at other wavelength to select rare classes of objects from their unique spectral properties (e.g., identifying AGN in Pan-STARRS).

WIDE (Tier 2): The WIDE survey component will cover $\approx$10,000 deg^2 down to 50 μJy/beam (1 σ) in the S-band with a resolution of 2.″1 (B-configuration). WIDE imaging will focus on portions of the sky for which major investments are already in place to gather optical/NIR spectroscopy, thus allowing meaningful astrophysical investigations of sources. Accordingly, WIDE will focus on covering a major portion of the 14,000 deg^2 area being targeted by the Dark Energy Spectroscopic Instrument (DESI), which will obtain optical spectra for tens of millions of galaxies and quasars, constructing a 3-dimensional map spanning the nearby universe to 10 billion light years.

At the proposed depth, the WIDE tier will be able to detect (5 σ) luminous star-forming galaxies (i.e., Luminous Infrared Galaxies; LIRGs) out to $z \sim 0.15$ and rarer ultra-luminous infrared galaxies (ULIRGs) out to $z \sim 0.5$, while additionally providing a good baseline sample of relatively nearby star-forming galaxies. According to White et al. 2007 (Fig. 3), WIDE should provide a 5 sigma detection for $\sim$20% of SDSS quasars.

As hundreds of thousands of spectra already exist (with many more coming from DESI), the radio data from WIDE will immediately enable investigations of stars, stellar remnants, galaxies, clusters, and AGN. For example, WIDE data will determine whether there is strong evolution in both redshift and luminosity in the radio-loud quasar population. This is fundamental for understanding the physics of quasars and the nature of their relationship to galaxy evolution, as today it remains unclear as to whether the radio-loudness of quasars is linked to redshift or bolometric luminosity.

GALACTIC (Tier 2): VLASS will map the Galactic plane and bulge regions down to 50 μJy/beam (1 σ) in the S-band to achieve sub-arcsecond (i.e., by combining A-configuration data with the ALL-SKY B-configuration data). The time request considers elevation-dependent $T_{\rm sys}$ (primarily spillover) effects to ensure a true sensitivity of 50 μJy/beam is achieved. The coverage will include a Galactic longitude range spanning -20 to 260 deg, along with a latitude range of $\pm$5 deg. This latitude range provides exceptional coverage of sources in the Galactic plane, overlapping with many infrared surveys of this region and providing significantly more survey area than many radio surveys of the Galactic plane. The Galactic bulge will be mapped between longitudes of $\pm$14 deg, with latitude coverage extending to $\pm$10 deg.

The key advantage of VLASS for Galactic science, over other existing and planned radio surveys, lies in its high spatial resolution capability, which motivates a broad range of Galactic science investigations. Thus, the Galactic survey component will address fundamental questions laid out in the previous Decadal Survey of Astronomy & Astrophysics including the mass-energy-chemical cycle in galaxies, star formation, the influence of rotation and magnetic fields on non-degenerate stars, nailing down the progenitors of type Ia supernovae, the end lives of massive stars, and what controls the parameters of compact stellar remnants.

DEEP (Tier 3): The DEEP survey component will cover a total of 10 deg^2 down to 1.5 μJy/beam (1 σ) in the S-band with a resolution of 0.″65 (i.e., A-configuration). A total areal coverage of $\gtrsim$10 deg^2 is required to both reduce the Poisson uncertainty for deriving statistically meaningful luminosity functions for star-forming galaxies, as well as to reduce sample variance due to large-scale structure, which is critical for developing our understanding of the link between star formation, galaxy mass, and environment. The DEEP imaging will be divided up into 3 separate fields: 4.5 (ECDFS), 3.5 (ELAIS-N1), and 2 deg^2 (COSMOS), the latter of which will leverage the existing deep imaging. Having these three separate fields allows potential issues from cosmic variance to be critically assessed and takes advantage of the huge multi-wavelength time commitments in each of these fields. Furthermore, to accurately measure the two-point correlation

function and conduct halo occupation distribution analyses, which in turn provides information on the underlying dark matter distribution in these regimes, structures on $> 2 - 3$ Mpc scales must be fully sampled in angular space. It is on these scales that one moves from the non-linear to linear regime. Consequently, the $\sim 50 - 60$ Mpc dimensions required to sample these large scales equates to a linear dimension of the survey of 2 deg, or a contiguous area of 4 deg^2 (we plan to map rectangles 1.5 deg by 3 deg = 4.5 deg^2 in ECDFS and 2 deg by 1.75 deg = 3.5 deg^2 in EN1). By observing three separate fields we can average over any field-to-field variations on the largest scales that are still present.

A 7.5 μJy/beam (5σ) detection threshold corresponds to a star-formation rate of $\sim$50 solar masses per year at $z = 1.5$ (i.e., L* galaxies at the peak of the cosmic star formation rate density). Using the joint information between the WIDE and DEEP tiers allows extragalactic objects of similar luminosity to be observed over a much wider range of distances, out to larger look-back times, and allows similar volumes of the universe to be studied at high and low redshifts. Consequently, VLASS provides an essential lever arm to disentangle the effects of differing luminosity from the effects of cosmic evolution of the source population being studied. Furthermore, the DEEP component provides a reference "truth" image for the both the WIDE and ALL-SKY tiers where they overlap, allowing accurate assessment of completeness and reliability in the shallower survey tiers.

TRANSIENT SCIENCE: VLASS will initiate a new generation of transient science by carrying out the all-sky, wide, deep, and galactic observations in multiple epochs in cadences consistent with the fidelity requirements and total observing time of each of the tiers. Thus VLASS will be the deepest (i.e., by two orders of magnitude) radio transient survey yet attempted. Consequently, VLASS will yield the detection of tens of radio supernovae, thereby determining the rate of obscured supernovae in the local universe. VLASS will additionally provide an observational measure of the rate and inverse beaming fraction of detectable radio orphan GRB afterglows, in turn providing a measure of the true rate of these events. The prediction for detections is poorly constrained, but VLASS will likely produce a small but extremely significant number of detections. From the Galactic component, VLASS will detect NS-NS mergers in the gravitational wave era. Rates are, once again, poorly constrained, hence uncertainty in the predictions for a-LIGO and Adv-Virgo. Any detection would be transformational. And, of course, VLASS will probe extreme AGN activity across many epochs.

The comprehensive approach of VLASS will additionally provide complementary information for the study of transients and variable sources through the WIDE and DEEP tiers. The DEEP tier will be observed with a more rapid cadence than the shallower WIDE tier, with depth being built up using many visits to the target fields, allowing studies of variability and transient phenomena on shorter timescales than in the WIDE tier. The WIDE tier, however, is better suited to finding rare, bright transient events. The combination of the DEEP and WIDE tiers enables the study of populations of the same objects at widely varying flux density levels, as well as the ability to find fainter populations that are completely missed in the shallower WIDE tier alone.

2 Introduction

We provide an overview of the Sky Survey, its components, and the motivation as well as an outline of the subsequent sections and organization of the paper.

Over the *past* two decades, a combination of increasingly sensitive telescopes and advances in data reduction techniques made it possible to complete a suite of comprehensive and sensitive radio surveys covering much of the radio band. Over the *next* two decades, a new series of telescopes will come online (e.g., the Low Frequency Array, the Karoo Array Telescope, the Australian Square Kilometre Array Pathfinder), all with key surveys as a prime component of their science programs. The Jansky Very Large Array (VLA), with its greatly enhanced unique suite of capabilities, is well positioned to conduct the first in a new suite of deep radio surveys. The VLA Sky Survey (VLASS) proposed here provides a qualitative improvement in observations of and understanding of the radio sky, will detect the radio counterparts to the current and emerging multi-wavelength suite of surveys (from the sub-millimeter to γ-rays) and will serve as a technical proving ground for future radio telescopes and their intended surveys. As discussed below, the VLASS has been designed with both SKA Pathfinders and the SKA itself in mind, and therefore showcases the unique capabilities of the VLA that will deliver science that cannot be achieved by any other facility until $\gg$2020.

The outline of this document is as follows: Below in §3, we first describe the motivation for and the process by which the proposed VLASS was created. In §4, we then summarize the scientific questions the survey will address and discuss how VLASS will stack up against the SKA Pathfinders and the SKA itself. Section 5 follows with a description of the components of the survey and their relation to specific science goals. A more technical description of the survey structure and its implementation plan are given in §6 and 8, respectively, which is then followed by a detailed discussion of the planned data products in §7. In §9, we discuss the opportunities for education and public outreach that will be enabled by VLASS. Finally, in §10 we briefly summarize the overall VLASS.

3 Motivation and Process

In July 2013 NRAO announced that it would consider a new radio sky survey using the Karl G. Jansky Very Large Array (VLA), after several members of the community approached the NRAO Director suggesting that it was time to think about a follow-on from NVSS and FIRST. These two surveys were ground-breaking in their time, but in the twenty years since their execution both the capabilities now available on the VLA following the Expanded VLA (EVLA) Construction Project, and the wealth of surveys, extant and planned, at other wavelengths that require *arcsecond* localization of associated radio emission, make necessary the consideration of a new radio survey. In particular, the availability of On-The-Fly (OTF) mosaics and the wide fractional bandwidth of the VLA provide the fast mapping speed, increased continuum sensitivity, and instantaneous spectral index information that would simply not have been possible prior to the improvements provided by the EVLA.

Given the potential impact a large survey would have on the use of the telescope, both in terms of the large-scale survey science that is simply not possible through the regular peer-review process, and on the resulting reduction in the availability of time for regular PI science should a large survey proceed, the survey science and definition had to be proposed and reviewed by the community. A process was therefore defined that would result in a community-led recommendation being provided to the NRAO Director, with NRAO facilitating the process. The process included, from the start, open *international* participation in the development of a VLA Sky Survey (VLASS) Proposal, with the final deliverables being public data and data products. Should the Proposal pass its Community Review, NRAO would implement the survey, deliver basic data products,

and support the community with higher-level data products as resources allow.

In preparation for a VLASS Science Planning Workshop held January 5, 2014 at the 223rd American Astronomical Society meeting in Washington, D.C., White Papers (WPs) were solicited from the community through the NRAO eNews, and a Scientific Organizing Committee (SOC) was convened to review the WPs and define the agenda of the Workshop. A total of 22 WPs were received, with contributions from 180 unique authors. It is interesting to note that of these authors, approximately 20% were *not* users of NRAO telescopes, and do not appear in the NRAO User Database (i.e., they have never been on a proposal to use an NRAO instrument, either as co-I or PI, nor have they registered in the User Database for any other reason). Therefore, the act of soliciting the WPs, in and of itself, already attracted interest from a broader community than the "traditional" radio astronomy community. The Workshop attracted $\approx$50 attendees, and comprised morning talks followed by afternoon discussion. Areas for debate became apparent, and some possible avenues for the survey began to be ruled out (such as a large-scale, high-frequency survey).

Following the Workshop the SOC was responsible for defining the process by which the VLASS Proposal would be developed. In February 2014 the Survey Science Group (SSG) was formed comprising several working groups (WGs), open to the entire community, and advertised in multiple eNews articles. The WGs topics were:

- Galactic
- Extragalactic
- Transients and Variability
- Programmatics
- Communication/Education/Outreach
- Technical

Each working group was led by two co-chairs, with the co-chairs comprising the SSG Governing Council. The SSG Governing Council itself had two co-chairs (Stefi Baum and Eric Murphy). Contributions to the WG discussions were enabled through the NRAO Science Forum (https://science.nrao.edu/forums/viewforum.php?f=59), with material also posted on the NRAO Public Wiki (https://safe.nrao.edu/wiki/bin/view/JVLA/VLASS), along with other methods of group communication such as Google Groups, as defined by the co-chairs of the individual WGs. In this way, contributions to the discussion on these WGs was expanded well beyond the original authorship of the WPs.

The process by which the VLASS survey definition proceeded from this point is worth documenting, as it may serve to guide the development of future surveys. Initially, the three scientific WGs (Galactic, Extragalactic, and Transients/Variability) were asked by the SSG Council co-chairs to specify their "ideal" survey designs, supported by key science goals. A "virtual face-to-face" meeting was then used to assess areas of commonality between the elements of the proposed surveys (frequency band, array configuration), and to identify areas that needed further discussion (number of epochs, depth of each epoch, monolithic vs. tiered). At this stage, the focus of the Galactic working group on thermal science, and therefore on higher frequencies than the Extragalactic or Transient WGs and with much less baseline understanding of the nature of the Galactic sky at those frequencies, led to difficulties defining a coherent survey that would justify being part of the VLASS rather than being proposed as a Large program through the regular NRAO proposal process. With this lack of consensus, the SSG Council co-chairs proposed a baseline all-sky, S-band, B-config, survey of $\sim$8500 hours, with the WGs proposing tradeoffs in time/area coverage needed to achieve their key science goals. The VLASS Proposal is the outcome of this process, and represents contributions from more than 200 astronomers over a 9 month period from November 2013 through July 2014.

The time committed to the proposed VLASS will reduce the time available for other VLA programs. However, the time spent on large VLA surveys have effects that increase the net science coming from the VLA.

These include:

1. VLA sky surveys have a science impact per observing hour that is demonstrably greater than the average VLA observing program. This is at least partly because surveys expand the usage of radio data beyond the usual radio astronomy community.
2. Once VLA sky survey products are available, many science projects that require pointed observations of a sample of objects (e.g., to measure spectral indices for a sample of quasars) can be carried out directly from the catalogs rather than requiring an observing proposal. That reduces the time requested for such observing proposals and so increases the time available for other projects.
3. The sky survey products themselves will become a key resource for radio astronomers in identifying targets and projects for followup proposals. That also leads to an increase in the science done by enabling projects that are not possible without the inputs from a sky survey.

The existing VLA sky surveys, NVSS (Condon et al. 1998) and FIRST (Becker et al. 1995, White et al. 1997), provide powerful evidence that the telescope time dedicated to these surveys repays the investment many times over. In Appendix A, we provide a detailed analysis that demonstrates the scientific impact of FIRST and NVSS as measured by publications and citations and data utilization.

4 VLASS - A Survey for the Entire Astronomical Community

Here we describe in detail the full range of science that will be delivered by VLASS. The science case is broken up into a number of interrelated and mutually supportive disciplinary areas. These include extragalactic, polarization, transient, and Galactic science cases, all of which benefit enormously from VLASS. We conclude this section by additionally pointing out that the science delivered by VLASS cannot be achieved with any of the SKA pathfinders coming online within the next 5 years, ensuring that VLASS will have a lasting legacy value well beyond $\gg$2020 into the SKA era.

4.1 Extragalactic Science

One of the fundamental challenges for astrophysics in the 21st century is finding a way to untangle the physical processes that govern galaxy formation and evolution in a range of environments. With VLASS we are well poised to break new ground on our understanding of the astrophysics and relative importance of these processes. A major strength of VLASS is that it takes full advantage of the VLA's long baseline capabilities and the benefits of observing in the radio part of the spectrum, delivering deep, sensitive full stokes imaging that is at much higher (sub-arcsecond) angular resolution than for example the current confusion-limited far-infrared (e.g., *Spitzer, Herschel) surveys*. In doing so, VLASS will probe fainter, higher-redshift galaxy populations, and be better matched to deep-field imaging observations from *HST*, *JWST*, and ALMA.

VLASS will probe galaxy-AGN co-evolution and AGN feedback as a function of cosmic time, stellar/black-hole mass, galaxy morphology, and environment. VLASS observations of galaxy clusters will probe the diffuse (Mpc-scale) synchrotron radio emission in galaxy clusters, elucidating the evolutionary processes shaping galaxies within the cluster environment. VLASS will play a critical role in properly measuring the star formation history of the universe, since radio luminosity provides a more reliable tracer of star formation rate than optical/UV luminosities, especially at high redshift where the latter are strongly affected by dust extinction.

In this section we highlight significant contributions VLASS will make towards a number of diverse, yet critically related topics in extragalactic astrophysics. These include: understanding

the physics behind quasars; characterizing the evolution of AGN while illuminating the relation between accretion and star formation processes; mapping the cosmic star formation history of the universe; investigating the complex physical processes occurring in galaxy clusters and their relation to galaxy evolution; mapping out large-scale structures in the radio for cosmology; and providing the first foray using weak lensing in the radio (a key science goal for the SKA).

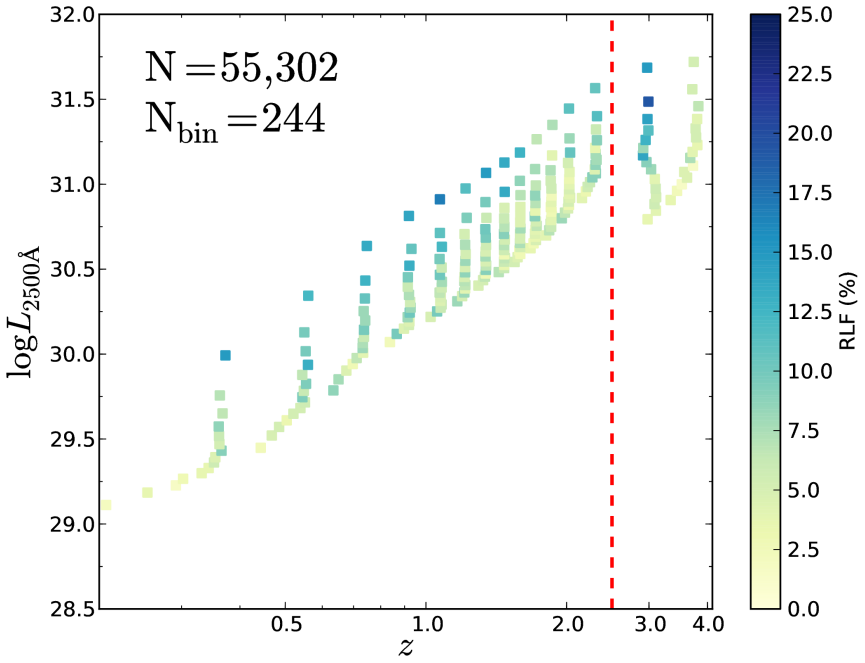

Figure 1: Fraction of quasars that are radio loud (colored blocks) as a function of luminosity and redshift. There appears to be evolution in both redshift and luminosity. Data are limited to the "uniform" SDSS sample and are robust only for $z < 2.5$ (dashed red line).

4.1.1 Quasar Science

Quasar Demographics: Although quasars were first discovered as radio sources, 50 years later we still do not understand the production of strong radio emission in that minority of quasars which are radio-loud or what selects a particular quasar to be a strong radio emitter. Although the Blandford & Znajek (1977) and Blandford & Payne (1982) mechanisms provide a way to tap the energy of a black hole and/or the accretion disk to produce jets, they do not tell us when that will happen or why it happens only a fraction of the time. Observationally, our best hope at further understanding of this phenomenon is to further probe the demographics of when and under what circumstances quasars can be radio loud and to understand whether the radio emission in radio-quiet quasars is due to a separate mechanism.

Recent work has investigated the evolution of radio emission, both in terms of the radio-loud fraction and in terms of the mean radio loudness of quasars as a function of optical luminosity, redshift, mass, accretion rate, and disk-wind properties (Jiang et al. 2007, White et al. 2007, Balokovic et al. 2012, Kratzer & Richards 2014). While much has been learnt about the demographics of radio emission in quasars, Kratzer & Richards concluded that incompleteness at the limit of the FIRST survey is preventing an understanding of whether the radio-loud fraction increases with luminosity and decreases with redshift, concluding that a wide-field survey at $\sim 3\times$ the depth

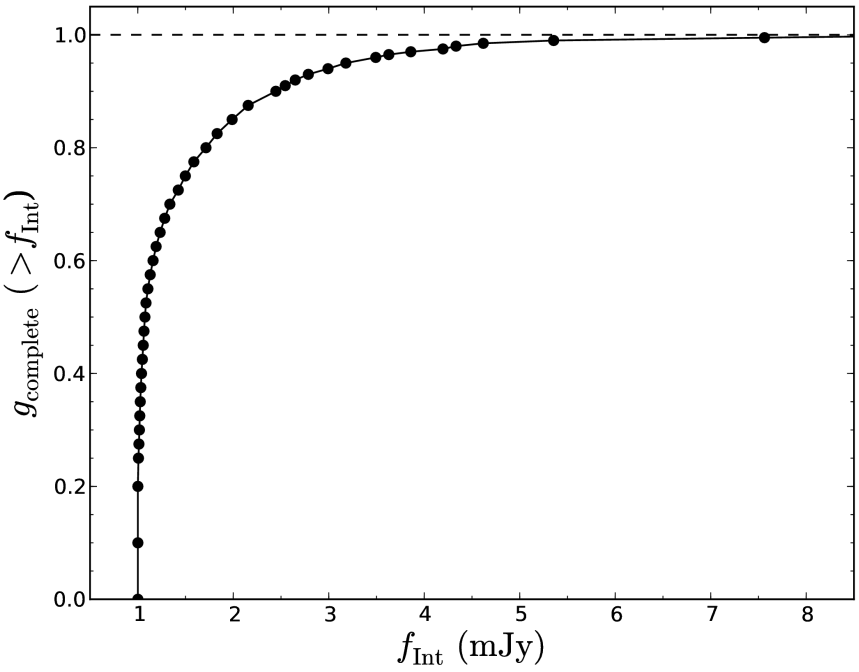

Figure 2: While Figure 1 shows that the radio loud fraction of quasars appears to evolve with luminosity and redshift, the depth of FIRST drops rapidly near the flux limit, as demonstrated here. The evolution could therefore simply be due to the limited depth of FIRST. Deeper radio data are needed to resolve this crucial question. (R. White, private communication: see Kratzer & Richards 2014 for more details).

of FIRST is needed to resolve this important question. While VLASS will miss more extended sources than FIRST, the evolution can be characterized with unresolved sources (which represents $\sim$ 85% of the sample; Ivezic et al. 2002). This apparent evolution is demonstrated graphically in Figure 1, which shows the radio loud fraction as a function of L and z. However, that evolution could simply be consistent with the incompleteness of FIRST at the nominal limit (Figure 2). Only with a solid understanding of the simple demographics of quasar radio emission can we hope to grasp the physics involved.

High-Redshift Quasars: Today over 60 quasars have been discovered at $z > 6$, and the first quasars at $z \sim 7$ have been found in near-IR surveys (Mortlock et al. 2011; Venemans et al. 2013). Although FIRST is relatively shallow, two of these quasars were selected from FIRST (McGreer et al. 2006; Zeimann et al. 2011), while two more have FIRST counterparts. At face value, this indicates that the radio-loud fraction remains high enough at $z \sim 6$ for radio surveys to provide an effective probe of the Epoch of Reionization (EoR). Indeed, it has been argued by Volonteri et al. (2011) that Swift detections of high-redshift blazars demand a substantially larger population of high-z radio quasars than currently known, unless there is significant evolution in the physical properties of jetted sources. A larger population may indeed exist if the fraction of optically obscured sources increases with redshift, an area where radio surveys have been particularly successful at complementing optical surveys (e.g., Glikman et al. 2013).

Orientations: Quasars are thought to have many axisymmetric structures (e.g., accretion disks, dusty torii, etc.) with associated observed properties that vary with viewing angle. Both continuum emission and broad emission line velocity widths depend on orientation and, critically, bias

black hole mass measurements (e.g., Wills & Browne 1986; Runnoe et al. 2013). As such, in order to enable corrections to quasar black hole mass estimates and to conduct other orientation studies, it is desirable to have orientation estimates. The jets of radio-loud quasars reveal their axisymmetry and provide the only reliable ways of determining quasar orientation. When the jet structures are clearly spatially resolved, the radio core flux relative to either the optical or extended radio emission can provide an estimate of orientation (e.g., Wills & Brotherton 1995). At higher redshifts, with young radio sources, or when dealing with lower resolution imaging, the jet morphology is not always clear and the radio spectral index is a more dependable orientation indicator (Orr & Browne 1982; Richards et al. 2001; Jarvis & McLure 2006; DiPompeo et al. 2012). Jet-on sources close to the line of sight are dominated by a relativistically boosted flat core spectrum, while more inclined sources are dominated by the steep optically thin synchrotron emission from the radio lobes. Currently, while FIRST is well matched to the SDSS, there is no equivalent survey of similar depth and resolution but a different frequency with which to obtain spectral indices.

4.1.2 AGN and the Evolution of Accretion Activity

While only roughly 5% of SDSS quasars meet a formal definition of being radio-loud, it is increasingly clear that even radio-quiet quasars are not radio-*silent*. Indeed, these lower-power AGN play a major role in the framework of galaxy formation. The energetic feedback from AGN appears to be a vital ingredient for reproducing some observed features, such as the stellar galaxy mass function (Croton et al. 2005; Bower et al. 2006), and the black-hole mass versus bulge mass (or velocity dispersion) correlation (Magorrian et al. 1998; Gebhardt et al. 2000; Ferrarese & Merritt 2000; Haring & Rix 2004). This suggests that AGN and star formation activity may have been concurrent, even though the origins of the above correlations are the subject of active debate. Indeed, the peak of quasar activity appears to take place at $z \sim 2$ (e.g., Croom et al. 2009; Hasinger et al. 2005), i.e. at epochs when star formation was also at its peak, and observational evidence has been found of the presence of an embedded AGN in 20–30% of $z \sim 2$ massive star forming galaxies in the GOODS fields (Daddi et al. 2007). Traditionally the provinces of separate research fields, it is now becoming clear that AGN and star-formation activity are intimately related, and the cosmic star formation rate appears to mirror closely the cosmic accretion rate onto AGN. However, a complete census of both star formation and AGN activity, especially at high redshifts, is complicated due to dust extinction and gas obscuration by circumnuclear material. The optimal combination of sensitivity and spatial resolution of the VLA allows the study of the entire AGN population from classical radio-loud sources down to the realm of radio-quiet AGNs ($P \sim 10^{22-23}$ W Hz^{-1}, Jarvis & Rawlings 2004; Wilman et al. 2008; Kimball et al. 2011; Condon et al. 2013), from z =0–6. This provides a complete view of nuclear activity in galaxies and of its evolution, unbiased by gas/dust selection effects.

Indeed, there is now strong evidence that the standard AGN unification paradigm (e.g., Antonucci 1993; Urry & Padovani 1995) does not give a complete picture. For example, observational evidence (e.g., Hardcastle et al. 2007; Herbert et al. 2010; Best & Heckman 2012) suggests that many or most low-power ($P < 10^{25}$ W Hz^{-1}) radio galaxies in the local universe (the numerically dominant population) correspond to a distinct type of AGN. These sources accrete through a radiatively inefficient mode (the so-called 'radio mode'), rather than the radiatively efficient accretion mode typical of radio-quiet optically or X-ray selected AGN (sometimes called 'quasar mode'); see Heckman & Best (2014) for a recent review covering these feedback processes. The role of these two accretion modes appears to be strongly influenced by the environment (e.g., Tasse et al. 2008) while the presence or absence of a radio-loud AGN appears to be a strong function of the stellar mass of the host galaxy (e.g., Best et al. 2005; Janssen et al. 2012). Deeper radio surveys covering areas of sky with the best multi-wavelength data are required to probe the evolution of these relationships and the accretion mode dichotomy over cosmic time; this is key information for any attempt to incorporate mechanical feedback from radio-loud AGN in models of galaxy,

group and cluster formation and evolution. In Figure 3 we show the predicted constraints on the radio luminosity function for AGN in three redshift bins of width dictated by the expected photometric redshift error of $\Delta z/(1+z) \sim 0.05$. It is only by having 10 deg^2 that the Poisson uncertainty for deriving the AGN luminosity functions will be reduced to something statistically meaningful, allowing us to properly investigate the role played by accretion in galaxy evolution over cosmic time.

Furthermore, the details of the mechanism(s) of interaction between radio-loud AGN and their environments, on all scales, remain unclear; such basic questions as whether the most powerful sources are expanding supersonically throughout their lifetimes (e.g., Begelman & Cioffi 1989; Hardcastle & Worrall 2000) or what provides the pressure supporting the lobes of low-power objects (e.g., Bırzan et al. 2008; Croston et al. 2008) remain unanswered. These questions can only be addressed by the accumulation of large, statistically complete samples of radio sources with good imaging and excellent, homogeneous multi-wavelength data. Information on both large and small-scale radio structure is required.

Key astrophysical problems related to AGN that VLASS will address thus include:

1) the relationship between AGN and star-formation activity (e.g., Bonfield et al. 2011; Rosario et al. 2013);

2) the evolution of low power AGN (including radio-quiet AGN), exploring the so-called "AGN cosmic downsizing" scenario, found for X-ray and optically selected AGNs (Hasinger et al. 2005; Babic et al. 2006; Smolcic et al. 2009; McAlpine, Jarvis & Bonfield 2013);

3) the relative contribution of different accretion regimes (radio vs. quasar modes), its evolution with redshift, and the role played by the environment (e.g., Best & Heckman 2012);

4) the relative contribution of radiative versus jet-driven (kinetic) feedback to the global AGN feedback in models of galaxy formation;

5) the mechanisms of that feedback and the evolution in the physical properties of radio-loud AGN with redshift (e.g. Mocz, Fabian & Blundell 2013).

4.1.3 Star Forming Galaxies and the History of Cosmic Star Formation

In almost all existing large-scale radio surveys, the vast majority of the sources detected are the accretion-dominated AGN and quasar populations. However, thanks to the well-known correlation between far-infrared (FIR) and radio emission (e.g., Helou et al. 1985; Appleton et al. 2004; Murphy 2009; Sargent et al. 2010; Ivison et al. 2010; Jarvis et al. 2010), the star-forming galaxy population becomes detectable at flux densities around $S_{1.4GHz} \sim 1$ mJy beam^{-1}, growing to dominate the source counts at fainter flux densities (e.g., Windhorst et al. 1985; Wilman et al. 2008; de Zotti et al. 2010). The radio is a particularly important tracer for this population, as it is relatively immune to dust extinction, providing an unbiased view into the basic features of galaxy formation across the history of the universe, including the volume-averaged star formation rate, its distribution function within the galaxy population, and its variation with environment.

Surveys of the cosmic star-formation rate as a function of epoch suggest that the star-formation rate density rises as $\sim$(1+z)^4 out to at least $z \sim 1$ (e.g., Lilly et al. 1996; Hopkins & Beacom 2006; Behroozi et al. 2013) and then flattens, with the bulk of stars seen in galaxies today having been formed between $z \sim 1-3$ in the so-called epoch of galaxy assembly. However, the effects of dust on the traditional optical and UV measurements of the star formation rate are still hotly debated (e.g., Carilli et al. 2008), with different star-formation indicators giving wildly different measures of the integrated star-formation rate density (see Hopkins & Beacom 2006). Moreover, the shorter wavelengths may miss the heavily dust-obscured IR bright-population entirely (e.g., Walter et al. 2012). The result is that the behavior of the cosmic star formation rate density at redshifts above

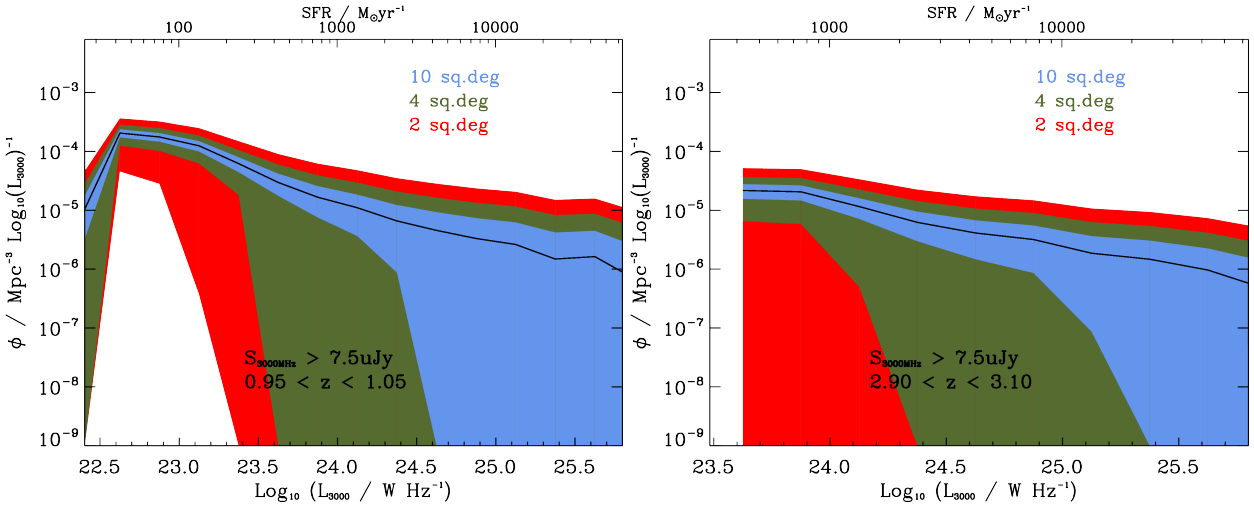

Figure 3: Predicted luminosity function at $0.95 < z < 1.05$ (left), and $2.90 < z < 3.10$ (right) for AGN in the deep continuum survey [based on the simulations of Wilman et al. (2008, 2010)]. The red regions shows the Poisson uncertainty for a 2 deg^2 survey, the blue region is for a 4 deg^2 survey and the cream regions is for the proposed 10 deg^2 survey. The equivalent star-formation rate is given on the upper x-axis.

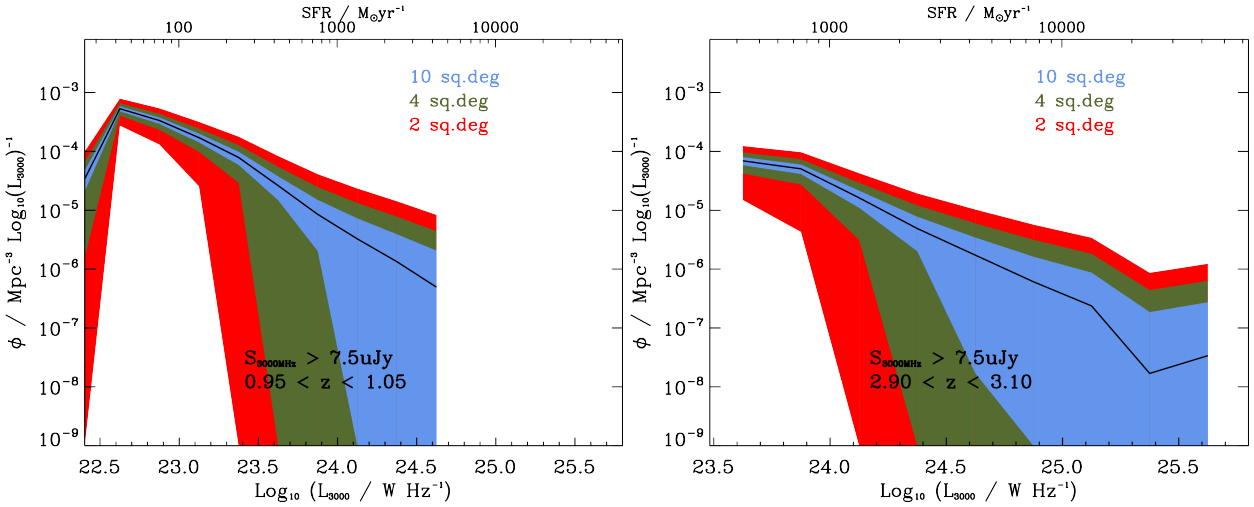

Figure 4: Predicted luminosity function at $0.95 < z < 1.05$ (left), and $2.90 < z < 3.10$ (right) for star-forming galaxies in the deep continuum survey [based on the simulations of Wilman et al. (2008, 2010)]. The red regions shows the Poisson uncertainty for a 2 deg^2 survey, the blue region is for a 4 deg^2 survey and the cream regions is for the proposed 10 deg^2 survey. The equivalent star-formation rate is given on the upper x-axis.

$z \sim 1$ is still uncertain. These problems are exacerbated by the effects of cosmic variance in the current samples (multi-wavelength surveys such as COSMOS and GOODS typically cover only modest-sized areas, $\lesssim$1 deg^2, corresponding to just $\sim$30 Mpc at z$\sim$23), as well as small sample sizes. In Figure 4 we show the predicted constraints on the radio luminosity function for star-forming galaxies in three redshift bins of width dictated by the expected photometric redshift

error of $\Delta z/(1+z) \sim 0.05$. One can see that moving from 2 deg^2, the area covered by the COSMOS survey, to 10 deg^2 greatly reduces the Poisson uncertainty on the luminosity function for star-forming galaxies. Figure 5 shows the sample variance due to large-scale structure in various survey areas for difference galaxy masses, demonstrating again that the move towards larger areas/volumes is key to developing understanding of the link between star formation, galaxy mass and environment.

Beyond constraining the global average star formation rate, forming a complete picture of galaxy formation and evolution also relies on understanding the nature and distribution of the star-forming galaxies by addressing a number of key questions:

How does star-formation proceed as a function of galaxy mass?: It is well established that in the local universe the stellar populations of the most massive galaxies formed earlier than those of less massive galaxies ('downsizing'; e.g., Cowie et al. 1996). Massive galaxies must therefore form stars rapidly at an early epoch before having their star formation truncated, but how and exactly when did this occur?

As the most massive and star forming galaxies are prone to extinction by dust, radio observations are required to provide high-resolution, dust-unbiased star formation rates as a function of galaxy mass and epoch.

What is the nature of the luminous starburst population?: We know from studies of polycyclic aromatic hydrocarbon features and FIR fine structure lines that the ultra-luminous infrared galaxy (ULIRG) population at $z \sim 2$ is quite different from that at low-z—likely dominated by multi-kpc-scale disks rather than by nuclear starbursts—but this evolution is yet to be understood. Studies of the radio properties of star forming galaxies, such as their sizes, polarizations and FIR/radio ratios, are necessary to constrain models for ULIRG evolution as a function of redshift and environment—particularly the unique aspects of the magnetic field in the ISM that can only be obtained from radio synchrotron emission.

What is the role of galaxy environment?: In the local universe, star formation is suppressed in dense environments (e.g., Lewis et al. 2002), an effect which diminishes with increasing redshift, with hints that it disappears altogether at $z \sim 2$ (e.g., Koyama et al. 2013; Ziparo et al. 2014). However, where precisely, in terms of epoch and environment, does this environmental influence begin to become important? To what extent is the build-up of galaxies into groups and clusters responsible for the sharp decline in the global average star formation rate below $z = 1$? Is this indeed an environmental effect or host galaxy mass dependent effect (e.g., Peng et al. 2010; 2012)? Current radio surveys are too limited to sample representative environments at all redshifts. Given that star formation is environmentally dependent, any investigation on the evolution of star-forming galaxies requires the ability to detect them over the full range of cosmic environments (e.g., from rich clusters to voids).

How does star formation relate to the growth of supermassive black holes, and AGN feedback?: As discussed in Section 4.1.2 above, it is widely thought that AGN activity (particularly radio-loud AGN) may be responsible for switching off star-formation in massive galaxies, but a direct observational link between AGN activity and star-formation at high redshifts remains elusive. Recent studies from both a theoretical (Silk 2013) and observational (Kalfountzou et al. 2012, 2014) perspective have shown that powerful radio-loud AGN may actually provide a positive form of feedback. On the other hand, there is little evidence for any type of feedback from radio-quiet objects based on the latest studies using *Herschel* (e.g., Bonfield et al. 2011; Rosario et al. 2013). Moreover, the interplay between jets (also rare AGN—requiring a large survey area) and associated satellite galaxies is even more poorly understood. As *Herschel* studies are limited due to resolution and confusion noise, and optical surveys miss all of the obscured galaxies, radio is again the best line of attack. However, current radio surveys are unable to probe radio emission from star formation over the epoch where AGN activity is having an impact on the environment. Given that different forms of

AGN feedback are invoked in current semi-analytic models of galaxy formation (e.g., Croton et al. 2006; Bower et al. 2006; Hopkins 2012), it is essential that we understand such processes if we are ever to understand the evolution of galaxies.

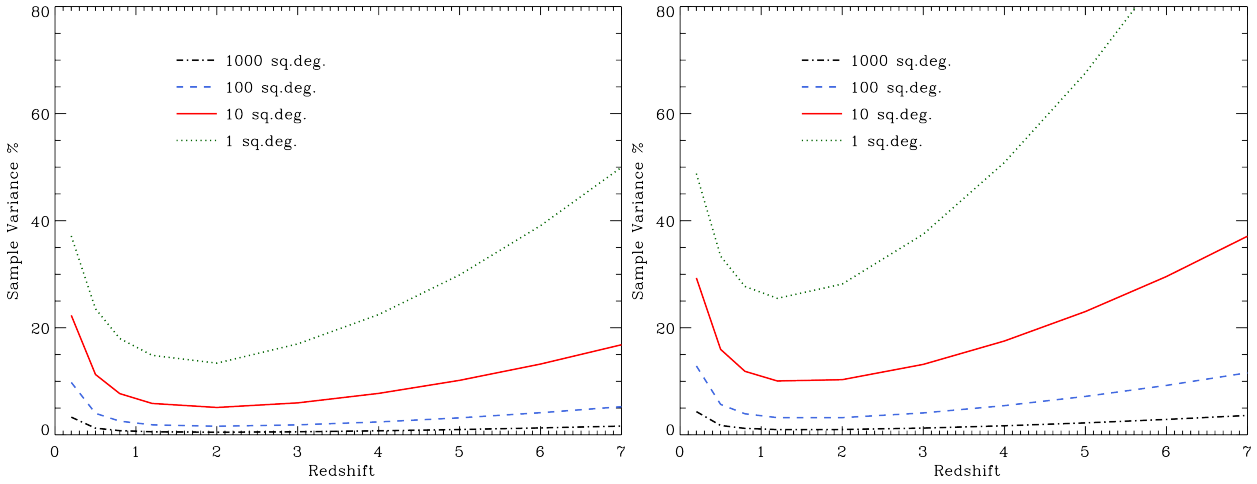

Figure 5: Sample/cosmic variance for galaxies of mass 10^{10} M_{odot} (left) and 10^{11} M_{odot} (right) for different survey areas. Moving from a 1 deg^2 area to 10 deg^2 reduces the sample variance from $\sim$ 15 per cent to $\sim$ 5 at the crucial epoch around $z \sim 2$.

4.1.4 The Physics of Galaxy Clusters

Clusters of galaxies are the largest gravitationally bound systems in the universe, and are dominated by dark matter ($\sim$80%). Clusters are thought to form hierarchically, with smaller galaxy clusters merging to form bigger ones. This process continues at the present time. Only a tiny fraction of a cluster's mass is in the form of stars in galaxies ($\sim$3–5%), while the rest ($\sim$15–17%) comprises the intracluster medium (ICM), which is a diffuse hot (10^7–10^8 K) gas detected in X-ray observations by its thermal bremsstrahlung and highly-ionized line emission. Radio observations play a key role in understanding the physics of galaxy clusters and the role of the intracluster environment in galaxy evolution. The proposed VLASS observations are particularly suited to (i) Study the interaction and feedback between the ICM and relativistic plasma from AGN, (ii) Determine the properties of cluster-wide magnetic fields, and (iii) probe cluster weather and turbulence through tailed radio galaxies. In addition, the high-resolution VLASS observations will enable the removal of compact sources from lower resolution images that are used to study large-scale diffuse radio emission in clusters (Feretti et al. 2012).

AGN Feedback: The hot gas in the center of relaxed clusters has a relatively high density ($\sim 10^{-2}$ cm^{-3}), which implies short radiative cooling times that should lead to strong cooling flows. However, only weak cooling is observed and thus some feedback source to heat the cool core is required. At present, it is hypothesized that the source of heating in cool-core clusters is the AGN activity of the brightest cluster galaxy at the center (e.g., Peterson & Fabian 2005). The details of this process are still far from being understood.

The radio feedback is thought to work through radio lobes which inflate bubbles (X-ray cavities) in the thermal gas, driving weak shocks and sound waves through the ICM. These bubbles are expected to detach and buoyantly rise through the ICM after the central AGN activity decreases. In addition to the energy injection, these rising bubbles provide a means of seeding the ICM with magnetic fields and relativistic particles. X-ray observations are only able to easily detect small

cavities near the plane of the sky at relatively small distances from the cluster core. Larger cavities farther from the core, where the ICM is more diffuse, as well as those at small angles from the line of sight do not provide sufficient contrast for detection in even moderately deep X-ray observations. On the other hand, radio observations provide methods to place observational limits on the energy injected into the ICM by AGN feedback by tracing the complete kinetic feedback history of the ICM over multiple AGN outburst cycles. Despite the many uncertainties, the study of the radio spectrum in the aged and active components provides critical information on the cycles of activity of, and the total energy output delivered into the ICM throughout the cluster lifetime (e.g., Giacintucci et al. 2012).

ICM Magnetic Fields: The study of polarized radio emission from cluster and background sources indicates that magnetic fields are ubiquitous in clusters. However, very little is known about the strength and structure of these fields and the origin of these fields is still being debated. Studies of the polarization fraction through Rotation Measures of both cluster and background sources provide a way tot determine the properties of ICM magnetic fields (e.g., Bonafede et al. 2010). Such a study is difficult to perform for individual clusters given the limited amount of polarized sources available. VLASS will provide a very large sample of polarized sources allowing binning the results for a large number of clusters.

Cluster Weather and High-z Clusters: Narrow and Wide Angle Tailed radio galaxies (NATs and WATs, respectively) are the most spectacular examples of radio emission from elliptical galaxies. Their shape is the signature of galaxy cluster membership, and is explained as the combination of motion of the hosting galaxy within the cluster and ICM bulk gas motion (e.g., Blanton et al. 2000). Spectral studies along the tails provide estimates of the age of the radio plasma, which in turn can be used to infer the galaxy velocity within the cluster, and information on the dynamical state of the cluster and the ICM. Due to their unique association with dense environments, NATs and WATs can readily be used to identify high-z galaxy clusters (Wing & Blanton 2011). High-z clusters require significant observational efforts for detection in the X-ray and optical bands, while they are fairly accessible with high resolution (arcsecond scale) radio observations. In this way, wide radio surveys that discover WATs and NATs nicely complement the ongoing surveys that exploit the redshift-independent surface brightness of the Sunyaev-Zel'dovich effect, which is now being used to locate previously-unknown clusters at high-z.

4.1.5 Cosmology and Large Scale Structure

Over the past few years there has been an increasing focus on using radio continuum surveys to address the fundamental issues related to the cosmological model, including determining the equation of state of dark energy and whether we can find evidence for departures from General Relativity on the largest scales (e.g., Raccanelli et al., 2012; Camera et al., 2012). Three key tests where one can use radio continuum sources as cosmological probes are: the Integrated Sachs-Wolfe effect (e.g., Raccanelli et al., 2008); the power spectrum of the radio source populations (e.g., Blake et al., 2004); and the cosmic magnification bias (e.g., Scranton et al., 2005). However, one of the key unknowns in our understanding of how well radio sources can help determine the underlying cosmological model is their bias, i.e. how they trace the underlying dark matter density field.

It is actually very difficult to determine this quantity directly from radio continuum surveys alone, although some progress has been made by measuring the angular two-point correlation function of radio sources cross-correlated with optical imaging and spectroscopic surveys (e.g., Lindsay et al., 2014a) and by assuming a redshift distribution (e.g., from the SKADS simulation of Wilman et al., 2008, 2010). However, such studies are hampered by only the low-redshift sources having reliable optical counterparts, thus limiting the redshift range over which the bias can be measured to $z < 0.5$. Given that the unique niche occupied by radio continuum surveys for

determining the cosmological model lie in the fact that their redshift distribution peaks at $1 < z < 2$ (depending on the precise flux-density limit), our lack of knowledge of the bias at $z > 1$ hampers our ability to use these sources as tracers of the universe on large scales.

This problem can be tackled in two ways with a deep VLA continuum survey. The first is to measure the two-point correlation function of the sources in the survey directly. This is analogous to what has been done at low redshifts, where the optical counterparts can be used in these deep fields to determine redshifts, using either photometric or spectroscopic redshifts. Such an experiment requires the necessary volume to determine the clustering of dark matter haloes, and with a single field of around 1 deg^2 such a measurement is extremely difficult. However, by moving to 4-5 deg^2 patches of sky then the two-halo term in halo-occupation distribution models begins to be measured at > 1 Mpc scales. Figure 3 shows the constraints that can be achieved by moving from a 1.5 deg^2 survey to a 4 deg^2 survey based on the clustering model prescribed in the SKADS simulation (Wilman et al., 2008). Additional information can also be used, such as the full galaxy catalogue from optical and near-infrared data. By measuring the cross-correlation of the much more abundant optical/near-infrared sources with the radio sources one can obtain much tighter measurements of the clustering of radio sources over all luminosity regimes, i.e. even for the rarer AGN (e.g., Lindsay et al., 2014b).

4.1.6 Weak lensing

Weak gravitational lensing is the effect whereby images of faint and distant background galaxies are coherently distorted due to deflection of their light by intervening large scale structures in the universe. This "cosmic shear" effect is recognized as one of the key cosmological probes that will allow us to precisely probe the nature of dark energy with future surveys (Albrecht et al. 2006; Peacock et al. 2006). The current state-of-the-art in terms of weak lensing comes from optical surveys covering 154 deg^2, i.e. the recent CFHTLenS results (Heymans et al. 2013). Although the lensing-derived constraints on the evolution of structure are currently not strong enough to meaningfully constrain the properties of dark energy, ongoing and future ground-based surveys, e.g., the KiDS (de Jong et al. 2013), DES[1], HSC[2], LSST[3] and SKA[4] surveys, and ultimately satellite missions such as NASA's *WFIRST-AFTA*[5] and ESA's *Euclid*[6] telescope (Laureijs et al. 2011), promise to revolutionize the field of weak lensing by allowing precision measurements of structure growth. In addition, lensing measurements can be used to test the nature of gravity in a complementary way to other cosmological probes (e.g., Simpson et al. 2013, Raccanelli et al. 2012).

The only detection of weak lensing in the radio band to date was made by Chang, Refegier & Helfand (2004) using the VLA FIRST survey (Becker et al. 1995). Since then progress in radio weak lensing studies has lagged behind the optical because of the much smaller number density of galaxies typically seen in radio surveys as compared to the optical bands. This situation is beginning to change with the advent of a new generation of radio telescopes. Indeed a number of relatively large observational programs in the radio have weak lensing as one of their primary science drivers. In particular the SuperCLASS[7] survey on the UK's e-MERLIN telescope aims to detect the weak lensing signal in a supercluster of galaxies while the CHILES[8] continuum and HI surveys, currently being undertaken on the VLA, will search for radio weak lensing effects in the COSMOS field. Large scale surveys with the LOFAR telescope and with the SKA pathfinder

[1]http://www.darkenergysurvey.org
[2]http://www.naoj.org/Projects/HSC/
[3]https://www.lsstcorp.org
[4]https://www.skatelescope.org
[5]http://wfirst.gsfc.nasa.gov
[6]http://sci.esa.int/euclid/
[7]http://www.e-merlin.ac.uk/legacy/projects/superclass.html
[8]http://www.mpia-hd.mpg.de/homes/kreckel/CHILES/index.html

telescopes, MeerKAT and ASKAP will also offer interesting opportunities for radio weak lensing studies (mainly through lensing magnification effects) in the run-up to Phase-1 of the SKA. However, it is the VLA that possesses the unique combination of excellent sensitivity and high angular resolution required to measure the weak lensing signal to high accuracy. This combination of sensitivity and resolution will remain unsurpassed until the advent of the SKA and will make the deep component of the VLA Sky Survey the world's premier resource with which to spearhead the development of radio weak lensing in preparation for the SKA.

The radio band offers unique and powerful added value to the field of weak lensing. Firstly, deep radio surveys will probe the lensing power spectrum at significantly higher redshift than most of the planned optical lensing surveys. The addition of radio can therefore offer a more powerful redshift "lever arm" with which to measure the effects of dark energy on the evolution of structure. Secondly, instrumental systematic effects are a serious concern for weak lensing studies for which a very accurate representation of the beam or point spread function (PSF) of the telescope is required. The highly stable and deterministic beam response of radio interferometers could therefore prove a major advantage for weak lensing science. Radio observations offer unique advantages over traditional lensing analyses by enabling fitting of galaxy shapes directly from uv-visibility data (Chang & Refregier 2002, Chang et al. 2004). Another unique aspect comes from the VLA's wide bandwidth at both L- and S-band which allows direct measurement of the frequency dependence of the beam. This is a potential major advantage over optical broad-band photometry since while galaxy optical-uv SEDs vary wildly, in the radio galaxies typically exhibit smooth power-law type spectra. Perhaps most importantly, the radio offers unique and novel opportunities to independently evaluate the effects of weak lensing such as through polarization measurements.

Polarization observations of weak lensing provide unique information on the intrinsic (unlensed) shapes of background galaxies. The position angle of the integrated polarized emission from a background galaxy is unaffected by gravitational lensing (Brown & Battye 2011). If the polarized emission (which is polarized synchrotron emission sourced by the galaxy's magnetic field) is also strongly correlated with the disk structure of the galaxy then measurements of the radio polarization position angle can be used as estimates of the galaxy's intrinsic (unlensed) position angle. Thus, polarization observations can be used to reduce the primary astrophysical contaminant of weak lensing measurements – intrinsic galaxy alignments (see e.g., Heavens et al. 2000, Catelan et al. 2001, Brown et al. 2002, Hirata & Seljak 2004) – which are a severe worry for ongoing and future precision cosmology weak lensing experiments. Additionally, depending on the polarization properties of distant background disk galaxies, the polarization technique has the potential to reduce the effects of noise due to the intrinsic dispersion in galaxy shapes.

4.2 The Polarized Sky

The WIDAR correlator has opened a major new window for wideband polarization work, enabling us to characterize properties of the magneto-ionic medium in AGNs and in galaxies across a wide range of redshifts. Faraday rotation in a magneto-ionic medium produces various external or internal depolarization processes (e.g., Burn 1966, Tribble 1991, Sokoloff 1998). These provide a unique and critical diagnostic of the magneto-ionic medium, but only when observed over a wide, continuous frequency range (e.g., O'Sullivan et al. 2012). Almost all studies to date have either relied on a selected number of narrow bands or have observed over a continuous but relatively narrow fractional bandwidth. However, both these approaches have severe shortcomings (Farnsworth et al. 2011). **Degeneracies between different types of depolarization behavior, and hence the underlying physical properties of polarized sources and foreground gas, can only be broken by wideband spectro-polarimetry.**

A 2–4 GHz (S-band) polarization survey will uncover previously unknown populations of sources with extremely large Faraday depths and those that are heavily depolarized. For many

sources, we will be able to combine these data with 1–1.5 GHz polarization measurements from ASKAP and AperTIF, which will enable the characterization of complex and interesting cases in compact and extended AGN regions, absorption line systems and galaxies, where magnetized relativistic and thermal plasmas are mixed.

Using broadband VLA data, we can uniquely address such questions as:

(1) What is the covering fraction, the degree of turbulence and the origin of absorption line systems? Mg II absorbers are associated with $\sim 10^4$ K photo-ionized circum-galactic medium in a wide range of host galaxy types and redshifts (see Churchill et al. 2005 for a review). These systems potentially trace outflows from star formation (e.g., Norman et al. 1996) and cold-mode accretion (e.g., Kacprzak et al. 2010). When seen against polarized background sources, the Faraday depth provides a direct measure of the electron density and the magnetic field strength in Mg II absorbing systems, parameters that are both currently poorly constrained. Bernet et al. (2008, 2013) and Farnes et al. (2014) have demonstrated the presence of large values of |RM| associated with Mg II absorbers, and have interpreted this as evidence for μG field at $z \sim 1$, possibly associated with outflows. We can use such data to test photo-ionization models, and to infer the evolution of large-scale magnetic fields over cosmic time. With deep observations and high angular resolution, we can use Mg II catalogs derived from SDSS (Quider et al. 2010, Zhu & Menard 2013) to identify sight lines through absorbers (current total number $\sim$ 40,000).

(2) What is the the magneto-ionic medium in AGNs, galaxies and their immediate environments? Feedback from AGN is important in galaxy formation: it is intimately linked to the star formation history (e.g., Hopkins & Beacom 2006), and could suppress cooling in massive galaxies, producing the bright-end cut-off of the luminosity function (e.g., Best 2006, Croton 2006). The nature of this AGN feedback is very much under debate: it has been shown that energy deposited by radio jets can either trigger or quench star formation (e.g., Wagner et al., 2012). AGNs are also thought to influence their surrounding intergalactic medium by enrichment of metals (Aguirre et al. 2001) and magnetic fields (Furlanetto & Loeb 2001). Thus, investigating how radio galaxies impart energies into the ISM/IGM is crucial.

While minimal interaction between radio lobes and the environment would lead to a thin "skin" of thermal material around the lobes (e.g., Bicknell et al. 1990), significant interaction should lead to large-scale mixing of thermal gas with the synchrotron emitting material throughout the lobe, causing internal Faraday dispersion. Recently O'Sullivan et al. (2013) fitted the depolarization trend of the lobes in one such radio galaxy, Centaurus A, and found a thermal gas of density 10^{-4} cm^{-3} well mixed in with synchrotron emitting gas in the lobes. A sensitive wide-band polarization survey allows statistical studies of this phenomenom through estimation of the thermal gas content in a large number of radio galaxies, covering a range of luminosities, redshifts, and environments.

Additionally, while we now have new extragalactic source catalogs of rotation measure vs redshift (e.g., Hammond et al. 2012), we are severely limited by our inability to correct polarization data for cosmological expansion. A "polarization k-correction" is only possible with wide-band polarization data, with which we can then infer intrinsic rest frame properties of the magneto-ionic medium in AGNs, galaxies and their immediate environments, and can then investigate how all these properties evolve with redshift.

(4) Emergence and growth of large-scale magnetic fields in galaxies? Spatially resolved images of the polarized synchrotron emission from nearby galaxies demonstrate the existence of μG azimuthal fields (e.g., Beck et al. 1996). However, the evolution of galactic-scale magnetic fields over cosmic time is poorly constrained, because this traditional approach becomes increasingly challenging for distant galaxies. An alternative approach is to utilize the statistics of integrated synchrotron polarization of unresolved galaxies to infer their overall magnetic field properties (e.g., Stil et al. 2009). In the presence of a large, scale galactic field the position angle of the integrated polarized radiation is aligned with the minor axis of the galaxy for rest frame frequencies above a few GHz.

At lower frequencies the effects of internal Faraday rotation from the galactic ISM both depolarizes the radiation and breaks the global symmetry of the observed field, leading to reduced polarized signal and variance of the correlation between the polarization position angle and the optical axes of the galaxy. On the other hand strong turbulence in starbursts can lead to depolarization that is largely independent of wavelengths.

Observations between 2-4 GHz spans the low and high depolarization frequency regimes, and can thus be used to test theoretical predictions from various galactic magnetic field generation mechanisms (see for example, Heiles & Zweibel 1997), with which we can provide the first constraints on the time scales for galactic magnetic field amplification and the strength of the initial seed fields (Arshakian et al. 2009). Average fractional polarization of unresolved Milky-Way type galaxies is a factor of 3–4 higher at 2 GHz than at 1.4 GHz (Stil et al. 2009; Braun et al. 2010; Sun & Reich 2012), a 2–4 GHz survey with sufficient sensitivity thus opens enormous potential for characterizing the development of galactic magnetic fields.

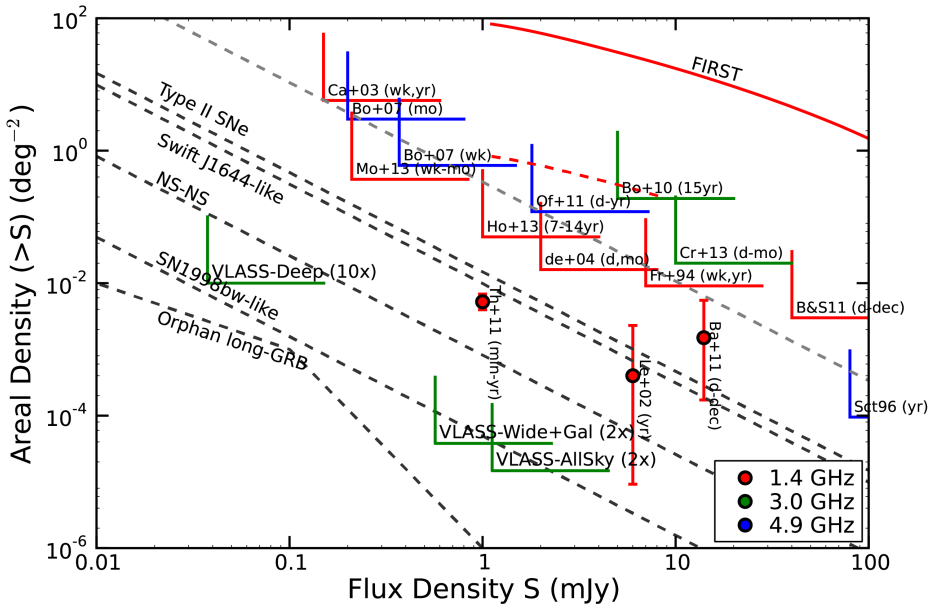

Figure 6: The phase space of slow extragalactic transients. The solid red line represent extragalactic source counts from FIRST. The dashed black lines give expected rates of different classes of transients at 3 GHz based on their known light curves and their occurrence per Gpc^3 per year. The rates for NS-NS and SN1998bw are from Frail et al. 2012, and those for orphan long-GRB afterglows are from Ghirlanda 2014. The dashed red line denotes the variable extragalactic source population (1% of the persistent sources; variety of references, e.g., Mooley et al. 2013 and references therein). The dashed grey line is the transient rate claimed by Bower et al. 2007. Wedges indicate upper limits to the transient rates form previous surveys, and errorbars (2-σ) are transient rates for past detections. The markers are color-coded according to frequency of observations.

4.3 Transient Science

The 2010 Astronomy and Astrophysics Decadal Survey highlights time domain astronomy as an arena with great potential for new discoveries. Space-based observatories, such as the Burst and

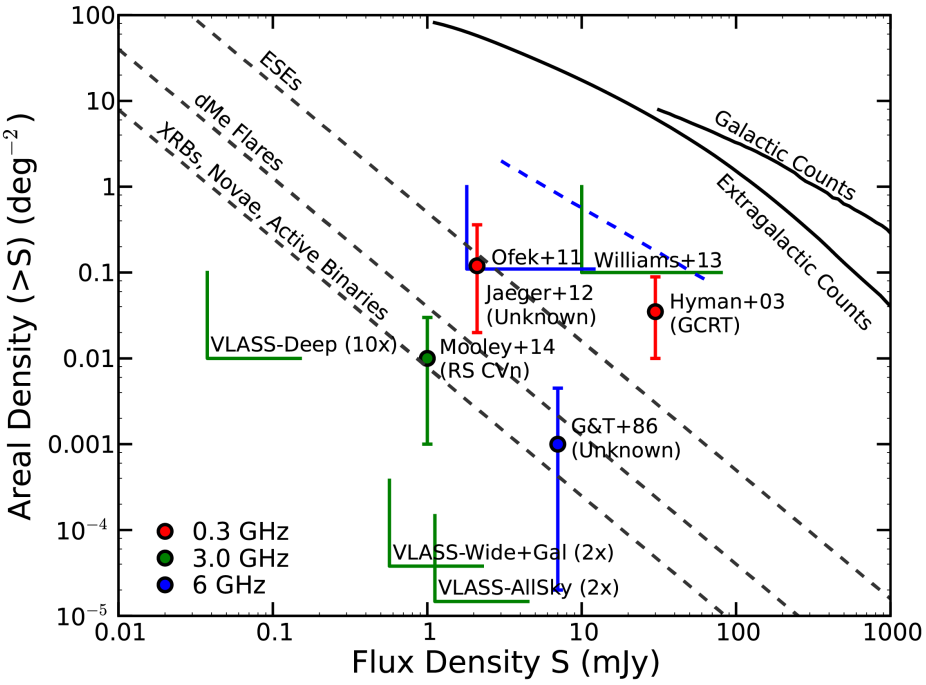

Figure 7: The phase space of Galactic radio transients at S-band. The solid black lines represent Galactic source counts from the MAGPIS survey [White et al. 2005, AJ, 130, 586] and extragalactic source counts from the FIRST survey. The dashed black lines give expected rates of different classes of transients from [Williams et al. 2013, ApJ, 762, 85]. The dashed blue line denotes variable Galactic population from [Becker et al. 2010, AJ, 140, 157]. Wedges indicate upper limits to the transient rates form previous surveys, and errorbars (2-σ) are transient rates for past detections. The markers are color-coded according to frequency of observations. Rates for novae are estimated from optical transient survey.

Transient Source Experiment (BATSE) on the Compton Gamma-ray Observatory, the Rossi X-ray Timing Explorer (RXTE), and more recently the Swift Gamma-Ray Burst Mission and the Fermi Gamma-ray Space Telescope, have pioneered real-time monitoring of large fractions of the X-ray and gamma-ray skies, while ground-based, large synoptic surveys such as the Palomar Transient Factory (PTF), the Catalina Real-time Transient Survey (CRTS), the Panoramic Survey Telescope and Rapid Response System (Pan-STARRS), and the planned Large Synoptic Survey Telescope (LSST), take advantage of progress in optical detector technology to open up new fields in the study of optical transients on timescales of seconds to years. In particular, the last two decades have seen these facilities reach the etendue necessary to routinely detect known populations of transients in synoptic surveys and to discover new classes of astrophysical transients. A good metric in the optical band has been the increasing rate of supernova detection, which is estimated to approach 1000 detections per night in the LSST era.

By contrast, the study of radio transients is a fledgling field; previous generations of interferometers have been ill-suited to the repeated imaging of large swathes of the sky with the sensitivity needed for the systematic exploration of the dynamic radio sky on timescales $>$ 1s (see Cordes et al. 2007 for a review). However, although comparatively poorly sampled, evidence suggests that the transient sky at radio wavelengths is equally ripe for discovery. Many new classes of ra-

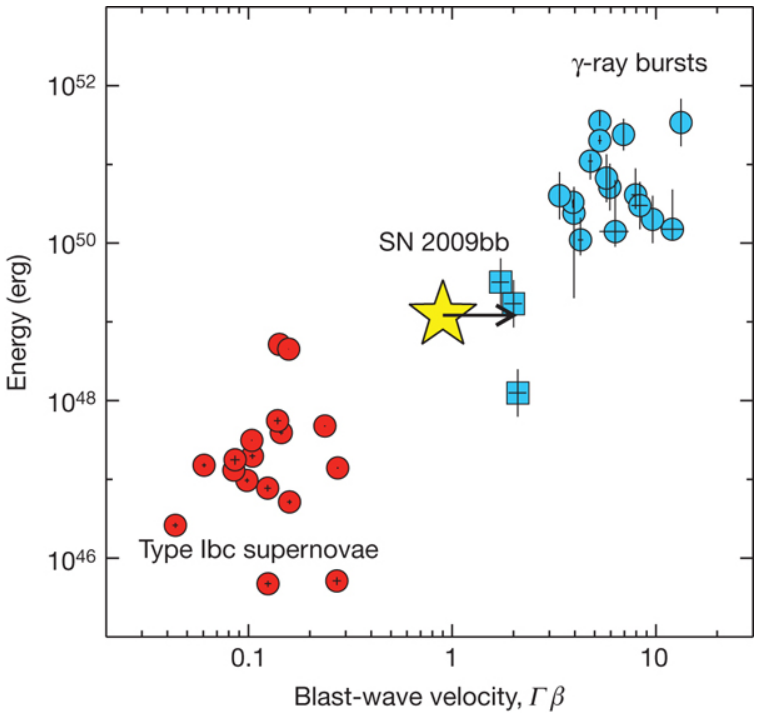

Figure 8: Kinetic energy in the fastest moving ejecta is plotted against shock wave speeds and compared for SNe and GRBs. It can be seen that the normal supernova shock wave carries a few orders of magnitude less energy than a GRB shock wave. Similar to the velocity space, energy distribution of SN and GRBs also appear bimodal. Events similar to SN 2009bb populating this parameter space remain to be discovered (Kamble et al., 2013; Soderberg et al. 2010).

dio transients have been discovered in follow-up observations of targets discovered in surveys at optical and higher energies. These include radio afterglows from gamma-ray bursts (GRBs; Frail et al. 1997) , a giant flare from a Soft Gamma-ray Repeater (SGRs; Cameron et al. 2005, Gaensler et al. 2005), the detection of periodic pulses from brown dwarfs (Hallinan et al. 2007) and a tidal disruption event around an otherwise dormant super-massive black hole (Zauderer et al. 2011).

Synoptic surveys offer the potential to systematically characterize radio transient phase space. For example, the detectable rate of extragalactic explosive transients may be much higher at radio frequencies than X-rays or gamma-rays, as the latter is often subject to narrow beaming that does not constrain the viewing angle for radio emission. Furthermore, transient events at radio wavelengths are often distinct in terms of emission processes, energetics, characteristic timescales and detectability from their counterparts in optical and higher energy wavebands, and in some cases are unique to the radio regime. There has been some success from blind searches for transients in archival VLA data (Bower et al. 2007; Thyagarajan et al. 2011, Jaeger et al. 2012). However, archival searches, while useful, are very much hampered by the lack of contemporaneous follow-up observations, precluding full characterization and association with higher energy counterparts. Optimized survey strategies (Macquart et al. 2014), rapid data reduction, transient identification and follow-up are essential to maximizing the success of future radio transient surveys. For example, see Table 1. of Lazio et al. (2014) for a summary of the relative energetics and evolutionary timescales for the radio and optical emission of various classes of transient populations.

The upgraded Jansky VLA is the first operational interferometer with the survey speed to probe known populations of extragalactic and Galactic radio transient populations with modest

time allocation (Figure ?). Furthermore, this capability has been demonstrated in pilot surveys of Stripe 82 (Mooley et al. 2014). The much larger area covered by VLASS will target a number of key radio transient science goals addressing fundamental outstanding questions, such as an unbiased measure of the SNe rate in the local universe and a determination of the true rate of neutron star merger events. Furthermore, the resulting dataset will provide image data for 75% of the entire sky that will serve as reference data for future radio transients searches, both targeted follow-up and synoptic surveys, with the high resolution of VLASS a particular advantage for cross-referencing with future datasets.

The VLA also offers a unique advantage for transient searches relative to any other facility, existing or planned. The VLITE system (center frequency 350 MHz, bandwidth 64 MHz) will be installed on the prime focus of 10 antennas of the VLA with a completion date of October 2014, with a proposed future upgrade (LOBO) extending this capability to all of the antennas (Kassim et al. 2014). This system will offer **commensal** observing of the P-band sky with little or no impact on standard observing at higher frequencies. The potential for transient science is particularly profound, as the low frequency system can probe an entirely distinct population of transients to the S-band VLASS, dominated by sources of coherent radio emission typically confined to such low frequencies. Blind searches of the Galactic Center have already demonstrated the presence of a population of coherent, pulsed sources as of yet unknown origin. A VLITE enabled VLASS will probe this population to much greater depth over a much larger swatch of sky.

4.3.1 The Death of Massive Stars

Phenomena associated with the explosive death throes of massive stars have been studied for decades at all wavelengths. These myriad phenomena include the various classes of supernovae (type Ia, type Ib, Ic and type II), the highly relativistic outflows of GRBs and the mergers of compact objects. As well as providing a window into the life cycles massive stars, such events also inform on the formation of compact objects and can provide a standard candle for precision cosmology. Heretofore, radio observations have been conducted as follow-up after the initial detection of such events at higher energies. The detected synchrotron emission has provided a unique window on the interaction of the associated stellar ejecta with the surrounding interstellar medium, typically providing the best means to undertake calorimetry of the explosion, independent of the initial asymmetry of the explosion. It is this very capability to provide an unbiased measure of the true rates of these phenomena that motivates their search via synoptic radio surveys such as VLASS.

Supernovae: A comparison of the star formation rate and supernova discovery in the local universe implies that as many as half of the supernovae remain undetected in the traditional optical searches, largely due to extinction via dust obscuration. This has far reaching consequences for models of stellar and galaxy evolution. Synoptic radio surveys, unaffected by dust obscuration, offer a means to reveal the radio afterglows of the core collapse supernovae population (type II, Ib and Ic) (Gal-Yam et al. 2006). Furthermore, Soderberg et al. (2010) and Margutti et al. (2013) have confirmed that the nearby, subluminous class of GRBs may generate relativistic ejecta yet lack high-energy emission, implying an additional population of energetic radio afterglows detectable in radio surveys, occupying the gap in energy and ejecta velocity between supernovae and GRBs (Figure 8).' Conversely, deep follow-up observations of type Ia supernovae suggest that population does not produce bright radio afterglows, likely reflecting the distinct environment of such events. As Figure 6 shows, VLASS will probe sufficient volume to rigorously constrain the rate of core collapse radio supernovae in the local universe.

Orphan Afterglows of Gamma-Ray Bursts: Long duration GRBs are a sub-class of type Ibc supernovae that produce a highly relativistic, collimated outflow powered by a central engine, thought to be an accreting black hole or neutron star. As might be inferred by their name, GRBs are pre-

dominantly discovered by space-based wide-field gamma-ray observatories. Detailed follow-up of exemplar candidates is carried out from X-ray to radio wavelengths, with radio observations, once again, key to establishing calorimetry of the explosion. Due to the highly collimated nature of the emission at gamma-ray wavelengths, only those bursts that are collimated in the direction of Earth are detected. Best estimates suggest this corresponds to a small fraction of the true GRB event rate, dependent on the typical opening angle of the collimated jet, with very poor constraints on the latter. The late time radio afterglow of such events, on the other hand, is largely symmetric, providing a means to directly constrain the true rate of GRBs (Cenko et al. 2013). Detection of a population of such "orphan afterglows" would provide an observational measure of the beaming fraction of GRBs. Indeed, given the current degree of uncertainty, even upper limits on this value would be a powerful constraint on models. In assessing the potential impact of VLASS is broaching this problem, we note that a very large degree of uncertainty in the true rate precludes a meaningful prediction, although we include an estimate for the expected rate based on the recent work of Ghirlanda et al. (2014) in Figure 6.

Binary Neutron Star Merger Events: Advanced LIGO (aLIGO) and Advanced Virgo (AdV) are scheduled to commence collecting data in 2015 and are expected to eventually yield the first direct observations of gravitational waves. The network will not be at full design sensitivity in 2015, but will grow in capacity over subsequent science runs (2016-2019) as detectors improve and with the eventual installation of a LIGO detector in India $\sim$ 2020 (LIGO Scientific Collaboration 2013).

One of the most difficult challenges in the wake of a gravitational wave detection will be detection of a corresponding electromagnetic counterpart, the 'smoking gun' that will confirm the gravitational wave detection, localize the source to a small enough region to be able to identify the host galaxy (e.g., Fong et al. 2013) and deliver diagnostic information to maximize the science delivered. With two gravitational-wave detectors, sources will be localized to regions of hundreds to thousands of deg^2; three detectors can potentially restrict the source to sky regions several tens of deg^2 in area.

Compact binary coalescences, particularly the inspiral of binary neutron star (BNS) systems, are expected to be the most common source for detection and also the most promising to yield a corresponding electromagnetic counterpart. For reasons similar to those discussed above for GRB orphan afterglows, the rate of BNS mergers is very poorly constrained ($10^{-8} - 10^{-5}$ Mpc^{-3} yr^{-1}), and, consequently, so is the predicted gravitational wave detection rate for eLIGO and AdV. Information gleaned from conventional astronomy thus far has been limited. BNS mergers are thought to be the likely progenitor of short gamma ray bursts (S-GRBs), but only a small fraction of such events are detected in gamma rays due to the narrow beaming of the emission (Fong et al. 2012). The fraction of S-GRBs that are not detected due to this narrow beaming is also poorly constrained. It is likely to be large however ($10^2 - 10^3$), as no S-GRB within range of aLIGO and AdV has been detected during the nine year Swift mission. It is clear that an unbeamed electromagnetic signature is required, both to 1) determine the true rate of BNS merger events to allow well defined predictions for the aLIGO and AdV era and 2) to provide a reliable means to unambiguously identify and localize a counterpart to a GW event.

The radio emission produced by the mildly relativistic outflows interacting with the surrounding medium in the wake of a BNS merger has recently been highlighted as one of the most promising means to detect such events (Nakar & Piran 2011). This radio afterglow would be produced in the weeks following the merger, peaking at $\sim$1.4 GHz. The false positive rate at 1.4 GHz has been shown to be extremely low (Frail et al. 2012; Mooley et al. 2013) and, in any case, the radio spectrum and characteristic timescale of a BNS merger afterglow is unlike that associated with possible contaminant events, such as radio supernovae afterglows. This is in contrast to the optical sky where counterparts to BNS mergers may be overwhelmed by false positives at the required depth of 22nd-23rd magnitude (Nissanke et al. 2013). We note that the expected luminosity and timescale of evolution for such an afterglow is strongly dependent on the density of

the surrounding circumbinary medium and thus the radio emission can provide a key probe of the environments of the associated progenitor BNS. Coordinated searches for radio afterglows, together with the faint optical/IR afterglow, dubbed a kilonova (Tanvir et al. 2014; Berger et al. 2014), may prove to be the most discerning means to conclusively localize these events.

VLASS will play a two-fold role in the search for such merger events, 1) determining or strongly constraining the true rate of merger events through identification of an unbeamed radio afterglow population (Figure 6) and 2) delivering reference image data on a large fraction of the sky with sufficient depth to allow constraining follow-up observations of potential GW events out to the aLIGO/AdV horizon (200 Mpc).

4.3.2 Black Hole Accretion

Active Galactic Nuclei: Intrinsic variability in the synchrotron emission from AGN invariably signals modification of accretion activity resulting in shocks in the associated jets. VLASS will probe this activity in an enormous population of AGN with unprecedented detail. Indeed, the survey will also likely offer a window into the earliest formation of AGN jets, as demonstrated by Mooley et al. (2014). Aside from intrinsic variability, those AGN of size ~ 1 mas or smaller will be subject to scintillation, which in turn informs on the density inhomogeneities in the ISM. The results from a recent VLA transient survey confirm that AGN variability on all timescales from days to decades, both due to intrinsic and propagation effects, dominates the extragalactic radio transient and variable population. Indeed, analogous to the foreground fog of M dwarf flares that contaminate transient searching in optical bands, AGN activity may likely constitute a background haze that must be carefully separated from other classes of transients. In this regard, the resolution offered by VLASS is a **critical** advantage in distinguishing radio populations of extragalactic explosive transients (SNe, GRBs, NS-NS mergers) from AGN activity.

Tidal Disruption Events: The detection of a transient associated with the otherwise dormant supermassive black hole at the center of a normal galaxy at $z = 0.354$ has revealed a new class of radio transient in the nucleus of normal galaxies. Initially detected as a hard X-ray transient, Swift J1644+57 (Burrows et al. 2011), subsequent follow-up observations revealed a bright, compact self-absorbed radio counterpart (Zauderer et al. 2011). This event has been attributed to tidal disruption of a star as it passed close to the supermassive nuclear black hole of the associated galaxy (Bloom et al 2011), providing a new means to probe the mass and spin of quiescent nuclear black holes. Whereas the X-ray emission from Swift J1644+57 was strongly beamed, the radio emitting region is mildly relativistic and therefore not narrowly beamed, indicating that blind radio searches may be a fruitful means to unearthing such tidal disruption events (TDEs). However, the population detected thus far is small (e.g., see Cenko et al. 2012 and Bower et al. 2013) and, once again, the inverse beaming fraction is poorly constrained and the true extent of the radio population can only be revealed by synoptic radio surveys such as VLASS.

4.3.3 Galactic Radio Transients

Galactic radio transients ($\sim 1\,s$ time scales) constitute an entirely distinct population to extragalactic radio transients, in terms of luminosity, progenitor population and time scale, some of which are preferentially clustered on the Galactic plane and some of which are effectively isotropic on the sky (e.g., flare stars and brown dwarfs). The potential inclusion of commensal observing with the VLITE/LOBO system (< 500 MHz) is particularly advantageous in the search for Galactic transients, as there are known populations of transient sources previously detected in blinds surveys at 330 MHz.

X-ray Binaries: At present the known black hole X-ray binary population in the Galactic field (outside of globular clusters) numbers a few dozen, which were detected exclusively during rare

X-ray outbursts. Deep radio observations provide a more unbiased method of discovering such systems. Although theoretical calculations for the total number of such systems expected in the Galaxy are poorly constrained, typical estimates of 10^4 quiescent black hole X-ray binaries would imply that we might expect to detect of order 5 such systems in the Galactic tier of VLASS, identified by their flat radio spectra, and their high radio/X-ray ratios. The Galactic tier will also detect many of the known persistent radio-emitting X-ray binaries, both black hole candidates and the high-luminosity Z-source neutron star systems. Finally, there is the possibility of detecting an outburst of either a neutron star or black hole X-ray binary, for comparison with X-ray monitoring data.

4.3.4 Novae

Approximately 35 Galactic novae explode each year, with about half of them occurring in the Galactic bulge (Darnley et al. 2006). However, most novae are detected in the optical, and due to the effects of dust and optical incompleteness, we usually only detect about a quarter of these, dramatically biasing our understanding of these most common explosions. With a radio survey of the Galaxy, we will carry out the first well-defined and complete survey for classical novae, with easily quantifiable selection effects that depend only on distance, ejecta mass, and ejecta velocity. With a 5-sigma sensitivity limit of 250 muJy/beam (Galactic tier of VLASS), we will be able to detect classical novae to the Galactic center (based on the light curve of the normal nova V959 Mon; Chomiuk et al. 2014, in preparation). Novae usually remain bright at radio bands for 2 years, implying that we will be able to observe them varying across multiple VLASS epochs (assuming spacing of 18 months). We therefore expect a yield of ¿ 100 classical novae over VLASS duration, increasing the number of radio-detected novae 5 fold, measuring the distribution of ejected mass and energetics (Roy et al. 2012) and enabling the most thorough test to date of the theory of nova explosions (Yaron et al. 2005).

Stellar Flares and Coronal Mass Ejections: Many classes of stars produce flares that are several orders of magnitude more luminous and frequent than any produced on the Sun, including young stellar objects, active M dwarfs and certain classes of tight binaries (eg. RS CVn systems). Such activity dominates the star's output over much of the electromagnetic spectrum, governs its angular momentum evolution and can also have a profound impact on the planetary systems orbiting such stars. In the latter case, higher X-ray and ultraviolet irradiation can lead to heating of the upper planetary atmosphere, resulting in photochemical reactions leading to significant atmospheric loss. In particular, studies of terrestrial planets in the habitable zone of M dwarfs, possibly the most abundant Earth-like planets in the solar neighborhood (Dressing et al. 2013), suggest that large flares and coronal mass ejections (CMEs) may potentially lead to catastrophic loss of the atmosphere of such planets (Khodachenko et al 2007; Lammer et al. 2007).

Radio bursts are a powerful means to detect and characterize flares and CMEs on the Sun and studies of radio bursts from nearby active stars can be similarly used to probe the local environment of impulsive flare and CME events with the potential for groundbreaking insight into the bulk motion of plasma in stellar coronae. Extremely bright bursts up to 1 Jy (Lovell et al. 1963) have been detected for decades from nearby M dwarfs, at luminosities that are up to 5 orders of magnitude more intense than any equivalent solar bursts. In more recent years, dynamic spectroscopy of stellar radio bursts has been carried out using the Very Large Array (VLA), Effelsberg, Jodrell Bank and Arecibo radio observatories(Osten & Bastian 2006 and references therein). In the case of the detected stellar radio bursts, the luminosities are orders of magnitude brighter than anything detected from the Sun, highlighting that the coronae possessed by active stars are very different to the solar corona. The radio emission properties clearly indicate coherent processes, probably associated with plasma radiation or electron cyclotron maser emission, the former providing direct measurement of plasma densities and the latter direct measurement of magnetic field strengths, while broadband dynamic spectra of bursts provide information of the size and extent

of the associated stellar coronae. Studying the coronae of such active stars provides a laboratory to investigate physical regimes unavailable with spatially detailed studies of our low-activity Sun. Furthermore, such bursts potentially provide direct insight on the density, velocity and energetics of mass ejection from stellar coronae and the associated impact on planetary atmospheres.

Active stars also produce large incoherent flares (Osten et al 2005), due to gyrosynchrotron radiation associated with the same nature of magnetic reconnection events that produce bright coherent bursts. Insufficient data exists on the relationship between the incoherent and coherent flare emission, but this can be probed by VLASS and VLITE/LOBO with the former probing the higher frequency incoherent emission and the latter probing the coherent emission more frequently confined to lower frequencies. The degree of circular polarization is often a good distinguishing characteristic between the incoherent and coherent emission. The measured rate of flares from active stars in previous surveys (Mooley et al. 2014) suggests that flares from M dwarfs in particular will prove to be one of the most frequent transient events detected by VLASS, with potentially 100s of events recovered in the All-sky and Wide tiers of the survey (Figure 7).

Substellar Auroral Emissions: A dozen or so low mass stars and brown dwarfs have been found to be radio sources in the last decade (Antonova et al. 2013 and references therein). A subset of these objects have been the subject of lengthy follow-up campaigns that have revealed the presence of 100% circularly polarized, periodic pulses, with the pulse period typically 2-3 hours and consistent with rotation (Hallinan et al. 2007, 2008; Berger 2009). This radio emission is thought to be electron cyclotron emission produced at the electron cyclotron frequency, in the same fashion as that detected from the auroral regions of the magnetized planets in our solar system. As is the case for such planets, it enables very accurate measurement of magnetic field strengths and rotation periods and has led to the confirmation of kilogauss magnetic fields in large-scale configurations for ultracool dwarfs. Indeed, radio observations have been the only method thus far capable of direct magnetic field measurements for L dwarfs; Zeeman broadening measurements are inhibited by the difficulty in obtaining high resolution spectra of these cool, dim objects (Reiners & Basri 2007).

Most recently Route & Wolszczan (2012) found the coolest radio brown dwarf yet detected, with the detection of radio pulses from the 900K T6.5 dwarf, 2MASS J10475385+2124234. Individual pulses were detected from this object in multiple short duration observations with the Arecibo observatory, resulting in a confirmed magnetic field strength of at least 1.7 kG near the surface of this extremely cool object. This significant discovery highlights the unparalleled diagnostic potential of radio observations of brown dwarfs, and their importance in constraining dynamo theory in the mass gap between planets and stars. VLASS will be the first survey with the depth to blindly detect brown dwarfs in both quiescence and outburst. The detection of late L, T and Y dwarfs would be of particular significance for ongoing empirical measurements of magnetic fields in this regime.

Galactic Center Radio Transients: Blind surveys of the Galactic Center region with the VLA have been used to search for radio transients with a considerable degree of success [Hyman et al. 2002, 2005, 2009), see Figure 9]. Most notably, a blind search program using the Very Large Array (VLA) at 330 MHz (90 cm) identified a mysterious, bright, pulsing source towards the Galactic Center inconsistent with any known class of radio source, labeled GCRT J1745-3009 (Hyman et al. 2005). 100% circularly polarized 1 Jy bursts of duration ten minutes each, reoccurring with period of 77 minutes, were detected in a 7 hours of VLA data taken in September 2002. In multiple follow-up observations, the transient was detected in two more epochs of observations with the Giant Metre-Wave Radio Telescope (GMRT) in 2003 and 2004, with flux levels greatly reduced relative to the original detection. At the last known epoch of emission detected in 2004, the source exhibited an unusually steep spectrum with $\alpha = -13 \pm 3$ ($S(\nu) \propto \nu^{\alpha}$). Very high circular polarization has also been reported. GCRT J1745-3009 may be as close as 180 pc to the Galactic Center but limits on distance, and thus brightness temperature, are otherwise weak. For distances d $<$ 70 pc from the Earth, the radio flux density constrains its brightness temperature to exceed the limit for in-

coherent synchrotron radiation thus requiring a coherent emission mechanism. The high circular polarization, spectral characteristics and intrinsic beaming of the emission support the assertion of coherent radio emission for this new class of radio source, christened "burper" (Kulkarni & Phinney 2005). We note that the 100% circularly polarized nature of the bursts from GCRT J1745-3009 favors parallel searches for transients in Stokes V where the galactic contribution will be reduced by many orders of magnitude relative to unpolarized Stokes I images.

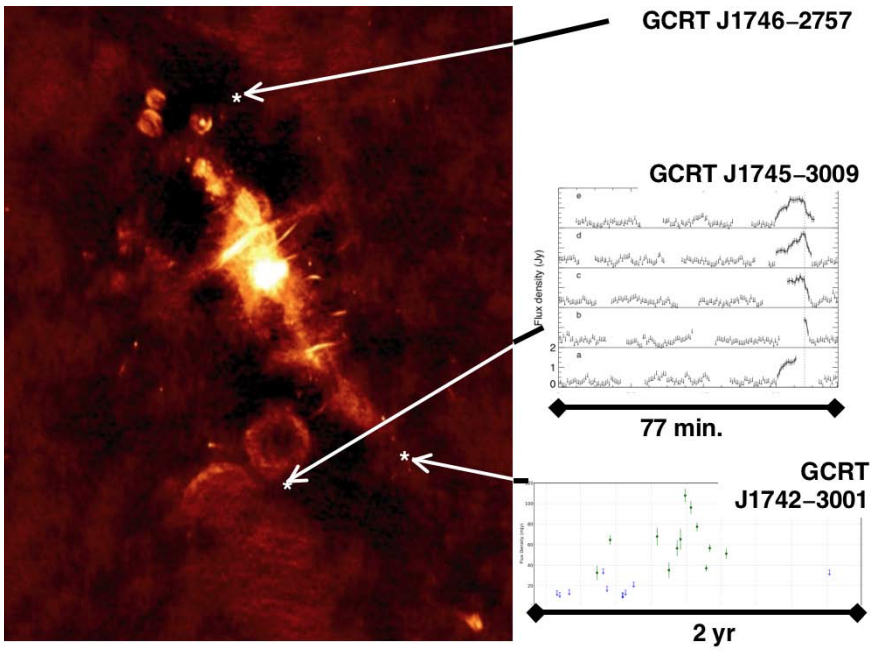

Figure 9: The diversity of the light curves for transients toward the Galactic center (Hyman et al. 2002,2005,2009]. The transient GCRT J1745-3009 burst several times (duration ∼10 minutes) during a 6-hr observation, with subsequent bursts detected over the next 1.5 yr; GCRT J1742-3001 brightened and faded over several months, preceded 6 months earlier by intermittent bursts; and GCRT J1746-2757 was detected in only a single epoch. None of these objects has been identified nor has a multi-wavelength counterpart been found. The background image is the Galactic center at 330 MHz. Figure taken from Lazio et al. (2009).

No counterpart was identified in observations at other wavelengths, largely due to the poor localization of the position of the transient in radio data. It remains unclear whether GCRT J1745-3009 is intrinsically close to the Galactic Center or rather simply lies in the direction of the Galactic Center; the latter case being feasible due to the biased nature of the survey, for which blind searches for transients were restricted to the Galactic Center. Proposed counterparts include a nulling pulsar, a double pulsar, a transient white dwarf pulsar, a precessing radio pulsar or a nearby pulsing brown dwarf or low mass flare star.

A second Galactic Center radio transient source (GCRT J1742-3001) was detected in multiple epochs of a 235 MHz transient monitoring program with the GMRT in 2006 and 2007 (Hyman et al. 2009). This was a very different class of radio transient, observed to brighten over a period of a month to a maximum of 100 mJy before fading in the subsequent 6 months. Once again, a very steep spectrum ($\alpha = -2$) was inferred. Discovering the frequency, nature and progenitors of these new classes of radio transients will open up new population of exotic objects to astrophysical study with the possibility of such transients being due to previously undetected populations of neutron stars being a particularly exciting possibility. The detection of two new classes of

transient in very limited blind searches towards the Galactic Center speaks to the huge potential for discovery associated with monitoring this region of the sky. VLASS will easily probe much deeper than any previous Galactic Center transient surveys. In particular, considering the steep negative spectrum confirmed for GCRT J1745-3009 and GCRT J1742-3001, the possible inclusion of VLITE/LOBO will be key to probing these particular populations as results from previous surveys suggest that the rate of detected transients would be ~ 0.2/hr with the upgraded VLA (Hyman et al. 2009).

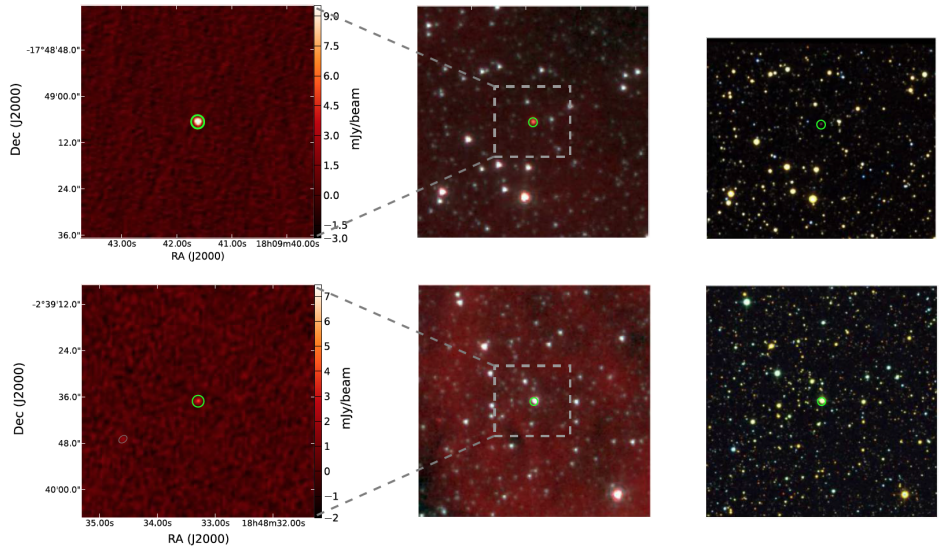

FIG. 4.—Example data from the CORNISH survey alongside three-color images from the *Spitzer* GLIMPSE (3.6, 4.5, and 8.0 μm) and UKIDSS (JHK) surveys. *Top*: A typical cometary H II region, G032.1502 + 00.1329. Notice the good correspondence between the radio emission and the brightest 8 μm emission in the GLIMPSE image. There is also strong extinction ahead of the cometary as expected if the OB star formed in a density gradient. *Middle*: A candidate PN that was previously unknown, G012.3830 + 00.7990. It is clearly seen as an isolated source at 8 μm with a very faint counterpart in the near-IR. In the longer wavelength *Spitzer* MIPSGAL data (not shown here) it is bright at 24 μm but fainter at 70 μm unlike H II regions that are brighter at 70 μm. *Bottom*: A previously unknown radio star, G030.2357 − 00.5719, that has blue colors in the near- and mid-IR. See the electronic edition of the *PASP* for a color version of this figure.

Figure 10: Figure 4 from Hoare et al. showing example data from the CORNISH survey of the Galactic Plane at 5 GHz. The top row displays a previously unknown planetary nebula candidate detected at radio wavelengths (left column) with a Spitzer image (middle column) and near-IR (JHK) image at right. The bottom row shows a previously unknown radio star in the same three wavelength bands.

4.4 Galactic Science

Galactic science covers a diversity of topics which collectively span the life cycle from stellar birth to death. Radio astronomical observations contribute to fundamental questions of how stars work and how they interact with their environments: understanding the mass-energy-chemical cycle in the Milky Way, and by extension, other galaxies; probing processes of star formation; examining the influence of rotation and magnetic fields on non-degenerate stars; nailing down the progenitors of type Ia supernovae; constraining the end lives of massive stars; and studying what controls the parameters of compact stellar remnants. A sensitive radio survey can contribute to all of these topics by detecting point-like sources for further radio and multi-wavelength characterization. We discuss the diversity of Galactic topics and the value of such radio measurements, divided in two broad categories of (1) learning about the physics of the stars themselves, and (2) the interaction of stars with the material around them over the course of their lives.

4.4.1 The Physics of Stars

The radio HR diagram shown in Figure 12 illustrates the centrality of radio emission to many types of stars and at a number of locations on and off the main sequence. Through thermal or non-thermal continuum emission, different physical processes can be probed that are important to a better understanding of how stars work.

Thermal emission from stellar winds exhibits a rising spectrum, with $F_\nu \propto \nu^\alpha$, with $\alpha \sim 0.6$ for free-free emission from an ionized wind. For massive stars, this wind emission is formed further out in the wind than other diagnostics like Hα or X-ray emission, so has different sensitivities to wind clumping and porosity. While the overall effect of this mass loss from hot stars is also important to a better understanding of how this matter interacts with its environment, the radio wind emission diagnostic is important to a detailed investigation of the wind flows of individual stars, particularly for comparison with measurements at other wavelengths. However, there are fewer radio-detected massive stars than the total number known: Rubin et al. (1962 AJ 67, 491) catalogued $\sim$ 1300 O-B5 stars within 3 kpc of the Sun within $\pm 5^\circ$ in Galactic latitude. There are only about 65 O-B2 stars with radio detections (Benaglia et al. 2009), and $\approx$70% of these show thermal emission. So there is a large potential for increasing the number of radio-detected hot thermal wind sources.

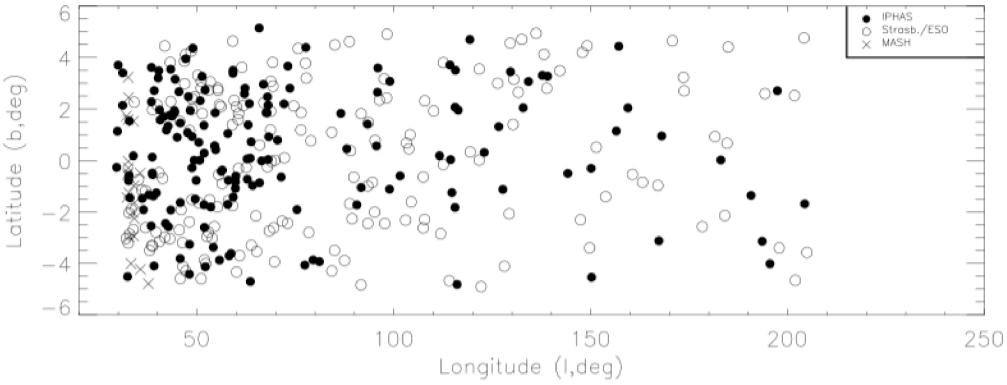

Figure 11: The distribution of detected planetary nebulae as a function of Galactic longitude and latitude, from Sabin et al. (2014). VLASS will easily expand on this by extending the longitude ranges probed in detail, and covering the Galactic bulge (which is not shown in this figure).

The thermal radio emission seen in young stellar objects originates in an inflow (accretion) or outflow (ionized winds or jets), giving crucial insights into these important processes. Since the thermal radio emission can originate from YSOs in evolutionary stages that run the gamut from objects deeply embeded in their natal cloud to fully formed stars, the radio emission effectively diagnoses the earliest stages at which these processes start, and contributes to understanding the relative importance of these effects during the initial life of the star.

The outflows associated with accreting white dwarf systems (novae, symbiotic systems) produce thermal radio emission, but radio emission has not traditionally been the vehicle for detecting these objects. A sensitive radio survey can identify additional candidates in these two classes; radio measurements are key to constraining the ejected mass and thus the characteristics of the explosion and the evolution of the white dwarf. Approximately 35 Galactic novae explode each year, with about half of them occurring in the Galactic bulge (Darnley et al. 2006). However, most novae are detected in the optical, and due to the effects of dust and optical incompleteness, usually only about a quarter of the total number are detected, dramatically biasing our understanding of these most common explosions. The number of Galactic symbiotic stars (red giant + accreting

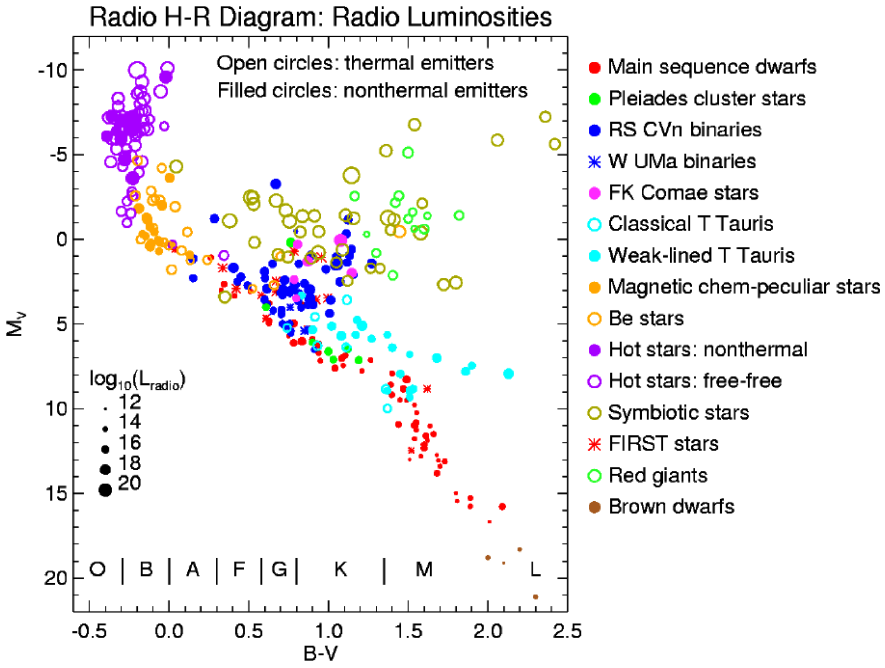

Figure 12: Radio HR diagram for stars, illustrating radio emission as a powerful probe of all phases of stellar evolution. Figure taken from White 1998 (NRAO Workshop Number 27) and updated based on recent discoveries. From thermal emission from massive star winds, to coherent emission from accelerated particles in the lowest mass stellar objects, practically all stellar types along the main sequence exhibit detectable levels of radio emission, and many important phases of post-main sequence stellar evolution also produce radio emission that can be used to study their structure and interaction with their environments.

white dwarf) is uncertain to two orders of magnitude (Munari & Renzini 1992, Lu et al. 2006), because these systems are time-variable and sometimes undergo long quiescent periods of several hundred days where traditional diagnostics (e.g., optical emission lines) disappear. The radio emission originates from the portion of the red giant stellar wind photoionized by the compact object. Symbiotic stars have long been suggested as Type Ia supernova (SN Ia) progenitor candidates, and have undergone a recent renaissance with the detection of several SNe Ia apparently surrounded by dense stellar envelopes (Patat et al. 2007, Dilday et al. 2012).

Nonthermal radio emission details the action of accelerated particles to stars, important for a better understanding of the physics of jets and influence of magnetic fields on the star. Many classes of stars and compact objects display nonthermal radio emission, illustrating the broad applicability that a radio survey tuned to point sources can have in elucidating the physics of these stellar objects. While most hot stars exhibiting detectable levels of radio emission are thermal sources, $\approx$30% are nonthermal, with $\alpha \lesssim 0$; the nonthermal emission is interpreted to be synchrotron emission from colliding winds of a massive star binary (Benaglia et al. 2009 astro-ph 0904.0533). There is no concensus about formation mechanisms to produce nonthermal radio emission from single OB stars. Recent results indicate that magnetic fields play a heretofore unrealized role in channeling wind emission (Wade et al. 2012 arXiv:1206.5163), with 6.5% of O and B stars surveyed exhibiting evidence of magnetic fields in their optical spectra. The radio emission from nearby active stars provides a unique probe of accelerated particles and magnetic fields that occur in them, which is useful for a broader understanding of dynamo processes in stars, as well as the particle environment around those stars. The stellar byproduct of exoplanet transit probes like Kepler and

TESS will yield information on key stellar parameters like rotation, white-light flaring, and asteroseismic constraints on stellar ages. These parameters can be used together to advance some of the fundamental questions ("How do rotation and magnetic fields affect stars?").

Radio and X-ray measurements of stellar mass black holes in a variety of states reveal a power-law relationship ($L_R \propto L_X^{0.6}$) between these emissions (Jones et al. 2011), illustrating the fundamental coupling between accretion processes (revealed by the X-ray emission) and the presence and action of a jet (probed by radio emission). At the present time the field (i.e. non-globular cluster) population of stellar mass black holes consists entirely of objects selected from X-ray outbursts, and contains only about 20 objects. The *known* stellar mass black holes have duty cycles in outburst that are typically less than a few percent, and many have not yet been seen to recur, suggesting a large reservoir of such objects.

4.4.2 The Interplay of Stars with Their Surroundings

The mass loss, ejecta, and inflows between stars and their environments mean that there is an active feedback between the stars and their surroundings. This impact is ideally probed at radio wavelengths through different phases of stellar evolution and throughout the Galaxy where extinction at many other wavelengths is typically a problem. Here we discuss the interplay of stars and their surroundings as a function of their evolutionary stage - from the impact of star formation on the surrounding medium to the expansion of the star's layers into the surrounding medium (i.e., planetary nebulae, supernova remnants).

The earliest stages of star formation in our Galaxy are well traced by the radio as these young stellar objects are still enshrouded by their natal material. Two types of compact radio sources characterize this early phase of star formation for stars of mass greater than 8 solar masses: (1) the earliest phase of radio "quiet" sources that are very bright in the mid and far infrared are known as massive young stellar objects (MYSOs) and may have lower levels of radio emission associated with inflow (accretion) or outflow (ionized winds or jets) onto the stellar disk; (2) the subsequent phase of radio "loud" ultracompact HII regions, which result when the star begins to ionize its surroundings (see Hoare et al. (2012) and references within). These two types of sources have different spectral energy distributions in the radio wavelength regime, therefore allowing multi-wavelength surveys to distinguish beteween them. Recent work by the CORNISH survey team (Hoare et al. 2012; VLA 5 GHz survey of the Galactic plane between 10 and 65 degrees longitude and +/1 1 degree in latitude) and other groups have suggested that large, unbaised radio and infrared surveys with matched resolution will allow these sources to be correctly identified with their stage of early star formation and therby begin to quantify what fraction of sources are in each stage. The CORNISH survey has paved the way for high resolution radio surveys that can match the increasingly higher resolution infrared surveys (such as GLIMPSE, MIPS-GAL), yet its coverage of the Galactic plane is not complete. Figure 10 shows an example from Hoare et al. (2012) of the kind of compact radio and infrared source characterization that can be accomplished with matched resolution. In the figure, identification of a previously unknown radio star and planetary nebula have been made.

Once massive stars reach the main sequence, they are important to study becuase of the impact of their considerable mass and energy input into the ISM and its effect on the life cycle of matter. Radio free-free observations trace the ionized wind, and are formed further out in the wind than other diagnostics like Hα or X-ray emission, so have different sensitivities to wind clumping and porosity. Rubin et al. (1962 AJ 67, 491) catalogued $\sim$ 1300 O-B5 stars within 3 kpc of the Sun within $\pm 5^\circ$. There are only about 65 O-B2 stars with radio detections (Benaglia et al. 2009), and $\approx$70% of these show thermal emission. So there is a large potential for increasing the number of radio-detected hot thermal wind sources, which will in turn help to assess the mechanical energy input into the ISM near regions of massive star formation.

At the end of a lower mass star's life, its *planetary nebula* phase represents the expansion of

its stellar layers into the interstellar medium. This ionized material emits free-free radio emission along with many optical spectral lines (Acker et al. 1992). In addition to their use as a tracer of the timescales for mass loss and stellar evolutionary processes, planetary nebulae are one of the best tracers of Galactic stellar and chemical evolution. These sources can be difficult to find optically (from optical emission lines) in the plane of our Galaxy. However, the radio emission from planetary nebulae is well understood and present in sources throughout the Galactic plane. The Strasbourg catalog, which seems to be the best one out there, is not well-selected; it preferentially selects compact and nearby objects. Population synthesis models predict a range of expected Galactic planetary nebulae (Sabin et al. 2014) yet the total number of known nebulae is far lower than even the most conservative expectations. Figure 11 illustrates the distribution of planetary nebulae from the Strasborg and follow-on optical catalogs and the need for even broader coverage in the sky.

Finally, the end stages of a massive star result in a violent and energetic outburst known as a supernova explosion. *The resulting supernova remnants are strong emitters of non-thermal radio emission* and exist in a vareity of shapes and sizes (need reference here). A number of these evolved systems represent the most extended and brightest radio sources in the sky. Radio images of supernova can reveal important diagnostics about the lifetime of this phase, the energy input into the interstellar medium and the tremendous wake that they produce. Currently missing from a census of supernova remants in the Galaxy are those with small angular diameters, which have traditionally been difficult to pick out in low-resolution radio surveys of our Galaxy (Green 2009), but yet can reveal important characteristics about the earliest phase of the expansion and energy input. The $\sim$1 arcmin-scale G1.9+0.3 was recently recognized as the youngest SNR in our Milky Way, just over 100 year old (Reynolds et al. 2008, Borkowski et al. 2010).

4.4.3 Searching for Exotic Radio Pulsars

Neutron stars born in supernova explosions are extraordinary laboratories for extreme astrophysics and general relativity. An imaging survey can identify candidate radio pulsars as compact sources, and has advantages over typical time domain pulsar surveys: angular scatter broadening is a much smaller concern than the equivalent pulse scatter broadening in the time domain, and imaging surveys are immune to the effects of acceleration in compact binary systems. The notion of using an imaging survey as a finding survey for a follow-up periodicity search has been demonstrated spectacularly, for example, with radio follow-up of unidentified Fermi sources (e.g., Ray et al. 2012).

Extreme double neutron-star (DNS) binaries must exist down to periods as short as 10 minutes owing to gravitational radiation. The double pulsar ($P_{orb} = 2.4$ hr; Lyne et al. 2004) requires post-Newtonian order 1.5 for its orbital description and has provided tests of GR to 0.05% (Kramer et al. 2006). More compact binaries will test general relativity to higher order and, with suitable geometries, will provide strong gravity tests from lensing. DNS binaries also provide better calibration of the event rate for LIGO.

Millisecond pulsars (MSPs) with especially high spin stability are being employed in pulsar timing arrays for gravitational wave detection. Standard periodicity surveys using single-dish telescopes will miss some MSPs, including some of the most interesting ones, because binary motion will not be mitigated by acceleration searches in the more extreme cases. Further, our current understanding of the equation of state of nuclear matter allows MSP spin periods as short as 0.5 ms. However, the fastest known MSP has a period of 1.4 ms (Hessels et al. 2006). Periodicity surveys suffer from selection effects (orbital motion and plasma scattering in the ISM) that are strongest for the shortest-period pulsars. A VLA finding survey may find sub-ms MSP candidates that can be identified as such in follow-up periodicity surveys. If these objects do not exist, then the combined hybrid approach will provide very important constraints on the evolution and physics of accretion-driven spin-up.

Neutron star–Black hole binary systems are not known yet, but they should exist on basic binary evolutionary grounds. The detection of a single NS-BH binary will be of profound importance because timing measurements will probe space-time around a black hole to much higher precision than any other technique.

Finally, *electron-density and magnetic field models for the Milky Way* will be calibrated and improved by column density and scattering measurements from confirmation observations of new pulsar discoveries in the Galactic plane and bulge.

4.5 A Lasting Legacy into the SKA Era

VLASS will not only deliver unprecedented science as described above, but will also build a lasting legacy well into the SKA era by consciously being designed to highlight the capabilities of the VLA that will remain state for the art well into $>>$2020. Specifically, the survey capitalizes on the exquisite point source sensitivity and high angular resolution that will not be superseded until SKA_1-MID begins operating in the Karoo. For comparison, MeerKAT/MIGHTEE will be able to detect the same sources as we would with the VLA in the DEEP tier, however it will be unable to characterize these sources from a radio perspective or unambiguously associate them with an optical/near-infrared counterpart. This is because the source density at these depths is $\sim$20,000 per deg^2 for the MIGHTEE-Tier2 survey, and the MeerKAT beam is approaching the confusion limit of $\sim$30 beams per source. Another crucial advantage that the VLA has over MeerKAT is its ability to resolve typical star-forming galaxies (and AGN) at all redshifts – MeerKAT will never be able to do this. This is a unique science case that will not be superseded until the SKA_1 is fully operational with $>$100 km baselines. Consequently, the first generation SKA_1 reference surveys, which are now being designed and will soon be proposed for, are currently being benchmarked against the deep imaging component of VLASS (Prandoni et al. 2014).

In addition to delivering deep, high-resolution imaging, the WIDAR correlator has opened a major new window for spectral index and wideband polarization work, enabling the characterization of the magneto-ionic medium in AGNs and in galaxies across a wide range of redshifts. The polarization for MeerKAT L-band surveys will be much more difficult than in the S-band, where depolarization will be lower. A deep S-band survey over the same fields as the MeerKAT deep survey will provide 3 GHz of frequency baseline to increase the signal-to-noise on polarization and rotation measure synthesis, opening up new and exciting science that combines the strengths of the VLA and MeerKAT, rather than setting them up to compete. For AGN science, the requirement to morphologically distinguish different types of AGN (e.g., FRI and FRII) from star-forming galaxies and the need for reliable cross-IDs is again the driver for doing this survey with the VLA rather than MeerKAT. However, the synergies between these two facilities and should be capitalized on. For example, MIGHTEE will provide accurate total flux densities and luminosities for extended AGN, whilst also providing a longer baseline for spectral index measurement that can be used to infer the physical state of the AGN and the environment in which is resides. Thus, not only will the deep, high resolution imaging from VLASS remain state of the art well into $>>$2020, the synergy of these observations (in frequency and resolution) with those of the SKA pathfinders coming online over the next $\sim$5 yr will ultimately enable even more new science than that which is discussed below.

From the point of view of the dynamic radio sky, the VLASS will also a unique snapshot of the Universe some 20 years after the FIRST survey, and leading up to the advent of the SKA pathfinders and SKA itself. Current large-area radio transient detection surveys, such as the recent Stripe82 survey of Mooley et al. (2014), successfully utilized the "Epoch 0" provided from FIRST as well as other historical VLA-based surveys, as a starting point for identification of newly appearing objects from the first new Jansky VLA epochs. As the JVLA surveys go deeper, the utility of FIRST and other earlier shallow surveys will decrease. The VLASS — with its depth, area, and angular resolution — will provide a new launching point for future surveys, taking us into the SKA and

LSST eras. This will be the case across the breadth of transient and variability studies touched upon in § transsci above, and well beyond. As a case in point, we note that later this decade the Advanced LIGO and VIRGO gravitational-wave observatories (GWO) are expected to turn on, ushering in a new astronomical land rush across the electromagnetic spectrum to make the first identifications within the large ($\sim 500\mathrm{deg}^2$) error regions of the first events[9]. The pre-existence of high quality dynamic radio images over a substantial region of the sky from VLASS will provide future GWO transient hunters a critical baseline which to discern newly appearing objects from extant static and run-of-the-mill variable sources. Crucially, we note that the VLASS All-sky tier is sufficiently deep to provide an unambiguous reference map for searches for counterparts to those first events, based on the range of predicted radio flux densities (Nakar & Piran 2011) for compact object mergers out to the detection horizon for the early Advanced LIGO and VIRGO runs (LIGO Scientific Collaboration 2013).

Finally, it is certainly worth mentioning that experience shows that when telescopes enter unexplored areas of observational phase space, as will be the case with VLASS, they make unexpected discoveries. Furthermore, it has been shown that the most significant discoveries with major telescopes often end up being those that were completely unexpected. As an example, of the top ten discoveries with *HST*, only one was identified as one of the key goals used to justify telescope. So while specific science goals detailed below have focused the design of VLASS, it may not be surprising if they do not end up being its greatest scientific achievements. It will undoubtedly be the scientific imagination and curiosity of community that will ultimately drive the best science to come out of VLASS.

5 Survey Strategy

In this section we describe the tiered approach that has been decided upon, briefly summarizing the technical aspects of the survey and their relation to the science goals described in detail above. This is done for each of the *symbiotic* survey components: All Sky, Wide, Deep, and Galactic. A detailed discussion of the survey components and their implementation can be found below in § 6 and 8, respectively.

5.1 All Sky Survey

5.1.1 Context

While deep, pointed observations are crucial for understanding the details of our universe, large-area sky surveys provide the laboratories in which these experiments are conducted. The Sloan Digital Sky Survey (SDSS) and the Faint Images of the Radio Sky (FIRST) surveys provide clear examples of how sky surveys can expand our existing knowledge and drive discovery in new directions. Each new generation of surveys has greatly increased our knowledge of the cosmos and has led to the discovery of heretofore unknown phenomena. Today we are on the edge of a new age in optical surveys with the genesis of Pan-STARRS, SkyMapper, DES, VST/VISTA, and SuMIRe. Ten years from now, LSST will begin constructing the definitive large, deep optical map of the universe. These surveys will probe new realms by covering large areas of sky to depths as faint as 28th magnitude with multiple epochs allowing new time-domain discoveries. Yet without multi-wavelength support, these surveys will fail to live up to their full potential as observations that span the electromagnetic spectrum are crucial for completing the picture of most astronomical sources.

[9] http://www.ligo.org/science/GWEMalerts.php

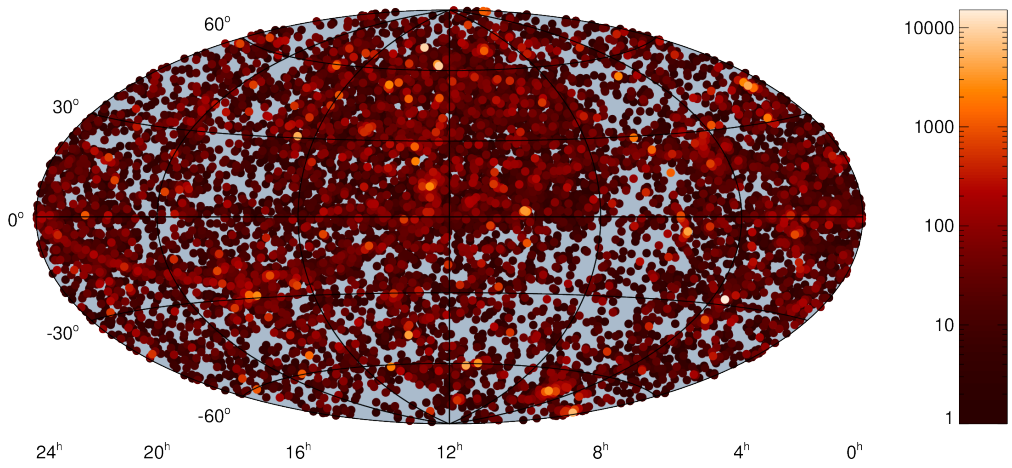

Figure 13: Distribution of Hubble observations across the sky. The color gives the number of observations in regions of approximately 2 deg^2. There are more observations in the SDSS area (roughly $0^\circ < \delta < 60^\circ$, $8^h < \alpha < 17^h$, where the WIDE tier will focus, see §5.2)), but there are also many observations outside SDSS.

It is in this light that we propose the first tier of VLASS provide a high-resolution radio reference for the entire northern sky. This tier will provide an all-sky survey at unprecedented combination of resolution and sensitivity, allowing astronomers to cross-identify interesting objects identified by both all-sky current and future photometric surveys (WISE, 2MASS, Fermi, eROSITA, WFIRST-AFTA) and by time- domain (variability, proper motion) surveys (Pan-STARRS, ZTF). With an RMS of 100 μJy beam^{-1}, it will be $\sim$3 times more sensitive than the NVSS (and roughly as sensitive as FIRST) to sources with $\nu\sim$0.7 radio spectral indices. Most importantly, the synthesized beam will have a FWHM $\sim$15 times smaller than the NVSS (more than 250 times smaller in area) and $\sim$2 times smaller than the FIRST beam, allowing radio sources to be confidently identified with optical and infrared counterparts at faint magnitudes. Such a tier for VLASS will have broad utility to the whole astronomical community.

Why all-sky? The reason to do an all-sky[10] survey is that there are astronomers doing research in every corner of that sky. If the radio sky layer is missing or incomplete, this forces astronomers to eliminate the radio domain as a factor in their study. This is reflected by a colleague's statement to Joe Lazio, who asked a few infrared astronomers what they would like from a new VLA sky survey:

> *"Make something like FIRST cover the entire sky. It is ridiculous that I type in coordinates and am told that they are out of bounds. That shouldn't happen for the extragalactic sky."*

The only reason to survey an area smaller than the entire sky is that one cannot afford the observing time to get to the required depth over the whole sky for a particular science goal - that is exactly why VLASS is designed as a tiered survey. But the wider the survey area, in general, the more the survey will benefit research in the community.

While the SDSS survey does drive a lot of science, astronomers really do study parts of the sky that are not observed by SDSS. This can be seen by looking at the distribution of Hubble Space

[10]"All-sky" for our purposes means the declination range than can be observed with reasonable uniformity by the VLA. Of course it excludes the area below the horizon. Our all-sky component includes 34,000 deg^2 north of declination -40°, which is 82% of the entire celestial sphere.

Telescope (HST) observations across the sky. HST observations are a good proxy for cutting edge science – they reflect the competitive allocation of a precious resource across a broadly representative array of science projects. Figure 13 shows that while 45% of HST observations north of declination -30° are in areas covered by FIRST (very similar to SDSS), 55% are outside the FIRST footprint. Since FIRST covers 1/3 of the sky north of -30°, that implies that the vast majority ($\sim$ 80%) of HST observations are distributed across the sky without regard to whether they are covered by SDSS. This argues strongly for an ALL-SKY tier to VLASS.

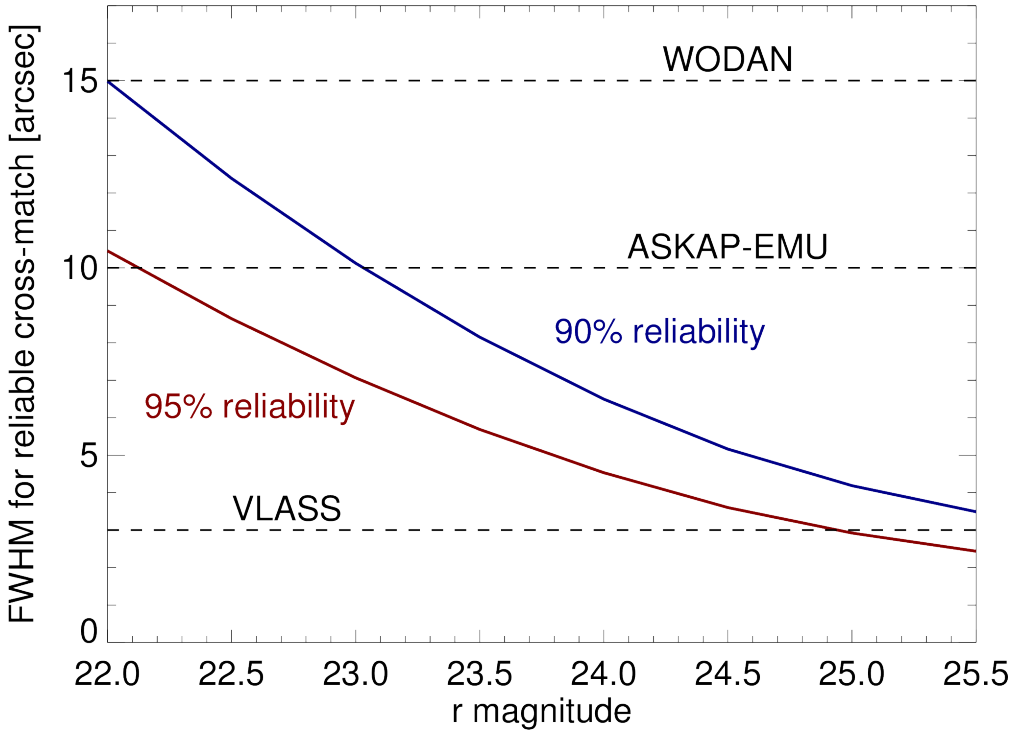

Figure 14: FWHM resolution required to achieve reliable cross-matches at fainter magnitudes using r-band galaxy counts. Two curves are shown for 90% and 95% reliable identifications, and the resolutions of VLASS, ASKAP-EMU and WODAN are shown. This confirms that the SKA pathfinders are at best marginally sufficient for identifications at SDSS/Pan-STARRS depths, while VLASS is usable all the way to $r = 25$.

Resolution and the SKA Pathfinders: While sky area is one of the two key parameters that define the value of a wide-area radio survey, the other key parameter is resolution, as this allows counterparts to be identified at other wavelengths among the dense populations of faint galaxies. Optical and infrared counterparts of even relatively bright radio sources are faint: only 33% of radio sources at the 1 mJy FIRST detection threshold have an optical counterpart bright enough to be detected in SDSS. That means potential counterparts are dense on the sky, and accurate radio positions are required to confidently associate radio and optical objects. For example, take the Pan-STARRS survey, which has now imaged the entire sky north of -30°. For Pan-STARRS, a FWHM resolution better than $7''$ is required for 95% reliability in radio-PS1 cross-matches, as demonstrated in Figure 14. That criterion is easily met by VLASS, but with resolutions of $10''$ and $15''$ respectively (FWHM), both ASKAP-EMU and WODAN fall short (Figure 14). Thus, despite their excellent flux sensitivity, the forthcoming SKA-precursor surveys will not have adequate spatial resolution for confident identifications of counterparts in Pan-STARRS.

A recurring claim is that the excellent $\sim$ 10 μJy rms flux sensitivity planned for the SKA-precursor surveys (WODAN, ASKAP-EMU) will lead to good positional accuracy for radio sources despite the relatively low resolution of those surveys. The evidence, however, suggests that this is incorrect – the positions of radio sources observed at low resolution do *not* actually converge to the optical counterpart position as the signal-to-noise increases. The wrong conclusion is reached due to simplistic assumptions about the structure of radio sources. In Appendix B we provide a detailed discussion and analysis (i.e., the "S/N model of positional accuracy") demonstrating that half of the optical counterparts to SDSS depth will be false matches using the matching radius that will be required for WODAN (e.g., see Figure 14). The false counterparts will obviously be an even problem for deeper optical surveys, such as the ongoing DES and HSC surveys and eventually for LSST. Thus the SKA-precursor surveys can not be substituted for the VLASS all-sky survey. This tier will have a long, useful, and heavily used lifetime even into the era of the SKA-precursor surveys.

5.1.2 Description

Area and Depth: The All-Sky component will cover $\approx$34,000 deg^2 north of declination -40°, which is 82% of the entire celestial sphere down to a 1σ RMS depth of 100 μJy, thus covering the entire VLA-visible sky down to FIRST depth.

Angular Resolution: The All-Sky component will be conducted in B and BnA-array, providing a uniform 2.″1 synthesized beam over the entire sky. Such high resolution is necessary for accurate positional matching with exising and forthcoming optical/NIR imaging surveys. This is also a factor at least 5 times finer than what is being delivered by similar all-sky surveys by other SKA pathfinders.

Cadence of Multiple Epochs: The entire sky will be imaged twice down to a depth of 140 μJy, providing two epochs of high-resolution maps and catalogs for immediate transient science as well as providing a critical baseline for all future transient surveys and follow-up of multi-wavelength transient events (e.g., gravity waves, LSST, etc.)[11].

5.1.3 VLASS ALL-SKY Survey Science

The primary driver for this tier is to create a set of legacy products that can be used for a very broad range of science by the whole multiwavelength astronomical community. As the entire sky down to -30° declination has already been covered by the Pan-STARRS survey – which is producing catalogs deeper than SDSS and which will be publicly released through the MAST archive in 2015, and as VLASS will have positions accurate enough for matching to new surveys such as DES – we can guarantee that the whole VLASS will be utilized for science as soon as it is available, providing this decades enhanced version of the powerful FIRST+SDSS combination.

There are many attributes of the ALL-SKY tier that will break new ground compared with existing surveys, including contemporaneous spectral indices, high-resolution polarization measurements, improved sensitivity, and higher frequency data. Many extragalactic sources will be resolved, enabling studies of the spatial distribution of the intensity and polarization. Some specific examples of science cases are listed below, but the results are sure to impact all areas of astronomy. The 1700 papers citing the FIRST survey cover the expected topics such as AGN and star-forming galaxies, but they also include many hundreds of papers on binary stars, neutron stars, X-rays sources, diffuse gamma-ray emission, gravitational lensing, galaxy clusters, the intergalactic medium and many other topics. Certainly VLASS ALL-SKY survey will become a top-level

[11]This is currently subject to OTF testing for fast slew rates (see §8.9).

resource for almost every area of astronomy. Below we call out in more detail, two illustrative areas of science that VLASS ALL-SKY will impact, quasar and polarization science.

Quasar Science The primary demand that quasar science – at high redshifts in particular – places on a radio survey is for a wide area. Quasars are rare, and the radio-loud sources account for only ∼5% of the population as a whole. To SDSS depth, the surface density of optically selected quasars is ~ 43 deg^{-2} at $0 < z < 5$ (Richards et al. 2006; Ross et al. 2013); of which only ~ 1.4deg^{-2} are at $z > 3$. Thus only one high-redshift, radio-loud quasar is detected per ~ 7 deg^2 of survey area. Building a large statistical sample of radio sources for demographical studies of, for example, the evolution of radio loudness with redshift (Jiang et al. 2007) requires significant sky coverage.

High-resolution is also important for understanding of radio-loud quasars. The typical spectral index for a radio quasar is $\alpha_\nu \sim -0.5$. Although this is relatively flat, it still argues for lower frequencies in order to achieve higher sensitivity for a given flux limit. In addition, there are hints that compact, steep-spectrum radio emission may be more prevalent at high redshifts (e.g., Frey et al. 2011). Such sources will be easily detected by planned low frequency (< 1 GHz) surveys with excellent sensitivity; however, these surveys will invariably have poor resolution. Efficient matching of radio sources to surveys at other wavelengths (particularly in the optical) requires ∼arcsecond resolution. In this way, a higher frequency VLA survey can provide an essential complement to the low frequency surveys, providing localization of radio sources at a much greater depth than FIRST. This is prerequisite to identifying candidates for spectroscopic campaigns to obtain redshifts, either in the optical/near-IR, or with ALMA.

VLASS ALL-SKY will provide reasonably accurate spectral indices for objects brighter than 3.5mJy (and wide will go deeper see below). For regions with spectroscopy, this will provide orientation measures for quasars, and for unexplored regions of the sky, this information can help with object classification.

In terms of radio-loud quasars at high-redshift, the limiting magnitude for detecting minimally radio-loud quasars at this depth is $i = 21.8$. At that depth, we expect roughly 20 quasars per deg^2, of which roughly 10% are radio loud. Thus, ALL-SKY should expect to observe of order 60,000 radio-loud quasars at $z > 2$. For quasars at $z \sim 6$, this depth would be sensitive to of order 1000 quasars, and will be helpful in identifying such sources.

Polarization Science In terms of polarization, the ALL-SKY tier provides the first high-resolution ($<45''$) large area survey of polarization at any frequency, therefore resolving most polarized sources. This will open the possibility for the discovery of new classes of polarized objects that are depolarized at longer wavelengths. Even after the POSSUM/WODAN surveys are available, it provides – at their high flux ends – determination of depolarization and complex Faraday structure. This tier will also detect new populations of polarized sources (in very turbulent environments: inner regions of jets, starbursts, etc.) that are depolarized at frequencies <2 GHz and will have sensitivity to larger Faraday depths ($>10^5$ rad m^{-2}) and extended structures in Faraday depth space.

5.2 Wide

The ALL-SKY component of VLASS will provide a legacy high-resolution dataset on the entire northern sky that will last through to the SKA era; however, it does not probe deeper than the FIRST survey. Similarly, while the DEEP component of VLASS will probe to far greater depths (as much as a factor of >50) and includes enough area to mitigate against cosmic variance, it will necessarily not survey enough area to produce statistically significant samples of those rare sources with low space densities but high intrinsic value. Thus it is crucial to include a tier that takes advantage of the existing and upcoming deep photometric and spectroscopic databases by breaking new ground (at high resolution) in term of depth (and thus redshift) for a statistically significant number of objects with low space density.

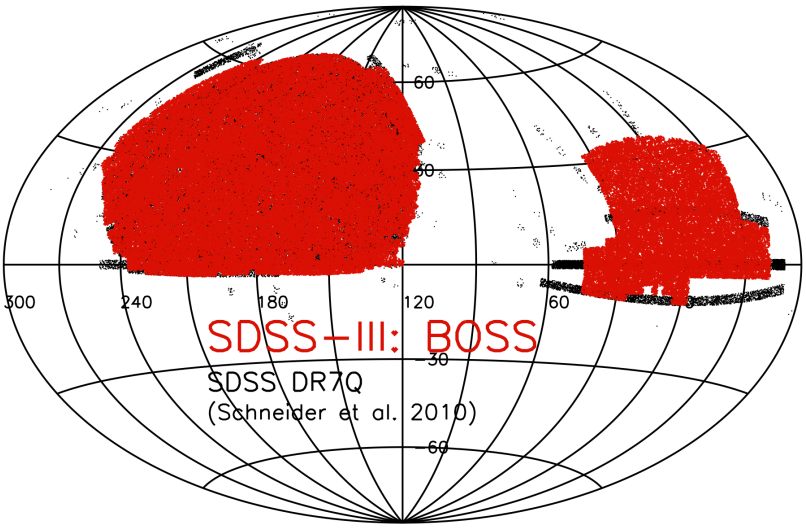

Figure 15: SDSS-III Footprint, which is the suggested area for the WIDE tier. DESI will further target this full area and HSC will target key parts of it.

Ideally we would simply extend the ALL-SKY tier even to greater depth (and possibly with more epochs for time-domain investigations), but the existing multi-wavelength photometry does not support such a strategy. It is more efficient to concentrate the added depth where it is most needed. In the long run, that will be the LSST area (with a co-added depth of i = 26.8), and these data will indeed serve as an important legacy dataset in combination with LSST. However, in the more immediate future, the Dark Energy Survey (DES) and Hyper-Suprime Cam (HSC) serve as better guides, with depths of i = 25.3 and i = 25.9, respectively—an order of magnitude deeper than Pan-STARRS.

It is for these fields that the high resolution afforded by VLA is most critical. At the limits of the DES, HSC, and LSST surveys there are 5, 8, and 14 galaxies in an ASKAP beam—never mind the number of stars. The higher S/N observations of EMU/Wodan will not mitigate this source density when it comes to associating optical and radio sources (see the Appendix), resulting in a high probability of misidentifications. B-array observations in the S-band provide sufficient resolution to bring these numbers down to $\lesssim$1 galaxy in the VLA beam without unnecessarily over-resolving extended radio sources.

Thus while the ALL-SKY tier provides the broadest sky coverage to maximize public utility and find the rarest of sources, and the DEEP tier will probe the faintest radio sources in those regions with ultra-deep multi-wavelength imaging, those two tiers alone leave a gaping hole in VLASS program. As such we propose a middle ("WIDE") tier where a fraction of the sky be covered to 50 μJy, roughly 3$\times$ deeper than FIRST, or roughly 2$\times$ deeper than FIRST for a typical extragalactic spectral index of $\alpha = -0.7$. This allows the detection of a statistically significant number of objects in source populations that are moderately fainter than the FIRST detection limit. This improved sensitivity, in combination with the high-resolution polarization measurements, contemporaneous spectral indices, and higher frequency data, will provide a legacy dataset with maximal public utility.

5.2.1 Description

Area and Depth: The WIDE component will cover ≈10,000 deg^2 down to a 1σ RMS depth of 50 μJy, covering the bulk of the 14,000 deg^2 area being targeted by the Dark Energy Spectroscopic Instrument (DESI), which will obtain optical spectra for tens of millions of galaxies and quasars, constructing a 3-dimensional map spanning the nearby universe to 10 billion light years.

Angular Resolution: Like All-Sky, WIDE will be conducted in B-array, providing a uniform 2.1″ sythesized beam over the entire field. This resolution is necessary to provide accurate positional matching with exising and forthcoming optical/NIR imaging surveys.

Cadence of Multiple Epochs: WIDE will be carried out in 4 epochs, each reaching a 1σ RMS of 100 μJy to enable the transient science described above.

Choice of fields: By focusing on the area of sky with the best spectroscopic coverage, we will maximize the return of these VLA data. The logical footprint for the WIDE tier is thus the DESI area, which has already been heavily covered by SDSS-I/II/III spectroscopy (2.2M spectra in all, including 440k quasars, 1.47M galaxies, and 260k stars) and will be covered in the near (and not quite so near) future by SDSS-IV, HSC, and DESI itself. This will allow HSC (and DESI) spectroscopic targeting based on VLASS. The bulk of this area is in the North Galactic Cap, but includes a significant region towards the South Galactic Cap where the extremely high spectral density (and multi-wavelength coverage) of SDSS Stripe 82 is particularly attractive (representing about 3% of the WIDE tier coverage). Figure 15 shows the approximate area that we propose to cover with WIDE.

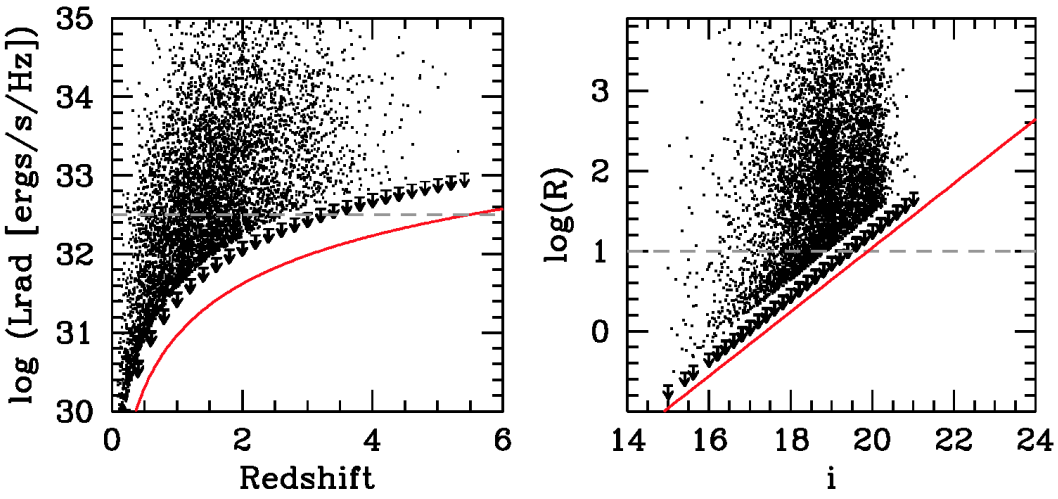

Figure 16: *Left:* Radio luminosity vs. redshift. The dashed line indicates a division between radio- loud and radio-quiet quasars according to the radio luminosity (e.g., Goldschmidt et al. 1999). Radio upper limits are shown by arrows (offset downward slightly from the actual limits and sparse sampled for clarity). The depth of VLASS WIDE tier (as indicated by the red line) allows us to push the redshift limit of radio-loud completeness from $z = 2.7$ to $z > 4$. *Right:* Radio loudness (as measured by the ratio of radio to optical flux) vs. i-band magnitude. The dashed line shows the traditional division between radio-loud and radio-quiet quasars of log(R)=1. Upper limits are given as arrows (offset downwards slightly and for clarity). The solid red line shows the improvement that results from VLASS WIDE tier. Not only will we be complete to radio-loud quasars to i = 19.9, combining with the deep optical data will allow us to study the most radio-loud objects to i $\sim$ 24 over a significant fraction ($\sim$30%) of the sky.

5.2.2 VLASS WIDE Survey Science

All of the extragalactic science enabled by the ALL-SKY tier will be strengthened by the WIDE tier, but this tier also allows a host of new investigations. For example, one of our science goals from §4.1 was understanding the evolution of the radio-loud fraction of quasars, for which the depth of FIRST and VLASS ALL-SKY will not be sufficient. This is just one example of many investigations where VLASS WIDE will have the simple, but powerful effect that comes from extending the depth on well studied parts of the sky. Thus, VLASS WIDE will capitalize on the investigations done with the FIRST survey by concentrating on the same area, but probing to fainter flux limits. This will enable science such as the study of the radio-loud fraction evolution that neither VLASS All-Sky, nor FIRST, allow. All-Sky will make sure that we don't miss any rare objects at the depth of FIRST, while providing the enhanced spectral, polarization, and transient science that the enhanced Jansky VLA now enables. WIDE will provide the area at greater depth to have sufficient numbers to do population studies (some examples below).

Star forming galaxies: Current surveys fail to provide a large baseline sample of low-z galaxies with well-established polarizations over a wide range in starburst luminosities. The WIDE tier will be able to detect luminous star forming galaxies out to $z \sim 0.15$ (LIRGs) or $\sim$0.5 (ULIRGs). By surveying a representative volume of the low-redshift universe, this tier will provide a good baseline sample of relatively nearby objects with which to compare the higher-redshift objects probed by the DEEP tier.

Polarization Science: Polarization studies will benefit from the combination of high resolution, depth and area provided by the WIDE tier. This includes increased detection rates for rare heavily depolarized sources, as in the ALL-SKY tier. Furthermore, by having good optical/NIR spectroscopic data included in WIDE, the properties of the magneto-ionic medium of absorption line systems can be more easily interpreted, and polarization k-correction can be made via accurate spectroscopic redshifts of sources. The WIDE tier will provide polarized number counts in a regime where 1.4 GHz measurements suggest a flatter slope (i.e., change in population?) from higher polarized fluxes. S-band also allows polarization detection of objects with high rotation measures (RM) not possible with ASKAP/MeerKAT.

AGN Science: The combined area and depth of the WIDE tier will allow us to gain a deeper understanding of the radio AGN population. For example, the breadth of the S-band, coupled with the depth and area of the survey enables robust spectral index measurements (good to $\Delta\alpha \pm 0.1$) for a significant number of objects (down to $\sim$ 1.75 mJy, which amounts to 60 sources per deg^2). Even the faintest FIRST sources will have spectral indices measured to better than $\Delta\alpha \pm 0.18$. This will enable, for example, AGN orientation measures necessary for a host of science investigations.

Quasar Science: The FIRST survey detects barely 10% of SDSS quasars, allowing only stacking analyses for the vast majority of sources. That is a real problem, as only about 10% of quasars are formally "radio-loud", leaving us with a very biased view of the radio properties of quasars, as well as many unanswered questions. For example, while the physics that leads to the generation of huge radio lobes in radio-loud quasars still eludes us, it seems clear that black hole mass (e.g., Lacy et al. 2001) and spin (e.g., Blandford & Znajek 1977; Blandford & Payne 1982) play key roles in this question. However, a deeper census of the demographics of radio-loud quasars is required in order to understand the coupling with the detailed physics of black hole accretion. By extending VLASS depth to 50 μJy, that fraction would increase to $\sim$20%, which would crucially allow the detection of radio-quiet (but not radio-silent!) quasars that FIRST generally does not probe. While VLASS will not be as sensitive as FIRST to extended sources, Ivezic et al. (2002) find that complex sources only account for 15% of the SDSS quasar sample. Moreover, Hodge et al. (2011) report on A-array observations (i.e., with better resolution than FIRST) to 3x the depth of

FIRST in SDSS Stripe 82 and found that 97% of known SDSS quasars are recovered in the higher resolution data. The WIDE tier will be sensitive to radio-loud quasars down to $i = 21.8$ (Figure 16), which corresponds to a depth of about 40 quasars per square deg, and an expected number of $z > 2$ radio-loud quasars of 40,000. Utilizing forced photometry, radio fluxes will also be measured for a large number of radio-intermediate sources, and many of the new spectroscopic quasars in the BOSS catalog ($2.2 < z < 3.5, r < 22$) and the upcoming eBOSS ($0.9 < z < 2.2, r < 22$). This tier should be sensitive to more than 600 quasars at $z \sim 6$ (based on Jiang et al.), many of which will be identified spectrosopically by either SDSS, DESI, or HSC. Moreover, the hundreds of thousands of existing spectroscopic quasars in the WIDE footprint will maximize the utility of these observations through stacking analysis of formally radio-quiet quasars. Such powerful investigations of objects not formally detected at 5 sigma are made possible by the high-resolution observations of VLASS, which are crucial at depths where deep optical surveys find as many as a dozen galaxies in a single ASKAP beam.

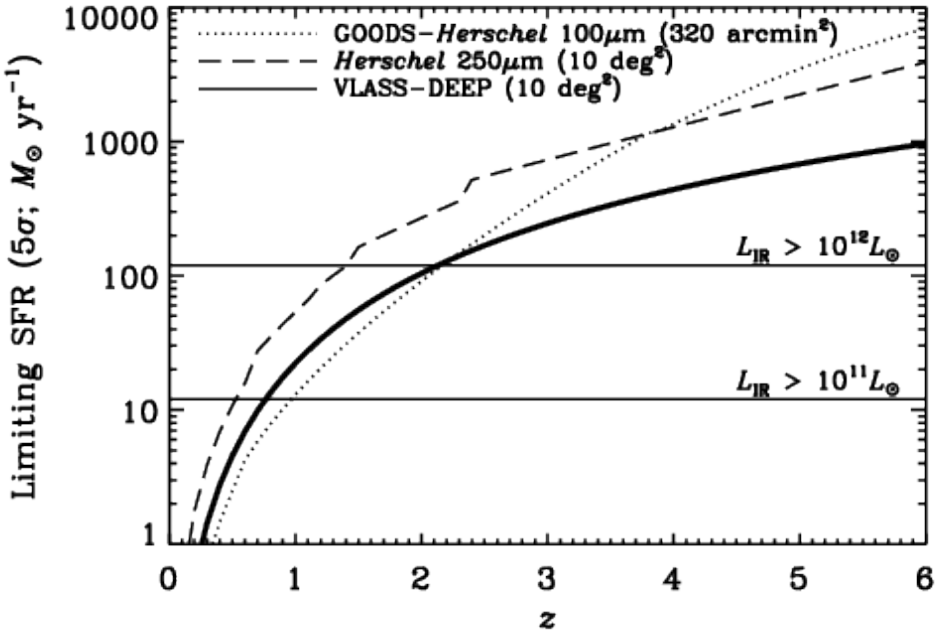

Figure 17: The VLASS-DEEP selection function (5σ) for unresolved star-forming galaxies in units of star formation rate. For comparison, we over plot the selection function (dotted line) of the GOODS-*Herschel* 100 μm (5σ) data, which are some of the *deepest Herschel* far-infrared extragalactic survey data ever taken, covering a total of $\approx$320 arcmin^2 in GOODS-N+S (Elbaz et al. 2011; Magnelli et al. 2013). (i.e., more than 100$\times$ less area than VLASS-DEEP). One beyond $z \sim 2$, the VLASS data are actually *more* sensitive to star-forming galaxies than the ultra-deep *Herschel* imaging. We additionally show the selection function (dashed line) for *Herschel*/SPIRE 250 μm (5σ) data, as these data are available for the full VLASS-DEEP 10 deg^2.

5.3 Deep

5.3.1 Context

There are three main reasons why VLASS contains a deep tier:

1. A deep tier allows objects of similar luminosity to those in the complementary, shallower but wider tiers to be observed at much greater distances and larger look-back times. This provides an essential lever arm to disentangle the effects of differing luminosity from the effects of cosmic evolution of the source population being studied.

2. The DEEP tier will be observed with a higher cadence than the WIDE and ALLSKY tiers, allowing studies of variability and transient phenomena on shorter timescales than possible in a wide survey. A deep survey also enables the study of entirely distinct transient populations than those detected in a wide survey, while additionally allowing transient populations detected in both deep and wide surveys to be studied at a range of flux density levels to investigate their evolution.

3. The DEEP tier provides a reference "truth" image for the WIDE and ALLSKY tiers where they overlap, allowing accurate assessment of completeness and reliability.

To date, the combined area of all extragalactic deep fields at $\lesssim 2\mu$Jy at S-band (or equivalent) constitutes <3 deg^2. Given that star formation is environmentally dependent, any investigation on the evolution of star-forming galaxies requires that we be able to probe them over the full range of cosmic environments (e.g., from rich clusters to voids). And, by having multiple fields covering such large areas, such survey will be able to overcome/test any remaining cosmic variance effects. As already shown above, we have chosen 10 deg^2 as the full survey area of DEEP as this is the only way to both reduce the Poisson uncertainty for deriving statistically meaningful luminosity functions for star-forming galaxies (see Figures 3 and 4) , as well as to reduce sample variance due to large-scale structure (see Figure 5), which is critical for developing our understanding of the link between star formation, galaxy mass and environment.

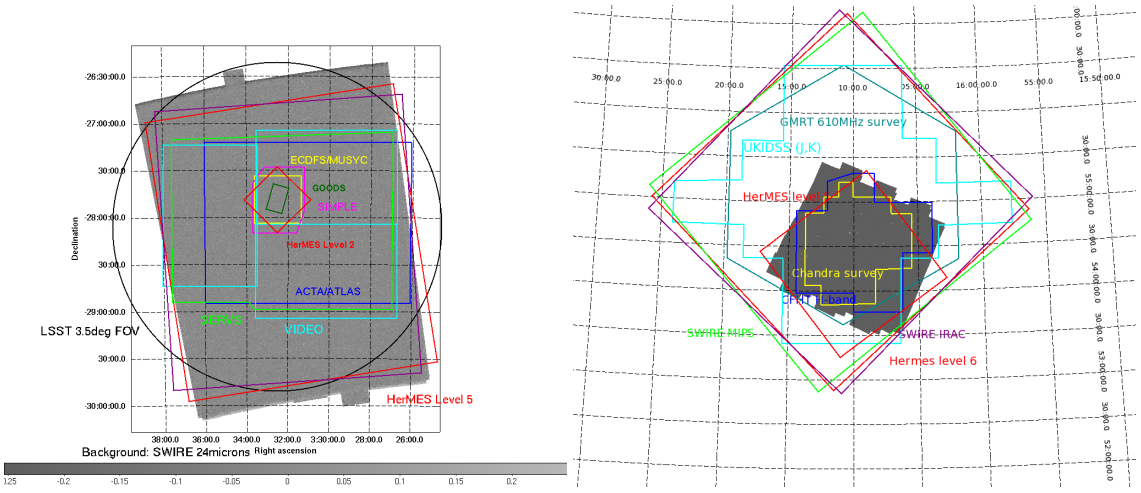

Figure 18: Multi-wavelength coverage maps of ECDFS (left) and EN1 (right), showing the wealth of degree-scale imaging over each field.

Table 1: Current/Scheduled 1–10 deg^2 Multiwavelength Coverage of the W-CDF-S

Band	Survey Name and Solid-Angle Coverage	Comments
Radio	Australia Telescope Large Area Survey (**ATLAS**; 3.7 deg^2)[a]	15 μJy rms depth at 1.4 GHz
	MIGHTEE Survey (Scheduled; 4.5 deg^2)[b]	1 μJy rms depth at 1.4 GHz
FIR	*Herschel* Multi-tiered Extragal. Survey (**HerMES**; 0.6–11 deg^2)[c]	5–60 mJy depth at 100–500 μm
MIR	*Spitzer* Wide-area InfraRed Extragal. Survey (**SWIRE**; 6.6 deg^2)[d]	3.6–160 μm
NIR	*Spitzer* Extragal. Representative Volume Survey (**SERVS**; 4.5 deg^2)[e]	2 μJy depth at 3.6 and 4.5 μm
	VISTA Deep Extragal. Observations Survey (**VIDEO**; 4.5 deg^2)[f]	$ZYJHK_s$ to $m_{\rm AB} \approx$ 23.5–25.7
Optical Photometry	Dark Energy Survey (**DES**; 9 deg^2 in 3 W-CDF-S fields)[g]	Multi-epoch *griz*; $m_{\rm AB} \approx 28$ co-added
	Pan-STARRS1 Medium-Deep Survey (**PS1MD**; 7 deg^2)[h]	Multi-epoch *grizy*; $m_{\rm AB} \approx 26$ co-added
	VST Optical Imaging of CDF-S and ES1 (**VOICE**; 4.5 deg^2)[i]	Multi-epoch *ugri*; $m_{\rm AB} \approx 26$ co-added
	SWIRE optical imaging (6.6 deg^2)[d]	
	LSST deep-drilling field (Planned; 10 deg^2)[j]	*ugrizy*; 20 000 visits total
Optical/NIR Spectroscopy	Carnegie-*Spitzer*-IMACS Survey (**CSI**; 6 deg^2)[k]	40 000 redshifts, 3.6 μm selected
	PRIsm MUlti-object Survey (**PRIMUS**; 1.95 deg^2)[l]	20 800 redshifts to $i_{\rm AB} \approx 23.5$
	VLT **MOONS** Survey (Scheduled; 4.5 deg^2)[m]	80 000 redshifts
	Spectroscopy of $\approx$ 900 radio and IR-luminous galaxies in ATLAS[n]	
UV	*GALEX* Deep Imaging Survey (7 deg^2)[o]	Depth $m_{\rm AB} \approx 25$

References: [a] Norris et al. (2006); Banfield et al. (2014); [b] `http://public.ska.ac.za/meerkat/meerkat-large-survey-projects`; [c] Oliver et al. (2012); [d] Lonsdale et al. (2003); [e] Mauduit et al. (2012); [f] Jarvis et al. (2013); [g] Bernstein et al. (2012); [h] Tonry et al. (2012); [i] `http://people.na.infn.it/~covone/voice/voice.html`; [j]`http://www.lsst.org/News/enews/deep-drilling-201202.html`; [k] Kelson et al. (2014); [l] Coil et al. (2011); [m] `http://www.roe.ac.uk/~ciras/MOONS/VLT-MOONS.html`; [n] Mao et al. (2012); [o] `http://galexgi.gsfc.nasa.gov/docs/galex/surveys/index.html`

5.3.2 Description

Area and depth The DEEP component of VLASS will cover 10 deg^2 to an RMS depth of 1.5 μJy in three well-separated fields to help mitigate against cosmic variance effects. At a depth of 1.5 μJy we will be sensitive to L* galaxies out to $z \sim 2$ (e.g., Gruppioni et al. 2013; see Figure 17). *At this depth, VLASS-DEEP is as sensitive to obscured star formation as the deepest Herschel survey data taken (i.e., GOODS-Herschel; Elbaz et al. 2011; Magnelli et al. 2014), but will cover more than 100$\times$ the area.*

Angular Resolution Sub-arcsecond resolution (A-array in S-band) is needed in order to make reliable identifications of faint star-forming galaxies.

Cadence of multiple epochs The exact number of epochs is field dependent, and the exact details can be found below in §6. However, in general, DEEP will have ≈8 epochs each reaching an RMS of around ∼4 μJy.

Choice of fields Our field selection includes 4.5 deg^2 in the Extended Chandra Deep Field South (ECDFS), 3.5 deg^2 in the ELAIS-N1 (EN1) field and 2 deg^2 in the COSMOS field. The chosen footprints for ECDFS and EN1 are largely based on the available deep NIR/VIDEO and warm *Spitzer*/SERVS data (see Figure 18). In Table 1 we provide a detailed list of the available ancillary data for our largest field, ECDFS, however, all three fields have medium-deep multi-wavelength data in X-ray through infrared bands, with typical 5σ depths of $r_{AB} \sim 25$ and $K_{AB} \sim 23$ in the optical/near-IR, mid-infrared depths of $S_{4.5} \approx 2\mu$Jy and $S_{24} \approx 300\mu$Jy, and *Herschel* SPIRE data to $S_{250} \approx$ 30mJy. Much of muliti-wavelength COSMOS data (imaging/cutouts, catalogs, etc.) is already readily available from IPAC/IRSA[12]. In addition, COSMOS has an existing S-band VLA survey to 2 μJy, which will be augmented with VLASS-DEEP imaging. EN1 has 0.1deg^2 to 1μJy sensitivity in C-band, and 1.1deg^2 to 7μJy at 610MHz, allowing us to obtain spectral indices for some fraction of the survey objects. While we prioritized southern fields due to visibility to ALMA

[12]http://irsa.ipac.caltech.edu/Missions/cosmos.html

(and eventually CCAT), along with having slightly better optical/NIR data, our second southern field choice, XMM-LSS, appears to be impractical due to RFI issues as it sits in the Clark satellite belt. We note though, having a northern field both helps with practical scheduling constraints, and will deliver a better behaved beam.

5.3.3 VLASS deep survey science

Star-forming galaxies: While the WIDE tier will detect luminous star forming galaxies out to $z \sim 0.15$ (LIRGs) or ~ 0.5 (ULIRGs), we need the DEEP tier to find them at $0.5 < z < 4$ to study the evolution of the radio properties. The proposed deep fields have *Herschel* data that is sensitive to ULIRGs at $z \sim 2$, but which is of low spatial resolution, making unambiguous identifications difficult. Radio data with good angular resolution is required as the bridge to cross-identify the *Herschel* sources with the deep near-infrared data in these fields (from Spitzer and VISTA surveys). The primary beam of ALMA is too small to make it an efficient survey instrument, so the VLA is needed. The deep component of VLASS will allow us to ask key questions about the evolution of the luminous starburst population as a function of redshift and environment, in particular magnetic field evolution (through both polarization studies and a careful comparison of the far-infrared-radio correlation for objects of equivalent luminosity).

Clustering and large-scale structure at high redshifts: The clustering properties of luminous star forming galaxies and radio-quiet/intermediate AGN can give valuable information on the masses of their underlying dark haloes. Making accurate measurements of the two-point correlation function, and conducting halo occupation distribution analyses, provides information on the underlying dark matter distribution in these regimes. To sufficiently constrain the two-halo clustering signal at large scales, where one moves from the non-linear to linear regime, requires structures to be fully sampled on $> 2 - 3\,\mathrm{Mpc}$ scales in angular space. Consequently, the $\sim 50 - 60\,\mathrm{Mpc}$ dimensions required to sample these large scales equates to a linear dimension of the survey of 2 deg, or a contiguous area of $4\,\mathrm{deg}^2$, which is not achieved even by COSMOS.

Weak lensing: The two crucial observational parameters that determine the quality of weak lensing measurements are the survey depth and angular resolution. An angular resolution $\theta_{\mathrm{res}} < 1''$ is required in order to facilitate the accurate measurement of typical galaxy shapes at redshifts $z \sim 1$. The choice of A-array at S-band ($\theta_{\mathrm{res}} = 0\farcs65$) is therefore well suited for weak lensing. In terms of survey area, a simple optimization procedure designed to maximise the signal-to-noise of the weak lensing measurement yields an optimal survey area of order $\sim 10\,\mathrm{deg}^2$. Thus the array configuration and survey area envisaged for the DEEP component is extremely well suited for weak lensing science.

AGN and implications for galaxy formation Radio jets are probably the key to understanding feedback processes in galaxy formation. Although strong "quasar mode" feedback is easy to find in the form of winds and powerful jets powered by the most luminous AGN, the duty cycle of such activity is so small ($\sim 10^{-2}$ even in massive objects at the epoch of peak of quasar activity). Jets and winds of relatively low kinetic luminosity are probably responsible for providing the bulk of AGN feedback outside of quasar outbursts in a "maintenance mode", whose characteristics are currently poorly understood. Measuring the AGN radio luminosity function down to the lowest AGN luminosities, where it merges with the radio luminosity function of starbursts is therefore essential. While the WIDE tier will allow us to obtain a good baseline at low redshifts, the DEEP component is needed to push out to $z \sim 1 - 2$, where feedback needs to be most active to prevent galaxy growth.

Quasar science Although SDSS-III/BOSS targeted FIRST sources nearly 3 magnitudes deeper in the optical than the main SDSS survey, a paltry 4% of BOSS quasars appear in the FIRST catalog (Paris et al. 2013). Clearly, a next-generation survey is needed to explore the radio properties

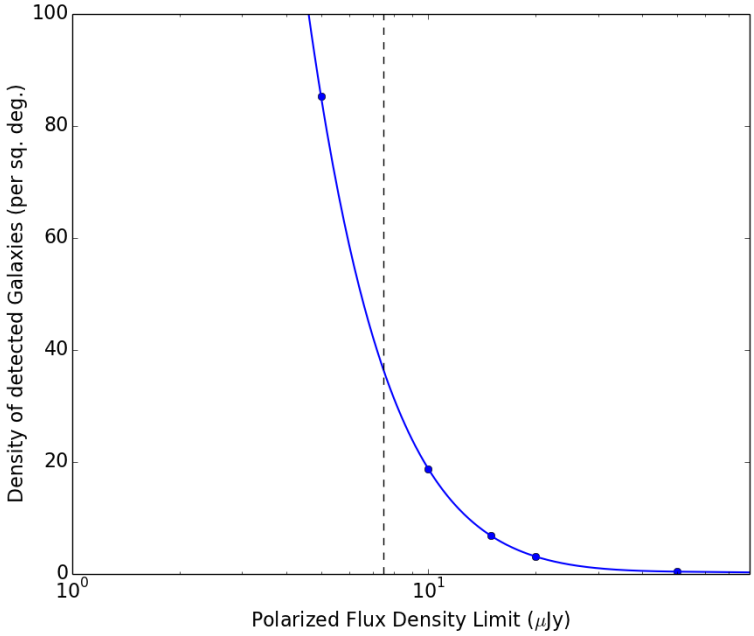

Figure 19: Number density per deg^2 of galaxies detected in integrated polarized emission as a function of detection threshold.

of these large quasar samples. While ALL-SKY and WIDE will more than double the number of SDSS quasars detected in the radio (not just radio loud), only with the DEEP tier will we detect the vast majority of radio-quiet quasars in the radio. Not only will DEEP provide truth tables that will inform what limitations the WIDE tier has, but achieving this greater depth is important to determining whether this (quiet) radio flux is intrinsic to the AGN or is due to star formation (e.g., Kimball 2011, Condon).

As with the fluxes, spectral indices in the DEEP tier will act as truth tables for the WIDE and ALL-SKY tiers. At the rms of DEEP, we can hope to measure relatively accurate spectral indices for quasars as faint as 52μJy, which generally represents a radio-quiet quasar. At the limit of the good spectral indices for WIDE, the error on the DEEP spectral indices will have statistical errors as small as $\Delta\alpha \pm 0.003$.

The DEEP tier will provide a small area where we are complete to SDSS quasars at all redshifts and to the depth of the imaging data. The DEEP fields have also been targeted as part of a spectroscopic survey of luminous mid-infrared selected AGN (Lacy et al. 2013), so radio luminosities of dust reddened AGN and quasars will also be obtained to compare to the normal quasar population.

Polarization science One of the primary aims for deep polarization observations is to chart the emergence and evolution of ordered magnetic fields in disk galaxies over cosmic time. Observations of nearby galaxies has shown that integrated polarized emission can be used as a tracer of ordered magnetic fields (Stil et al. 2009). In the presence of a large, scale galactic field the position angle of the integrated polarized radiation is aligned with the minor axis of the galaxy for frequencies above a few GHz. At lower frequencies the effects of internal Faraday rotation from the galactic ISM both depolarizes the radiation and breaks the global symmetry of the observed field, leading to reduced polarized signal and variance of the correlation between the polarization

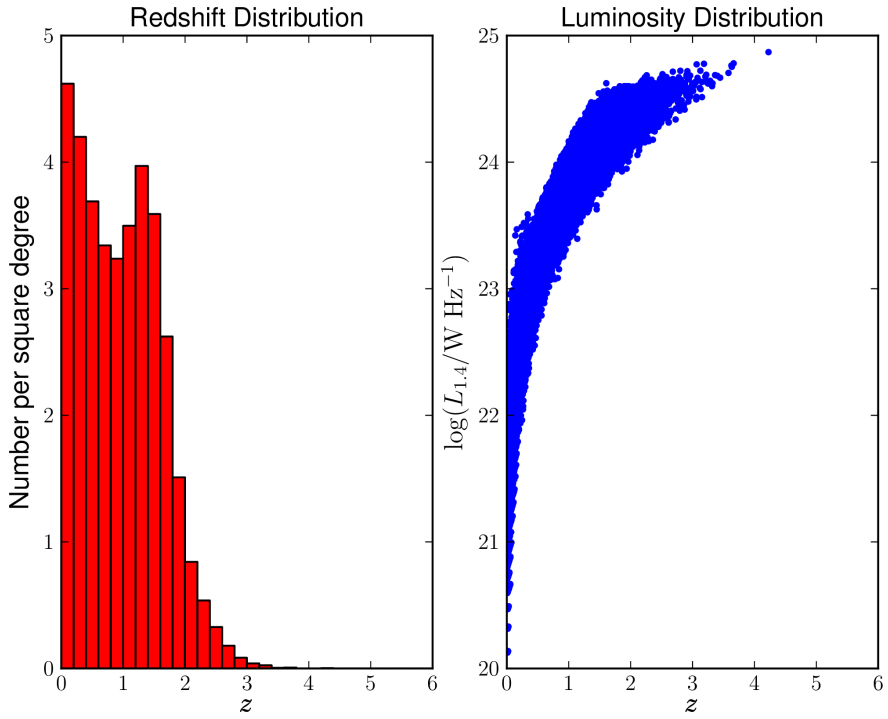

Figure 20: Redshift distribution and luminosity versus redshift for galaxies detected in polarized radion emission at $p > 7.5\,\mu$Jy.

position angle and the optical axes of the galaxy. Observations at S band between 2-4 GHz span these two frequency regimes, and with sufficient sensitivity will allow study of the emergence and growth of large scale fields in galaxies over cosmic time scales, the properties of the thermal magneto-ionic interstellar media, and their relation to star formation history.

This science goal requires detection of the polarized emission from a statistically significant sample of galaxies to cosmology distances. Predictions based on Monte Carlo simulations using properties of nearby disk galaxies show that sensitivities of order 1 μJy are required over solid angle of order 10 deg^2. Figure 19 shows the number density per deg^2 of galaxies that will be detected in polarized emission as a function of detection threshold. There is a dramatic rise in the number density below 10μJy. At a detection threshold of 5 μJy we will detect $\sim$100 per deg^2. This drops to $\sim$10 per deg^2 at a threshold of 10 μJy.

Figure 20 shows the distribution in redshift of galaxies detected in polarization down to 5 μJy, as well as the radio luminosity distribution versus redshift. With a 5σ threshold of 7.5μJy beam^{-1} over 10 deg^2, we will detected polarized emission from of order 400 galaxies to redshifts beyond $z \sim 2$.

5.4 Galactic

We first give the context of other Galactic surveys and then describe how a VLASS Galactic component will make unique and important contributions to Galactic science complementary to work that is being done by other radio surveys and many multiwavelength surveys of the Galaxy.

5.4.1 Existing Galactic Surveys

In recent years, surveys of the Galaxy have provided some of the highest resolution and most sensitive images of the stellar and interstellar environment over very large areas, which have improved our understanding of the life cycle of stars and gas across the Milky Way. Surveys, such as the infrared GLIMPSE and MIPS-GAL surveys carried out with Spitzer (Benjamin et al. 2003; Churchwell et al. 2009; Carey et al. 2009), Hi-GAL with *Herschel* (Molinari et al. 2010), and UKIDDS (Lucas et al. 2008). Complementary efforts across the radio spectrum have been made to try to match the spatial resolution (typically a few arcseconds or better) and sensitivity to put together a complete picture of the astrophysics of star birth and death and the interstellar medium in our Galaxy. Along these lines, the CORNISH survey was designed to provide a 5 GHz complement to the GLIMPSE survey (and other infrared surveys) of the inner Galaxy. CORNISH sampled a longitude range of 10 to 60 degrees and +/- 1 degree in latitude at arcsecond resolution (Hoare et al. 2012). CORNISH demonstrated yet it had a fairly restricted survey area, and omitted both the Galactic bulge and center, two unique regions for understanding the interplay between the stellar and interstellar medium. Recently, a follow up survey to CORNISH, GLOSTAR (VLA/14A-420; PI. Menten), has begun observing the Galactic plane with the new wideband C-band receiver using multiple configurations and targeting a latitude range of +/- 1 degree in the Galactic plane.

Using the VLASS "All Sky Survey" component as a starting point (to reach RMS noise levels of approximately 100 *mu*Jy sensitivity over the entire visible sky as described above), we propose additional time in the A-array configuration to target the entire observable Galactic plane and bulge regions, and a broader range in latitude than almost 20 existing infrared and radio surveys (see Hoare et al. 2012's Table 1). This Galactic component is well positioned to make a significant improvement to such studies by surveying a large region of the Galaxy at both high spatial resolution and with excellent sensitivity.

5.4.2 Description of Galactic Survey Component

Area: The Galactic component will cover 3160 deg^2 defined by a longitude range of -20 to 260 degrees, and a latitude range of +/- 5 degrees (this latitude range will provide exceptional coverage of sources in the Galactic plane, overlapping with many infrared surveys of this region and provide significantly more survey area than many radio surveys of the Galactic plane). In addition, our Galactic component includes a special extension in latitude to include the "Bulge region," a region defined to be between longitudes of 5°–10° and $-5°$ to $-10°$, additional latitude coverage up to $\pm 14°$ (a corner goes below declinations of $-40°$ and will be out of reach).

Resolution and Need for A-array: In order to carry out the optimum Galactic science described below, **sub-arcsecond A-array resolution** is critical. Most major Galactic surveys at other wavelengths (X-ray, optical, infrared, far-infrared and millimeter) have spatial resolutions of $\sim 1''$, and so for source identification and classification, the addition of A-array observations will make VLASS-Galactic component much more useful by astronomers across the electromagnetic spectrum. In turn, this will allow VLASS to have much higher legacy value among all astronomers interested in Galactic science.

Requested Sensitivity: The requested final sensitivity in the region described above is **50 μJy**, which includes A-array data that will be added to the B-array coverage of the Galactic plane and bulge included in the ALL-SKY mapping (the B-array alone will get to an RMS of $\sim$100 μ Jy).

Multiple Epochs: At a final depth of 50 μJy, we can easily get at least 4 epochs, based on the imposed data rate limitation for OTF of 25 MB/s. Factoring in the true usable bandwidth and the elevation dependent $T_{\rm sys}$, it is likely that we will obtain at least 6 epochs on the bulge. Multiple epochs will be very important for transient science (many of the above sources, in particular the stellar sources and stellar systems) in the Galaxy.

5.4.3 VLASS-Galactic Survey Science

Thermal and Non-thermal radio emission from YSOs: The increased sensitivity of the VLA, combined with the large area coverage of the Galactic Plane tier, will be able to increase the numbers of radio-detected objects, perhaps up to a factor of 4 [see Ortiz-Leon et al. (2013)[13] for early EVLA results]. Temporal variability is an important factor affecting the radio emission, and motivates multiple epochs for detections. High spatial resolution observations of young stellar objects are needed for classification, and a large in-band frequency coverage constrains the spectral index to determine thermal or nonthermal emission. The fraction of objects detected in previous pointed centimeter wavelength observations varies with mass and evolutionary phase, but is low, 10-50% (see discussion in Osten & Wolk 2009 ApJ 691, 1128).

Planetary nebulae used to map Galactic structure: Since the distances to PNe can be obtained in a straightforward manner this might help us to map out the back side of the Galaxy. The known foreground PNe are almost all in NVSS, and the Zijlstra 1989 catalog contains pretty much only sources at at least a few mJy – so we should be able to find PNe as mildly resolved, well-detected objects out to 30 kpc or so without much trouble if we get to a detection limit of 0.1 mJy. For some of them, it might require follow-up observations in recombination lines to get the distances. At large distances, radio emission from planetary nebulae might actually be one of the best tracers of the Galactic structure out at large distances through the Galactic Plane, since they are quite bright and with some follow-up work, reliable distances can be obtained.

Non-thermal emission from Active Stars: Radio luminosities of the nonthermal emission from active stars span a large range, 10^{13}-10^{18} erg s^{-1} Hz^{-1}, allowing probes of different types of cool stars: ultracool dwarfs out to 10-20 pc, active stars out to a few tens of pc, and magnetically active binaries out to 1.8 kpc. Both incoherent and coherent emission occurs, with a large degree of variability (factors of 100-1000) even within one object. The stellar byproduct of exoplanet transit probes like Kepler and TESS will yield information on key stellar parameters like rotation, white-light flaring, and asteroseismic constraints on stellar ages. These parameters can be used together to advance some of the fundamental questions laid down the Astro2010 decadal survey (How do rotation and magnetic fields affect stars?). Constraints on the particle populations around stars are also key to an understanding of the environment of the nearest potentially habitable planets: Dressing & Charbonneau (2013 ApJ 767, 95) claim with 95% confidence that the nearest non-transiting planet in the habitable zone of a cool M dwarf is within 5 pc.

A Complete Search for Symbiotic Stars: A more accurate estimate of the number density of symbiotic stars will serve as a critical input and test of binary population synthesis models (Yungelson et al. 1995), while constraining the fraction of SNe Ia that might plausibly have symbiotic star progenitors. Radio observations are a straightforward, extinction-free technique for detecting symbiotic stars, as they are simply sensitive to the ionized red giant wind (Seaquist et al. 1984). Reaching 250 μJy 5 σ sensitivity will uncover a large sample of symbiotics and enable a high-quality estimate of their number density; we will be able to detect a typical D-type symbiotic star (dusty, with an AGB-like giant) to the Galactic center, and a typical S-type symbiotic (wherein the giant is consistent with the first-ascent red giant branch) out to $\sim$3.5 kpc (Seaquist & Taylor 1990). Multiple epochs will enable us to—for the first time—probe the radio variability of symbiotic stars, constraining the energy source that powers these interacting binaries (accretion or nuclear fusion on the white dwarf surface?).

Radio Emission from Massive Star Stellar Winds: A VLA Sky Survey can contribute fundamentally to this field by using non-thermal radio emission as a probe for the evidence of magnetic fields. The bandwidth of the S band observations can discriminate between thermal and non-thermal emission. As hot stars are usually located in clusters, the spatial resolution of A array is

[13] http://adsabs.harvard.edu/abs/2013prpl.conf1K004O

required for unambiguous identification.

Thermal Emission from Novae - an unbiased search for Classical Novae: A radio survey of the Galaxy, we will carry out the first well-defined and complete sample for classical novae, with easily quantifiable selection effects that depend only on distance, ejecta mass, and ejecta velocity. With a 5 sigma sensitivity limit of 250 μJy/beam, we will be able to detect classical novae to the Galactic center (based off the light curve of the normal nova V959 Mon; Chomiuk et al. 2014, in preparation). Novae usually remain bright at radio bands for $\sim$2 years, implying that we will be able to observe them varying across multiple VLASS epochs (assuming spacing of $\sim$18 months). We therefore expect a yield of greater than $\sim$ 100 classical novae over VLASS duration, increasing the number of radio-detected novae $\sim$5 fold, measuring the distribution of ejected mass and energetics (Seaquist & Bode 2008, Roy et al. 2012) and enabling the most thorough test to date of the theory of nova explosions (Yaron et al. 2005).
Quiescent stellar mass black holes: Radio detections in quiescence will be much less severely biased than X-ray detections in outburst. If we take 10000 black holes as the total number expected in the Galaxy, we should detect of order 5 in this survey, meaning that we will at least be sensitive to the case where the existing number is much larger than standard model predictions.

Non-thermal Emission from Supernova Remnants: A dozen or more young (age less than 1000 yr), angularly small SNRs are likely hidden along the Galactic plane ($b \sim 1^\circ$, Green 2004), and VLASS will enable identification via morphology and spectral index. The high resolution and good sensitivity of VLASS will yield a complete survey for compact SNRs; with 50 μJy/beam sensitivity, VLASS will easily detect sources similar to G1.9+0.8 (flux density of 0.6 Jy and a diameter of 92$''$, Green et al. 2008). Galactic VLASS will likely double the number of known young SNRs, honing our estimate of the Milky Way SN rate and enabling detailed study of particle acceleration and stellar feedback with follow-up spanning low frequencies to gamma-rays.

In summary, a 50 μJy survey of the Galactic plane and bulge (obtained by combining ALL SKY and Galactic tier data) will:

- Provide significant increases in the radio detections of active stellar coronae and hot stellar winds in the Galaxy.
- Use PNe to measure Galactic structure: PNe should be detectable to a distance of 30 kpc and throughout the disk for the first time, making them a novel tracer of Galactic structure.
- Find exotic pulsars: of the many pulsars detectable at this survey depth, 10-30 will be exotic or suitable for use in pulsar timing arrays seeking to make the first direct detection of gravitational waves.
- Quintuple the known population of classical novae: all classical novae in the Galactic bulge will be detectable, increasing the number known by 100 and enabling statistical tests of theories of nova explosions.
- A complete survey of compact supernova remnants in the Galaxy.

6 Survey Structure

The VLASS science case is comprehensive and motivates a multi-tiered survey consisting of tiers at three depths: ALL-SKY (Tier 1) at 100 μJy/beam rms, WIDE and GALACTIC (Tier 2) at 50 μJy/beam rms, and DEEP (Tier 3) at 1.5 μJy/beam rms. The observing time required for the three tiers is 1804 hours for ALL-SKY in Tier 1 (exclusive of the WIDE region) , in Tier 2 totals of 3020 hours for WIDE and 812 hours (exclusive of ALL-SKY) for GALACTIC, and 3430 hours for DEEP in Tier 3. The total observing time in VLASS, including overhead, is **9066 hours**, for our primary 5-year survey schedule (§ 8.4).

6.1 Tier 1 (ALL-SKY)

Table 2 summarizes Tier 1, the All-Sky component of the VLASS. The all-sky tier covers the entire sky visible to the VLA north of Declination -40°, approximately 34000 deg^2 (33885 deg^2 for 82.14% of the sky). It will be carried out using On-The-Fly Mosaicking (OTFM) at a constant scan rate. This tier will be observed in two epochs separated by 12–36 months (16–18 months following the current configuration cycle schedule). In the proposed schedule (§ 8.4) the area to be observed in the region excluding the WIDE footprint will be split into two sets of blocks, to be observed in pairs of the total four observing cycles.

Table 2: Summary of All-Sky (Tier 1)

Parameter	**Value**
Total Area	33885 deg^2, $\delta > -40^\circ$ 23885 deg^2 exclusive of WIDE
Cadence	2 epochs, separated by at least 12 months
Continuum Image RMS (Stokes I)	$\sigma_I \geq 100\,\mu$Jy/beam combined $\sigma_I \geq 141\,\mu$Jy/beam per-epoch
Integration Time	1443 hr total (exclusive of WIDE) 604 hr per epoch,
Observing Time (25% overhead)	1804 hr total (exclusive of WIDE) 755 hr per epoch,

6.2 Tier 2 (WIDE and GALACTIC)

Table 3 summarizes the Tier 2 WIDE and GALACTIC components of the VLASS, which reach an imaging depth of 50 μJy/beam rms. Tier 2 covers a total of 13160 square degrees, including 3160 square degrees of the Galactic plane and the Galactic Bulge, plus 10000 square degrees in the region covered by the SDSS-III footprint (see Figure). The sensitivity required in this tier is a continuum image rms $\sigma_I = 50\,\mu$Jy/beam, to be uniform over the regions covered. Tier 2 observations will also use OTFM to cover these large areas with high observing efficiency.

The total observing time in Tier 2, in addition to the coverage provided as part for Tier 1 in these regions, is **3075 hr**, including overhead.

6.2.1 Tier 2 — WIDE

The WIDE sky area of 10000 square degrees will be observed to a final depth of 50 μJy/beam, in four epochs of 604 hr integration each for a rms image depth of $\sigma_I = 100\,\mu$Jy/beam per epoch. The WIDE portion of Tier 2 will have a total on-sky integration time of 2416 hours (3020 hours with 25% overhead), all to be observed in B-configuration. This region is treated separately from the Tier 1 ALL-SKY area in these depth calculations.

The proposed observing scenario for WIDE is

- four epochs with roughly 12-24 month cadence (TBD)
- single-epoch continuum image rms (Stokes I) $\sigma_I = 100\,\mu$Jy/beam
- per-epoch on-sky time of 604 hours, taking 755 hours observing with 25% overhead
- total scheduled time is 3020 hours

Table 3: Summary of Tier 2

Component	Parameter	Value
WIDE		
	Total Area	10000 deg^2, in SDSS-III footprint
	Cadence	4 epochs, separated by at least 12 months
	Angular Resolution	2.6″ (B configuration)
	Continuum Image RMS (Stokes I)	$\sigma_I = 50\,\mu$Jy/beam combined $\sigma_I = 100\,\mu$Jy/beam per-epoch
	Integration Time	2416 hr total 604 hr per epoch,
	Observing Time (25% overhead)	3020 hr in total observing, 755 hr per epoch
GALACTIC		
	Total Area	3160 deg^2 (560 deg2 in Galactic bulge, $-10^\circ < \ell < 10^\circ$, $\lvert b\rvert < 14^\circ$ 2600 deg2 in Galactic plane, $-20^\circ < \ell < -10^\circ$ and $10^\circ < \ell < 260^\circ$, $\lvert b\rvert < 5^\circ$)
	Cadence	4 epochs, separated by at least 12 months
	Angular Resolution	0.76″ (A configuration)
	Continuum Image RMS (Stokes I)	$\sigma_I = 50\,\mu$Jy/beam combined (with ALL-SKY) $\sigma_I = 114\,\mu$Jy/beam per-epoch (exclusive of ALL-SKY)
	Integration Time	840 hr total in region 649 hr in addition to ALL-SKY, 162 hr additional per epoch
	Observing Time (25& overhead)	812 hr (in addition to ALL-SKY) 203 hr additional per epoch

6.2.2 Tier 2 — GALACTIC

The Tier 2 GALACTIC survey area comprises 3160 deg^2, with 560 deg^2 of the central Galactic Bulge ($-10^\circ < l < 10^\circ$, $|b| < 14^\circ$) plus 2600 deg^2 in the Galactic Plane from $-20^\circ < l < -10^\circ$ and $10 < l < 260^\circ$ for $|b| < 5^\circ$. This GALACTIC region includes significant areas that must be observed at low-elevation even around transit, so integration times are scaled by 1.1× to reflect the higher system temperature (R. Perley, private communication); this scale factor assumes observations will be scheduled within +-45 minutes of transit. For 3160 square degrees, it will take a total of 840 hours of integration to reach a uniform $\sigma_I = 50\,\mu$Jy/beam. The Tier 1 B-configuration observations will have integrated for 191 hours, so 649 additional hours of integration are needed. The new Tier 2 time will be entirely in A configuration. Tier 2 GALACTIC requires an additional 810 hours observing (with overhead).

The proposed scenario for Tier 2 GALACTIC observing spreads the additional observations between 4 cycles in A configuration:

- four epochs with 12–24 month cadence in A configuration
- in 4 unique A-configuration epochs, on-sky observing time of 203 hours each
- single-epoch continuum image rms (Stokes I) $\sigma_I = 114\,\mu$Jy/beam in each of the four A-configuration epochs
- single-epoch continuum image rms (Stokes I) $\sigma_I \sim 141\,\mu$Jy/beam (in each of two B-configuration ALL-SKY epochs)
- total scheduled time is 812 hours

6.3 Tier 3: DEEP

The deep tier comprises observations of 3 deep fields with multi-wavelength coverage in a total area of 10 square degrees. The fields are: COSMOS (2 square degrees, 10h00m28s, 02d12m21s), ECDFS (4.5 square degrees, 03h32m28s, -27d48m30s), and Elias-N1 (3.5 square degrees, 16h08m44s, 56d26m30s). The cumulative depth for each field will be an image rms (Stokes I) of 1.5 μJy/beam in A-configuration. There is an multiplicative factor of 1.23$\times$ applied to the integration time needed, to compensate for its low elevation assuming observations within 1.5 hours of transit. For COSMOS, there is an existing 2 μJy/beam S-band C plus A-configuration dataset (12B-158, Smolcic et al.). Note that although these fields are all included in Tier 1, and all but ECDFS is in Tier 2, the amount of time in those tiers in those areas ($<$ 1 hour total per square degree) is not significant enough to count in the total, so we treat Tier 3 as independent. If desired, the B-configuration Tier 1 and 2 data can be included in Tier 3 imaging to provide additional sensitivity to extended structure. These smaller fields can be efficiently mapped using pointed mosaics, so OTF need not be used for the deep fields unless it is desirable to cover these multiple times in a single day for more uniform uv-coverage.

The total scheduled observing time in Tier 3 is 300 hours for COSMOS, 1960 hours for ECDFS, 1170 hours for Elias-N1, which totals **3430 hours**.

Table 4: Summary of DEEP (Tier 3)

Field	Parameter	Value
COSMOS		
	Total Area	2 deg^2, centered at $10^h00^m28^s$, $+02^\circ12'21''$
	Total Tier 3 Integration Time	234 hrtime (300 hr with 25% overhead) (302 hr of Archival observations, 12B-158)
	Continuum Image RMS (Stokes I)	$\sigma_I = 1.5\,\mu$Jy/beam combined
ECDFS		
	Total Area	4.5 deg^2, centered at $03^h32^m28^s$, $-27^\circ48'30''$
	Total Tier 3 Integration Time	1570 hr (1960 hr with 25% overhead)
	Continuum Image RMS (Stokes I)	$\sigma_I = 1.5\,\mu$Jy/beam combined
Elias-N1		
	Total Area	3.5 deg^2, centered at $16^h08^m44^s$, $+56^\circ26'30''$
	Total Tier 3 Integration Time	937 hr (1170 hr with 25% overhead)
	Continuum Image RMS (Stokes I)	$\sigma_I = 1.5\,\mu$Jy/beam combined

COSMOS This field will be observed for 6 hr centered near transit, without suffering elevation induced sensitivity losses. The notional observing scenario is to break the observations into 7.5 hr blocks. For 300 hr total, we need 40 blocks. We will observe this field in four epochs:

- four A configuration epochs

- each epoch 10 passes of 7.5 hours observing each (6 hours each integration time, 60 hours integration per epoch)
- single-epoch continuum image rms (Stokes I) $\sigma_I = 4.5\,\mu$Jy/beam
- single-pass continuum image rms (Stokes I) $\sigma_I = 10\,\mu$Jy/beam
- total scheduled time 300 hours (75 per configuration)

Alternative scenarios include spreading the 300 hours among 5 A-configurations (60 hours in each).

ECDFS This field should occur witin 2 hours of transit, so we break the observations of this field into 5 hr blocks (each should get 4 hr integration). We will need 392 such blocks total. A plausible scenario is to spread these over four cycles of A configuration epochs.

- four A configuration epochs
- 98 passes of 5 hr each (490 hr) per epoch
- single-epoch continuum image rms (Stokes I) $\sigma_I = 3\,\mu$Jy/beam
- single-pass continuum image rms (Stokes I) $\sigma_I = 30\,\mu$Jy/beam
- total scheduled time is 1960 hr

An alternative scenario is to spread the observations between 5 epochs, with two getting 79 passes (395 hr) and three getting 78 passes (390 hr).

With observations closer to transit (e.g., within 1.5 hr), elevation losses could be decreased, with a concomitant reduction in overhead (1.28$\times$ increase). However, 3.75 hr blocks would require 128 passes per epoch (over 4 epochs), which is more than 4 months with observations every day. Such a scenario is likely to have serious logistical problems in scheduling, and we choose to take an extra 2% loss in efficiency to observe longer blocks. If 98 passes are too many, one could observe 2.5 hr from transit at 1.33$\times$ penalty (2008 hr total) and take only 80 passes per epoch.

The efficiency loss due to the low elevation has been estimated from a plot of system temperature versus antenna elevation angle at various frequencies in S-band (courtesy R. Perley). Our estimate is uncertain at the few percent level, and could be either too lenient or too conservative. Further testing on the VLA through a trial observation of the ECDFS (e.g., a single pass) will be scheduled as soon as is practical (best done in the upcoming C-configuration or wider).

Elias-N1 This field can be observed for long blocks due to its high declination. However, we restrict to around 6 hour integration per block so that they better fit in with dynamic scheduling (but can be observed over a wide range of start times). These blocks will be 7.5 hr long with overhead, and thus we need 156 blocks total (giving 936 total hours integration, just under our target). Again we split these into four cycles:

- four A configuration epochs
- each epoch 39 passes of 7.5 hr observing each (292.5 hr per epoch)
- single-epoch continuum image rms (Stokes I) $\sigma_I = 3\,\mu$Jy/beam
- single-pass continuum image rms (Stokes I) $\sigma_I = 18.7\,\mu$Jy/beam
- total scheduled time is 1170 hr

An alternative scenario is to divide the observing among 5 epochs, in which case each epoch gets 234 hr (31 passes).

6.4 Sensitivity Assumptions

The sensitivity of the Jansky VLA for mosaicking is computed using the procedure given in the Guide to VLA Observing: Mosaicking[14]. For continuum (Stokes I) at S-band (2–4 GHz) we assume a Survey Speed (SS) of

$$SS = 16.55 \left(\frac{\sigma_I}{100\,\mu\mathrm{Jy/beam}} \right)^2 \mathrm{deg}^2\,\mathrm{hr}^{-1} \quad (1)$$

of on-sky integration time for an assumed image rms of σ_I. This assumes 1500 MHz of useable bandwidth (after RFI excision) and an image averaged over the band using multi-frequency synthesis. The integration time needed to survey a given area to a depth is given by dividing that area by the survey speed.

6.5 Overhead Assumptions

In the estimates for total observing time, the assumption is made that a global 25% overhead for slewing, setup, and calibration applies to the survey. Thus all integration times are mulltiplied by 1.25 in order to arrive at the "clock time" needed to execute the VLASS components. In practice, this will depend on exactly how the survey componenets are scheduled and how much calibration can be shared between blocks. For example, the S-band Stripe-82 observations of program 13B-370 (Hallinan et al.) were observed using dynamic scheduling and independent 3-hour blocks, and thus had a 33% overhead. We fully expect to be able to meet (or come in under) the global 25% overhead for (i) observing blocks of 6 hours or longer, and (ii) short blocks that can share calibration with other blocks observed around the same time. Due to the need to observe the Tier 3 ECDFS near transit, special attention will be required to optimize the calibration overhead for that component of the survey. Verification of these assumptions are listed under the Test Plan below.

7 Data Products

The VLASS data products are described below. Products are broken into classes of "Basic" and "Enhanced," with the former being simple enough to proudce by NRAO's standard (or soon to be standard) data processing system, or modest extensions. Enhanced data products will require domain expertise, so they will be left for community members to define and produce.

7.1 Basic Data Products

The Basic Data Products (BDP) of the VLASS consist of:

1. raw visibility data
2. calibration data and process to generate calibration products (current best version as well as past released versions maintained in archive)
3. quick-look continuum images
4. single-epoch images and image cubes
5. single-epoch basic object catalogs

[14] `https://science.nrao.edu/facilities/vla/docs/manuals/obsguide/modes/mosaicking`

6. cumulative "static sky" images and image cubes (generated after epoch beyond the first)

7. cumulative "static sky" basic object catalogs (generated after epoch beyond the first)

The resources for processing, curating, and serving will be provided by NRAO, as described in § 7.3. Teams led by NRAO, but including external community members where possible, will carry out the activities required for the processing and Quality Assurance (QA) of the products.

Details of individual BDP are now described.

7.1.1 Raw Visibility Data

The raw visibility data for the VLASS will be stored in the standard VLA archive. These data will be available immediately after observation with no proprietary period. As the VLASS is being observed using standard data rates (25 MB/s maximum averaged over the project) there are no special resources required for the storage and distribution of these data. Data will be downloadable by users from the archive web pages as normal.

7.1.2 Calibrated Data

VLASS data will be processed using a modified version of the normal CASA-based VLA cailbration pipeline. By the time of the VLASS observations, the VLA pipeline will have the requisite functionality to process VLASS data (full polarization, many individual target fields generated in OTF mode). The VLA pipeline is currently run on most VLA observations and is well tested. The VLASS will use a version specifically tested on VLASS pilot observations.

In summary, the output of the pipeline will consist of:

- a set of final calibration tables
- (possibly) a set of sky models used in calibration
- one or more sets of flagging commands
- the final flag column
- QA reports and plots
- the set of pipeline control instructions or script necessary to calibrate the raw data

Once the pipeline has run and after QA assessment, users will gain access to the calibrated data from the archive. Physically archiving the calibrated visibility data for long-term storage would double the amount of archive space required, which is too costly. Instead, the VLASS will archive calibration products and maintain scripts to generate the calibrated dataset. Scripts to apply calibration products will be based on CASA. Upon first processing of a Scheduling Block the calibrated data will be available for a short time for transfer to subsequent processing teams.

7.1.3 Quick-Look Images

The identification of transient and variable objects is a key science goal of the VLASS. This requires the capability to process and image the data within a short period after the data is taken. We have set the requirement on this to be 48 hours maximum, with a goal of 24 hours. The primary output of the Quick-Look Calibration and Imaging Pipeline (QLP) will be continuum images (Stokes I) that can be used by the Transient Object identification teams (see below under Enhanced Data Products) to produce alerts for transient objects and arrange for follow-up studies. As these images will be constructed through mosaicking, there will also be a corresponding rms sensitivity (noise) image.

Of secondary (but still high-utility) priority are the polarized continuum images (Stokes Q,U,V). The Q and U images will be most important for linear polarization studies. The V image is mainly useful as a cross-check on systematics, but may provide useful information for some classes of transients if our imaging and calibration pipeline can produce high-quality V images. There will need to be a noise image for each of these also. There are thus a total of 8 images to potentially be produced by the QLP per trigger: 4 images (I, Q, U, V), and their corresponding noise maps. As detailed in § 8.8 these images take a substantial (350TB) but not prohibitive amount of space. The amount needed after a given observation day to search for transients and generate alerts is much smaller. It will be most practical to keep only a buffer of current and some number of past image sets from the same epoch, and only archive long-term the QLP instructions to re-generate previous epochs QL images (most likely in a "postage stamp" limited area) by "processing on-demand" (POD). This is particularly true for QL products as these will be streamlined and fast pipelines. We will assume in the resourcing of QL storage that this will be the case.

These Quick-Look images will be publicly available from the VLASS archive promptly upon production.

7.1.4 Single-Epoch Images

Within 2 months (Tiers 1 and 2) or 6 months (Tier 3) of completion of the observations of a given "epoch" (observations in a given configuration), fully calibrated and quality-assured images as detailed below will be produced and available in the archive. These will be generated using a specialized CASA-based Imaging Pipeline. This pipeline will be developed by the NRAO staff, with the involvement and guidance of the VLASS teams.

The VLASS single-epoch wide-band continuum images will include:

1. Flux density calibrated beam-corrected Stokes IQUV continuum (band averaged) images covering the full mosaic area
2. Sensitivity (rms noise) images for the IQUV continuum images
3. Spectral Index and uncertainty images for Stokes I (generated using Multi-Frequency Synthesis)

There are thus 10 single-epoch continuum image products.

In addition to continuum images, there are potentially cubes of 1024 channels at full spectral resolution for each of:

1. Flux density calibrated beam-corrected Stokes IQUV continuum per-channel image cubes covering the full mosaic area
2. Sensitivity (rms noise) images for each of the cube images

There are thus 8 single-epoch image cube products. These will contain a wealth of information on the SED and polarization necessary for deriving RM and other computed products. In addition, these will be important for QA purposes and diagnosing RFI problems. Thus they will need to be generated with the processing of a given epoch. However, we note that it will be expensive to store these long-term in the archive for each epoch for Tiers 1 and 2 at least. It is thus attractive to consider a POD on-the-fly processing service for these cubes, as described for the QL continuum images (§ 7.1.3), hosted on-site or externally (e.g., through XSEDE). It will be of great benefit if this capability is available for Tiers 1 and 2. In addition to efficiency, POD imaging will provide flexibility for choosing coarser frequency resolution in cubes, and the abiity to control whether beam-corrections are done or not.

We assume that for Tiers 1 and 2 only modest short-term storage is required for the large full-resolution cubes for QA purposes. We will only provide long-term archiving of full-resolution

cubes for Tier 3. These are likely sufficiently deep and costly to produce that we will assume that cubes are created once and stored in the archive. It is likely that the channels in two or more entire spectral windows with 64 channels each (e.g., the first two at the bottom of the band) will be entirely flagged, and so we assume we need cubes for only 896 channels.

For all tiers, it is practical and useful to produce and archive coarse cubes where planes are imaged for each of the 16 spectral windows (64 channels, 128MHz bandwidth) in the dataset. In addition to coarse SED and RM information, these cubes can provide QA diagnoses of RFI or other frequency depended errors. Those would be for the same 9 quantities described above for the full-resolution cubes. Note that it is likely that due to RFI 2 or more of these spectral window planes will be fully flagged and omitted from these cubes. We assume these will require storage for 14 planes. For all tiers we plan to archive and serve the 14-plane coarse cubes per epoch. If storage is a concern, these would be compressed or made at reduced spatial resolution.

7.1.5 Single-Epoch Basic Object Catalogs

There are many object finders used in the community for identification and classification of objects from images. It is expected from surveys such as the VLASS that basic object catalogs be produced and released along with the images. Over the next year, we will carry out a study of the available object finders suitable for use on the VLASS data and select and test one (or more if necessary) for production use by the team.

We consider the Basic Object Catalog entry for an "object" to contain:

1. Position, and uncertainty (likely centroid of I emission)
2. Peak Flux Density (continuum) in IQUV, and uncertainty
3. Spectral Index at Peak (Stokes I) and uncertainty
4. Integrated Flux Density (continuum) in IQUV, and uncertainty
5. Integrated Spectral Index (Stokes I) and uncertainty
6. Basic Shape information IQUV (TBD)

7.1.6 Cumulative Images

Within 6 months (goal) of the completion of observations of each epoch after the first (1 year for Tier 3), continuum images for the cumulative data will be made. These will be the same set of images as described above for the single epochs. Accommodation for variable objects in the imaging will be required across the multiple epochs.

The VLASS cumulative wide-band continuum images will include:

1. Flux density calibrated beam-corrected Stokes IQUV continuum (band averaged) images covering the full mosaic area
2. Sensitivity (rms noise) images for the IQUV continuum images
3. Spectral Index and uncertainty images for Stokes I (generated using Multi-Frequency Synthesis)
4. Spectral Curvature and uncertainty images for Stokes I (generated using Multi-Frequency Synthesis)

There are thus 12 cumulative continuum image products. These are the images produced for the individual epochs (§ 7.1.4), with the addition of the spectral curvature MFS image, plus its uncertainty.

In addition to continuum images, there are cubes of 1024 channels for each of:

1. Flux density calibrated beam-corrected Stokes IQUV continuum per-channel image cubes covering the full mosaic area
2. Sensitivity (rms noise) images for each of the cube images

There are thus 8 cumulative image cube products.

The same considerations apply to the cumulative image cubes as for the per-epoch cubes (see § 7.1.4). The archive will store and serve only the most recent cumulative image cube for each Tier. If the POD capability is available, users can request images from previous cumulative epochs (or possibly other selections). Note that the storage needs for these full-resolution cubes is considerable, and fallback options to reduced resolution or compressed cubes will be necessary to implement in the absence of enhanced archive resources.

It is practical also to create and store the spectral window averaged coarse image cubes (14 planes, 128MHz resolution) at little extra cost. There are 8 of these also. Only the most recent cumulative coarse cube image will be retained.

7.1.7 Cumulative Basic Object Catalogs

As in the case of the single-epoch catalogs, these basic catalogs would be made available along with the cumulative images. These are largely based upon the continuum images, we do not foresee using the cubes for these.

We consider the Basic Object Catalog entry for an "object" in the cumulative catalogs to contain:

1. Position, and uncertainty (likely centroid of I emission)
2. Peak Flux Density (continuum) in IQUV, and uncertainty
3. Spectral Index at Peak (Stokes I) and uncertainty
4. Spectral Curvature at Peak (Stokes I) and uncertainty
5. Integrated Flux Density (continuum) in IQUV, and uncertainty
6. Integrated Spectral Index (Stokes I) and uncertainty
7. Basic Shape information IQUV (TBD)

7.2 Enhanced Data Products

The Enhanced Data Products (EDP) are those that require more domain expertise, and so will be defined and produced by the VLASS community outside the NRAO. These data products will require external support to define, produce, and validate. However, these products are seen as essential to the VLASS science case, so both BDP and EDP (where practical) will be curated and served by the NRAO. EDS (§ 7.3) will be required for curation and distribution of EDP beyond the capabilites of NRAO to support.

Some examples of EDP include (but are not restricted to):

1. Transient Object Catalogs and Alerts

2. Rotation Measure Images and Catalogs
3. Improved Object Catalogs
4. Light curves (intensity and polarization) for objects and/or image cutouts
5. Catalogs of multiwavelength associations to VLASS sources

Beyond requiring extensive domain expertise, these areas are also ideal for nucleating multi-wavelength community groups and resources to work with and enhance the VLASS.

A special case of a EDP is the support for commensal observing at P-band (230–470MHz) using the VLITE system. There is no NRAO processing or archive support currently budgeted for VLITE data products, and thus use of VLITE with VLASS should be considered as a EDP (and EDS) provided in partnership with NRL.

Other areas for EDP will undoubtedly become apparent. Once the survey is approved, we will take proposals for new EDP to be included in the list above. Criteria for including EDP in the VLASS archive will be relevance to the VLASS science case and cost of curating and serving the products. As an incentive to include EDP in the VLASS archive, we ask that the NRAO encourage authors that use EDP to acknowledge groups that produced them.

7.3 Enhanced Data Services and the VLASS Archive

A comprehensive survey like the VLASS will produce a diverse set of data products and will require a full-featured archive to serve it to the public. A baseline plan is to serve products from a website hosted by the NRAO. This site will feature basic search capabilities of catalogs and products, as has been done for FIRST[15] and NVSS[16]. Previous VLA surveys only provided catalogs and images, so at a minimum the VLASS will extend that search capability to visibility data, calibration products, and deep/multi-epoch images. The NRAO will also provide data analysis scripts to apply calibration to raw data.

However, astronomy is increasingly a multi-wavelength discipline with a diverse set of tools for comparing observations from different observatories. If the VLASS archive exists only as a stand-alone NRAO-hosted service, it would not be as useful as one integrated with the tools available at places like IPAC[17] or the Virtual Observatory [18].

We are investigating options for having catalogs and/or images served by organizations outside the NRAO. This would extending the reach of the VLASS outside the radio community and open access to powerful tools for multi-wavelength analysis. The VLASS community, including the co-authors of the VLASS proposal, will be writing an NSF proposal to support VLASS data analysis and a more effective archive. These Enhanced Data Services will greatly augments the utility of the VLASS and its basic and enhanced data products to the wider astronomical community.

Another area that would be greatly improved through EDS is the capability for "processing on-demand" (POD) of images or image cubes. This would alleviate storage volume concerns, and enable more flexible angular and spectral resolution of the resulting products. We expect to utilize the NSF XSEDE network for modest use of POD-like processing for the pipeline. Fully enabled POD for VLASS could be carried out through partnerships with NSF supercomputing centers or with DOE science labs. Exploration of these options will commence upon approval by NRAO for VLASS.

[15] `http://sundog.stsci.edu/cgi-bin/searchfirst`
[16] `http://www.cv.nrao.edu/nvss/postage.shtml`
[17] `http://www.ipac.caltech.edu`
[18] `http://www.us-vo.org`

As noted above, data archive and distribution support for commensal observing at P-band (230–470MHz) using the VLITE system is not currently budgeted for support by NRAO. Archive serving of VLASS should be considered as a EDS provided in partnership with NRL.

8 Implementation Plan

Here we present an overview of the implementation plan and observing logistics. Details of the observations and observing plan are given in the VLASS Technical Implementation Plan document. The TIP will be reviewed internally by NRAO as a Conceptual Design Review prior to the VLASS Science Review. The CoDR report will be provided to the science reviewers.

8.1 Mosaic Observing Patterns

In order to carry out the VLASS, we will need to observe the sky using a large number of mosaicked pointings of the VLA. At 2–4 GHz, the VLA has a field-of-view given by the primary beam response of the 25-meter diameter antennas. This approximately follows a Gaussian response, with a full-width at half-maximum (FWHM) given by

$$\theta_{FWHM} \approx 45' \left(\frac{1\,\mathrm{GHz}}{\nu} \right) \tag{2}$$

at observing frequency ν, and thus over the S-band the FWHM varies from 22.5′ at 2 GHz to 11.25′ at 4 GHz, with FWHM of 15′ at 3 GHz mid-band. In order to optimally cover a given sky area in an efficient manner, the array must either conduct a raster scan using "on-the-fly" mosaicking (OTFM), or tile the area with a number of discrete pointings in a hexagonal packed configuration ("Hex-pattern Mosaicking"). The choice between these techniques is determined by the extent to which the extra overhead (from 3 to 7 seconds) needed to move the array and settle at each pointing in the discrete hex-pattern mosaic becomes a burden on the observations, and thus OTFM is favored.

The techniques of OTFM and Hex-pattern Mosaicking and the calculations and procedures needed to set these up are described in the *Guide to VLA Observing: Mosaicking*[1] section. The salient features are

OTFM: There is very little move-and-settle overhead as the array is in continuous motion over a row of a raster with only a small startup (∼10–15 sec) at the start of a row. In OTFM the phase center of the array is discretely stepped on timescales of a few seconds or longer, so no phase smearing of the images results. However, because the primary beam response pattern is moving with respect to the sky, there are errors introduced in the amplitudes by the moving beam in a single visibility integration time. Thus, the main cost of OTFM therefore is that for fast scanning rates the fundamental integration ("dump") times in the dataset must be short (10% or less) compared to time it takes to cross the FWHM of the primary beam. This in turn increases data rates from those otherwise required (e.g., to avoid time-smearing of the loci in the uv-plane). The secondary cost of OTFM occurs in the imaging process, where the effects of the moving primary beam over the time at which the phase center is fixed must be compensated for by the imaging algorithm at significantly increased computational cost over that required for a similar observation taken with a fixed pointing center. This is currently done by the CASA software package in its `clean` deconvolution task. This has been used successfully in the S-band Stripe82 program of 13B-370 (Hallinan et al.), and has produced images of comparable quality to those using a traditional hex-mosaic (see below). More detailed testing of the efficacy and efficiency of the use of the CASA imaging for OTFM is part of the testing plan given below. For the purposes of this plan, we will assume that OTFM datasets can be imaged with sufficient accuracy to be practical for the depths (and dynamic ranges) required for the Tier 1 and 2 observations.

Hex-pattern Mosaicking: It takes the VLA 3–7 s (depending on the direction of motion in azimuth-elevation coordinates, usually around 6–7 s if not optimized) to move and settle between nearby pointings. This time is dominated by the oscillations of the antennas due to our current (aging) antenna servo system (a replacement is planned, but the array is not likely to be fully outfitted for this survey). The settling time is worst in the undamped azimuth direction.

In order to keep the overhead from this motion to be 25% or less, one needs to spend at least 28 s integrating on each pointing. For a hex-pattern, each field gets 67% of the total integration time desired on-sky, so observations where the VLA Exposure Calculator[19] indicates an on-source time of 42 seconds or less will incur significant overhead if not done with OTFM. For VLA S-band, the calculated exposure time is 7.7 seconds at a rms image sensitivity of 100 μJy/beam, and thus observations desiring a depth shallower than around 43 μJy/beam in a single pass will prefer OTFM. Thus, our Tier 1 and 2 observations with single-pass depths $> 100\,\mu$Jy will require OTFM, which the deep Tier 3 observations (single-pass depth $< 34\,\mu$Jy/beam) can be carried out with straightforward Hex-pattern Mosaicking. Note that it is in principle possible to arrange the order in which the fields are observed to make the motions to be predominantly in the elevation axis which damps the telescope settling, and has been shown to lose only 3–4 seconds. However, this optimization is dependent on the local time at which the observations are made requiring restricted LST scheduling blocks, and is difficult to arrange over large areas of the sky. We will try where possible to use this optimization to further reduce overheads in the Tier 3 mosaics.

8.2 Scheduling Considerations

The Jansky VLA is normally operated using a "Dynamic Scheduling Queue" where the individual Scheduling Blocks (SBs) are created in the VLA Observing Preparation Tool (OPT) to be able to be executed in a prescribed range of LST, and submitted to the VLA Scheduler software (OST) to be queued up for observation by the array in a manner dictated by weather and priority. It is our intent that the Tier 3, along with some of the Galactic Plane Tier 2) observations, where possible for each pass, be observable using standard Dynamic Scheduling. This requires that these blocks contain sufficient calibration to stand alone or be boot-strapped from other VLASS SBs executed nearby in time.

For Tier 1 and most of Tier 2, it would be advantageous to construct the schedules in large blocks to be observed at specific LST start times. This would allow maximum efficiency in calibration and control of slewing (e.g., telescope wraps). In practice, due to considerations such as the ability to allow interrupts for target-of-opportunity observations, and fault tolerance (e.g., for power outages, weather, etc.), the schedule will need to be broken in to modestly sized blocks. Ideally, the VLA Scheduler software would be able to handle sets of SBs that are linked (e.g., in a particular order or in alternate sets). However, this capability does not currently exist, and there may not be resources in the software group to allow this. Instead, the most straightforward plan is to make sets of SBs for submission (see below) and submit only a day ahead. This will require an "Astronomer on Duty" (AoD) for VLASS who will keep track of what SBs are ready to observe, make sure they are submitted, make sure that they run, and make any modification necessary (e.g., due to TOO or weather interrupts).

The VLASS will ultimately consist of many SBs (e.g., 3000 3-hour SBs for 9000 hours total) that will be submitted through the OPT for execution. Currently, when the OPT is filled with even a modestly large (> 100?) number of SBs for a given user, its performance is very slow. Some thought, and possibly some software modification, will need to be made on how to handle a program like this that will execute a large number of scheduling blocks. A fallback would be to delete already processed SBs from the project manually relying upon separate storage of the ascii scan lists (and/or XML representations output from the OPT) for record keeping.

[19] `https://science.nrao.edu/facilities/vla/docs/manuals/propvla/determining/source`

Target-of-Opportunity Interrupts: For the long-block observations in Tiers 1 and 2 (and some of Tier 3), provision will be made for the possibility that observations will be interrupted for time critical TOO programs (e.g., for triggered transient observations). There is currently no mechanical provision in the way schedules are constructed or executed for the supension and restarting of schedule blocks. Therefore, the most straightforward implementation is to break all schedules into blocks of 2–3 hours in length, and to allow TOO interrupts to simply stop the execution of the current schedule and possibly pre-empt the execution of the following one or more SBs. After TOO obserations are complete, the VLASS schedule would resume with the next appropriate block. The AoD would be informed of this interruption, and would examine the archive record to determine the missing observations and construct a "make-up" SB to be run at the first appropriate opportunity. The plan for the construction of schedules (see below) will take this need into account.

8.3 Schedule Construction

It will be impractical to use the VLA OPT in standard interactive mode to construct the thousands of hours of schedules for thousands of pointings that must be in the Source Catalog Tool. Instead, we will create some lightweight software in Python to construct the ascii lists that the OPT and SCT can read. This feature has been used by the 13B-370 Stripe-82 observers (mainly Caltech graduate student Kunal Mooley) with success to schedule those observations. Our plan is to use and modify as needed the Python code developed for that project. These scripts and code would be made available to the community for their own use for similar surveys.

8.4 Overall Observing Schedule

The VLASS as proposed will be carried out over the course of 4 or 5 cycles of JVLA in its A and B configurations, spanning a total of 5–6 years (52–70 months or more). The cycles start with an additional A-configuration tacked onto the beginning of semester 2015B (which would normally transition to D from the A configuration of 2015A). We assume the array follows the current standard cycle order of B followed by A. We also assume that each configuration is the current 4-month duration, but note that accommodating the VLASS could involve extending some of the durations in the more loaded sessions.

In this scenario the VLASS is a 5-year survey with a total of 9066 hours of observing spanning parts of 5 cycles spanning a total of 64 months or more (if we keep to 4 months per cycle minimum):

Cycle	Config	ALL-SKY	WIDE	GALACTIC	COSMOS	ECDFS	Elias-N1	Total
1	A	0	0	203	0	490	292.5	985.5
2	B	451	755	0	0	0	0	1206.0
2	A	0	0	203	150	490	292.5	1135.5
3	B	451	755	0	0	0	0	1206.0
3	A	0	0	203	0	490	292.5	985.5
4	B	451	755	0	0	0	0	1206.0
4	A	0	0	203	150	490	292.5	1135.5
5	B	451	755	0	0	0	0	1206.0
Tot		1804	3020	812	300	1960	1170	9066.0

This starts with an extra 41 days (986 hours) added on to the A configuration that ended 2015A. If a start in 2015B is not possible, one could move the first A session to the end, making a survey that spans a minimum of 52 months (the most compact survey that we consider). In this schedule, no configuration has more than 1206 hours (50 days) of VLASS observations. The B-configuration

ALL-SKY (excluding the WIDE area) has two epochs distributed in four cycles, so each pass of the area will be split evenly between two cycles.

8.5 Calibration

The goal of the VLASS Calibration process is to determine, on the basis of *a priori* factors and from observations of standard calibration sources, the corrections to the raw data amplitude, phase, and visibility weights to be applied to the data. This process also determines the flags that are needed to remove bad data due to instrumental faults, RFI, and other causes of error. When applied to the VLASS data, this calibration will allow the production of images in the next processing stage. This process only includes the derivation of the complex gain and bandpass calibration factors known through previous measurements or determined by the observations of calibrators and transferred to the VLASS target observations. The self-calibration of VLASS data is included in the Imaging stage of processing.

VLASS data will be processed using a modified version of the normal CASA-based VLA cailbration pipeline. By the time of the VLASS observations, the VLA pipeline will have the requisite functionality to process VLASS data (full polarization, many individual target fields generated in OTF mode). The VLA pipeline is currently run on most VLA observations and is well tested. The VLASS will use a version specifically tested on VLASS pilot observations.

As mentioned earlier when discussing Data Products, it is more efficient to store the calibration tables, flags, and pipeline commands and the create the calibrated dataset upon request from the archive, rather than to store both raw and calibrated datasets. Should it be deemed appropriate and possible, we might consider also archiving off-site the full calibrated dataset (e.g., through Enhanced Data Services by a community partner).

8.6 Imaging

The VLASS is at its heart a wide-band continuum imaging survey. The science goals of the survey are predicated on the ability of the instrument and data processing to deliver images of sufficient quality to be able to identify objects and measure the salient properties (e.g., flux density, position, spectral index, polarization, light curve). In order to keep up with the observing, the VLASS Imaging Pipeline must be able to process and image the data at a rate commensurate with the observing rate. This will be effected through the parallel image processing of sub-mosaics on NRAO-based clusters or externally provided systems (e.g., through XSEDE).

There are three imaging processes that need to be handled by the pipeline:

- Quick Look (QL) imaging triggered after every scheduling block is observed (e.g., for transient identification)
- per-epoch imaging triggered after the last observation each configuration
- cumulative imaging triggered after each epoch beyond the first, incorporating all previous data

For each of these, there are three kinds of images that may be produced:

- Wide-band (2–4GHz) continuum images
- Full-resolution (2MHz channels) image cubes
- Coarse-resolution (128MHz spectral windows or similar) image cubes

Imaging is done in all Stokes parameters (IQUV) for polarimetry capability.

Continuum imaging can include higher-order Taylor terms in the spectral dimension (e.g., spectral index, spectral curvature) depending on image depth (e.g., for processing beyond the Quick Look). CASA has Multi-Frequency Synthesis (MFS) algorithms for this that have been used in past programs, and further development of these capabilities is underway. Full-polarimetric imaging is a key part of VLASS, and the use of accurate polarized "primary beam" maps of the VLA field-of-view during imaging and analysis are critical to the production of science ready images. Self-calibration (through the use of previous sky models as well as true self-calibration from iterative imaging) is also an integral part of the image processing.

We assume for all image size calculations that in the ideal case the images will be pixellated at a sampling level 0.4 of the (robust weighted) resolution at the highest frequency of the band (4 GHz), rounded to a convenient value. For A-configuration, this is $0.2''$ (resolution $0.49''$ at 4GHz), giving 324Mpix per square degree. For B-configuration, this is $0.6''$ (resolution $1.58''$ at 4GHz), or 36Mpix per square degree. In practice we will refine this based on imaging performance and we may be able to get by with less oversampling. In addition, individual sub-images will likely need some amount of extra padding to accomodate odd shapes. Overall we should treat these estimates as reasonably conservative, uncertain at the around the 25% level. However, this optimal level of resolution leads to large image archive sizes (see § 8.8) and thus a key issue for testing is the determination of the lowest acceptable resolution in the images and image cubes that will still enable the key science with the Basic Data Products. It may be possible to reduce the image data volumes by significant factors (2–8) in this manner. In addition, image compression algorithms (lossless and lossy) can also improve storage efficiency and will be investigated in the Test and Development Program.

The image cubes are needed as input to more advanced processing for Rotation Measure determination, spectral line surveys, and more detailed SED modeling of sources. Most of these would be provided as Enhanced Data Products and Services. Note that the storage and distribution of the large full-resolution cubes will be a challenge for the archive (see § 8.8), and options for external hosting and "on-demand" image processing should be explored (e.g., as an Enhanced Data Service). As a fallback we would carry out compression through a combination of reduced angular resolution (e.g., $0.3''$, Nyquist at 3GHz) and spectral resolution (average 8 channels, 32MHz).

8.7 Image Analysis and Sky Catalogs

The main image analysis task for the VLASS is the production of the basic object catalogs for the Quick-Look and standard images.

A good study of the performance of radio continuum image source finders is Hancock et al. (2012MNRAS.422.1812H), which considers the available options in the context of ASKAP. The upshot is that there are options available that should have acceptable performance for the basic catalogs for VLASS. Note that inclusion of the spectral index images and polarimetric images from VLASS will likely require some extensions to these source finders, which in turn will require some developer or astronomer time.

Also available as a proof of concept is the source finding carried out for the JVLA Stripe-82 surveys by Mooley et al. (in preparation). There is also a comprehensive discussion in Mooley et al. (2013, ApJ.768.165M) in the analysis of archival VLA ECDFS multi-epoch data. It is our current assessment that one or more of these methods will be suitable for the basic catalogs from the VLASS.

More advanced catalogs and source finding algorithms could be developed and produced as an Enhanced Data Product.

8.8 Archiving and Data Distribution

The primary interface that the user community will have to the VLASS is through the archive and data distribution system. Raw data will be served via the normal JVLA archive, available with no proprietary period as soon as it has been ingested into the archive system.

The archive, or at least some archive, will have to also serve the VLASS data products as described above. It is the responsibility of NRAO and the VLASS to make the Basic Data Products available through this archive mechanism. Enhanced Data Products may or may not be made available through the NRAO-hosted VLASS archive, this will need to be negotiated and is largely dependent upon resources required. The VLASS products, either in basic form or further processes, may also be made available via alternative Enhanced Data Services, as described above.

The estimated ideal data volumes required for storage of the VLASS data and data products are:

1. raw visibility data — 783TB
2. calibration data — $<$ 10 TB
3. quick-look continuum images — 279TB
4. single-epoch continuum images — 314TB
5. single-epoch image cubes — 2918TB
6. single-epoch basic object catalogs — $<$ 10 TB
7. cumulative "static sky" continuum images — 230TB
8. cumulative "static sky" image cubes — 76874TB
9. cumulative "static sky" basic object catalogs — $<$ 10 TB
10. **Total:** continuum images — 823TB; image cubes — 80PB

These volumes have been calculated assuming the angular and spectral resolutions defined in § 8.6, for the data products listed in § 7.1. More details on this storage calculation are given in the TIP.

For reference, the current JVLA archive has capacity for around 400TB. The normal expansion of this capacity, if driven by archiving of visibility data only, would be expected to be at the 100–200TB/year rate, and thus we would expect around 1.6PB of storage available in 2020. This does not include storage for images from future general image pipelines. We conjecture that support for storage of around 10PB by the end of VLASS is just within the practical envelope for funding within the NRAO budget, and even that assuming a extremely strong recommendation by the VLASS science review for this level of data support. Beyond this, partnerships with the community and other agencies will be necessary (see § 7.3).

The VLASS continuum image volume is within the range of expected storage capability. However, the 80 PB of image cubes exceeds the currently extrapolated capacity of the JVLA archive by a factor of 50, and the wildly projected upper envelope by a factor of 8. Therefore, barring outside support through a EDS partnership, severe compression of the final cubes (in either angular or spectral resolution) is required.

The detailed calculation of these data volumes is given in the VLASS Technical Implementation Plan. The individual data products are described below in § 7.1.

8.9 Test and Development Plan

There are a number of issues related to the VLASS that must be addressed before the survey can be observed on the telescope, though none of these appear "show-stoppers" that are likely to prevent the survey from being carried out at all, and most have obvious work-arounds. Fundamentally, these are schedule and resource risks rather than functionality risks, in that it will take longer and will be more costly in computing and human resources to process the survey, impacting the data product delivery schedule. However, they do need to be addressed, and we propose a VLASS Test & Development Program leading up to and through the survey start, for example through small test observations or through larger pilot observations, or through analysis of archival data from previously observed projects such as Stripe-82 13B-370. These will require signifcant astronomer resources to carry out, and thus we are unable to fully prosecute this program before submission of the VLASS proposal — approval for the observation of VLASS would be necessary before allocating the resources to carry out this test program. This is particularly true for the issues in Tier 3 imaging, where the tests using archival data will be time-consuming at the depths required. There would be a final technical design review before survey observations commence, and that point we will have dealt with the high and medium risk issues sufficiently to proceed.

We also include here the actual development and testing of the pipelines for VLASS. These will be based on the general VLA pipelines that are now being deployed and used, tuned for VLASS specific cases. Testing on suitable projects (current and archival) will be an important aspect to pipeline test and development.

The areas we have initially identified for further testing, exploration, and development include:

- General Flagging, Calibration, and Imaging issues
  - Tests of RFI occurence, RFI flagging efficacy, bandwidth lossesto RFI in VLASS sky coverage area
  - Assessment of reliability of wide-field polarized beam maps (2–4GHz) and need for further measurements
  - Tests of general wide-band wide-field polarimetry, including application of beam maps to data
  - Determination of optimal vs. practical options for image pixel resolution (critical for archival storage planning)
  - Exploration and development of image and image cube compression options for VLASS
  - Assessment of effects of source variability (intensity and polarization) on deeper static-sky imaging performance
- OTFM tests and development (primarily for Tiers 1 and 2)
  - Tests of Imaging errors from OTF scanning (continuum intensity and polarimetry)
  - Tests of Fast integration fast scan system and imaging performance (for depths shallower than 100 μJy/beam rms)
  - Tests of Galactic Plane and Bulge region imaging (complicated source structures, crowded fields)
  - Development of improved algorithms required (if any) for OTFM imaging
  - Development of automated and semi-automated pipelines for Tiers 1 and 2
  - Development of plan for small test or pilot observations for Tiers 1 and 2

- Deep Mosaic Imaging tests (Tier 3)
  - Assessment of Imaging performance for deep mosaicked fields (continuum intensity and polarimetry) based on archival data
  - Development of optimal scheduling for deep observations (e.g., scanning for best uv-coverage)
  - Development of improved algorithms required (if any) for deep imaging and polarimetry
  - Development of automated and semi-automated pipelines for Tier 3
- General Logistical Tests
  - Determination of observational overheads (slew, setup, calibration)
  - Determination of actual increase in integration times needed for low-elevation observations
  - Exploration and testing of calibration issues for VLASS (e.g., sharing of calibration between blocks, cadence)
  - Exploration of optimal and practical scheduling options (fixed LST vs. dynamic)
  - Exploration and development of optimal/practical compression options for VLASS
  - Assessment and improvement of calibrator source lists for VLASS

Many of these are currently being carried out by VLA staff and resident observers as part of the normal development and science support, and by the user community in their research activities. However, new resources (additional staff, post-doc, or student time, computing, and telescope test time) will be required to fully implement this plan before the start of the VLASS.

More details on the VLASS Test and Development Program are given in the Technical Implementation Plan.

9 Education and Public Outreach

The activities of communication, education and outreach cover a very large, and often overlapping, sets of activities, which, however, present interesting opportunities for dissemination. We discuss how VLASS science, results and data will be publicized and made available to interested persons. Wherever possible, we leverage off existing infrastructure and resources, adopting and adapting as necessary. The overall objective is to disseminate VLASS science, results and data to the widest audiences.

9.1 Audiences

We identify these unique audiences for VLASS, each with its own style of communication and interaction, and grouped into 4 categories:

9.1.1 Scientists

- experienced radio astronomers, experts at analyzing radio data
- novice radio astronomers, content experts but who many have little to no experience with retrieving and analyzing radio data

- Professional astronomers are primarily interested in how VLASS products can be used to further their research objectives.

For expert radio astronomers, access to the data and calibrated products is relatively easy, as is the analysis. For astronomers who are familiar with other methods of data acquisition (optical telescope spectra and images) or delivery methods (e.g., calibrated HST or Chandra data products) figuring out how to obtain, manipulate and understand and integrate unaccustomed data structures can be challenging. Thus, the first group is likely satisfied with access to a catalogued database. The second group would prefer to have calibrated data products in a form they can use with their familiar tools, for example a FITS image of the M87 Halo in 90 cm continuum halo (Image courtesy of NRAO/AUI and F.N. Owen, J.A. Eilek and N.E. Kassim). This group is keenly interested in timely updates - for example, the most recent data release. Methods of communication include email newsletters, the Astronomers Facebook Group, The American Astronomical Society, and similar venues.

9.1.2 Staffers, Managers

- NRAO directorate and upper management
- AUI officers and board of trustees
- Funding agency program officers
- Congressional staff

Members of this audience are probably most interested in receiving encapsulated information e.g., progress reports, press releases, summary of results.

9.1.3 Educators

- Teachers in accredited K-12 schools, 2 and 4 year colleges
- Informal science educators, e.g., after school programs, science centers, planetaria and so forth
- Disseminators of information, e.g., journalists, bloggers

This grouping has teachers who serve a variety of demographics, namely pre-college and undergraduate students in formal educational institutions, subject to curriculum requirements. Informal science educators serve students, but also include families as well as the general public. The needs for this group as a whole are easily accessible materials, with appropriate pedagogical backing.

9.1.4 General public

The broadest category which includes people of all ages, interest level and residency (US, international and so forth). The public is far from monolithic, with very wide range in age, education level, socioeconomic status and preferred means of obtaining information.

9.2 Social media and communication

Interest in science and astronomy among the general public has been on the rise and is at least partly facilitated by the ease of sharing information and engaging with scientists using social media. The Very Large Array Sky Survey can build on the existing audience and practices of NRAO social media and rely on the breadth of expertise and personalities working with the project.

Examples of active NRAO social media accounts (as of 7/9/2014):

- Facebook - https://www.facebook.com/TheNRAO - 40,041 likes
- Twitter - https://twitter.com/thenrao - 5186 followers
- Google Plus - https://plus.google.com/117435324254706605576/posts - 235 followers, 22,378 views

A sound social media project includes defining clear goals for the communications, picking which specific platforms to use, and ensuring regular posting and interaction with the community (Bohon et al. 2013). Though some of the work of VLASS can be worked into the existing framework of NRAO social media projects, work from VLASS's many participants would be appreciated as well. This would particularly be true of the NRAO's Facebook presence, which is by far its largest audience.

One model for additional participation is to have a weekly "host" of a twitter account that uses the week to communicate their particular aspect of the science being done with VLASS. Examples of such accounts already in use are @realscientists (https://twitter.com/realscientists), @WetheHumanities (https://twitter.com/WetheHumanities), and @astrotweeps (https://twitter.com/astrotweeps). Other collaboration members who are already active on social media can use a specific hashtag to join the conversation. To date, we have adopted the simple hashtag #VLASS.

Another outlet for VLASS news and communication would be in blog form so that long format stories can be told. Such a blog would be modelled after the CANDELS Blog (http://candels-collaboration.blogspot.com/). This site has two editors who ensure that new and relevant content is posted on a regular basis. These editors invite members of the collaboration to submit posts on their specific science, their role in the survey, biographical profiles, or explainer articles on broad and basic scientific concepts. A blog hosted by Wordpress.com is free and is easy to use for collaborative projects. The URL vlass.org is also available (that is, has been privately reserved) for use for either this blog or for a broader public website if desired.

Although it is now considered and "old" form of web communication, emails lists are still a popular method of communication as it ties directly into the users daily email routine and does not require visiting an external app or site. Email lists can also be audience specific (as in separate lists for teachers, general public, and professional astronomer) and are opt-in by the user. At the very least, a periodic email list should be made available for professional astronomers interested in the status of the survey and its data products.

All of these methods of communication have little to no cost for the accounts but incur costs in the person-hours to develop content and communicate with the community.

9.3 Examples of CEO activities

9.3.1 Picture of the Week

Each epoch of VLASS data acquisition lasts approximately 8-12 weeks. Starting with the first week, VLASS should release a picture of an interesting object, along with explanatory material and a press release delivered through as many channels as maximize exposure. The very first image could be simply a 'pretty picture' just to get started, though thereafter in addition to being good looking, the POTW should be of scientific interest, whether as a unique object or one that

demonstrates a specific instrument capability. In this category are the "most": distant, brightest, faintest, dusty, nearest, resolved etc. VLASS scientists pick the targets ahead of time, reduce the data and generate the 'picture'. Someone expert in visualization will need to work with VLASS scientists on these pictures. This is very similar to the way HST among others, generate interest in its surveys (PHAT, Frontiers Fields) and attract attention.

9.3.2 Citizen Science

Public participation in science has grown in the last few years with access to new technologies and data sharing techniques. Projects range in participant involvement from collection of data (e.g., variable star observations) to web-enabled classification and data analysis (e.g., Galaxy Zoo, CosmoQuest) to passive use of computing resources (e.g., SETI@home). With the exception of projects that just use computing resources with no human intervention, citizen science projects tied to large surveys such as VLASS are best suited for problems that need human interaction through simple tasks that cannot be handled automatically by a computer. Searching for transients that might be missed by traditional source finding techniques is one such application of a citizen science task.

Audiences: general public, with access to the internet. Can also tie into K-12 education with appropriate teacher materials.

9.3.3 Science Stories

An ongoing VLASS blog, where VLASS personnel contribute individual entries, can generate and sustain interest in the survey. Individual stories could include descriptions (by the parties involved) of the deliberations undertaken to arrive at the final survey plan, life of an astronomer during the week of, and the like. New postings are advertised via social media apps, email, on the web page. Readers can post comments (moderated, of course).

Audiences: all

9.3.4 Education Activities

Here, the objective is to take advantage of existing resources at NRAO, its partner institutions (RIT, CalTech) and extant networks (e.g NightSky Network), to share VLASS science in ways that are compatible with the objectives of formal and informal educators. Partnerships with other national and international institutions with experience in this area (International Astronomical Union's Office for Astronomy Development, Galileo Teacher Training Program) would be helpful as well.

Audiences: K-12 and Higher Education

10 Summary

The proposed VLASS definition comprises a cohesive and aggressive science program that will benefit the entire astronomical community, deliver unique forefront scientific discovery, and keep its legacy value well into the SKA-era. The scientific legacy, impact, and efficiency of deep and all sky surveys are clearly established - from the Hubble Deep Fields to GALEX to NVSS/FIRST to Sloan and the next US optical/NIR ground-based priority LSST. The proposed VLASS finds its place within this tried and true tradition of modern astronomy. Analysis of the statistics from NVSS and FIRST (as with the Hubble Deep Fields) clearly indicate that the impact on PI science from these kinds of community surveys is positive, as might seem counterintuitive. This is true not only in terms of the extensive usage of these data by wide swatches of the community, resulting in startlingly high publication rates, but also due to the new inquiry driven PI science they enable,

that could not otherwise have been conceived or survived the proposal process without the critical enabling data and demonstration science from the surveys. The proposed VLASS will continue the integration of radio astronomical data into the multi-wavelength astronomical community, putting the U.S. broad astronomical community in an optimum position to make substantial use of the SKA when it comes online.

Appendix

A Impact of VLASS Sky Survey on Overall EVLA Science: The High Impact of Surveys

The time committed to the proposed VLASS will reduce the time available for other VLA programs. However, we argue that the time spent on large VLA surveys has effects that increase the net science coming from the VLA:

1. VLA sky surveys have a science impact per observing hour that is demonstrably greater than the average VLA observing program. This is at least partly because surveys expand the usage of radio data beyond the usual radio astronomy community.

2. Once VLA sky survey products are available, many science projects that require pointed observations of a sample of objects (e.g.,, to measure spectral indices for a sample of quasars) can be carried out directly from the catalogs rather than requiring an observing proposal. That reduces the time requested for such observing proposals and so increases the time available for other projects.

3. The sky survey products themselves will become a key resource for radio astronomers in identifying targets and projects for followup proposals. That also leads to an increase in the science done by enabling projects that are not possible without the inputs from a sky survey.

The existing VLA sky surveys, NVSS (Condon et al. 1998) and FIRST (Becker et al. 1995, White et al. 1997), provide powerful evidence that the telescope time dedicated to these surveys repays the investment many times over. Below we present some statistics on the usage of the FIRST survey data and on the impact of FIRST and NVSS as measured by publications and citations.

A.1 FIRST survey data usage

The FIRST image server[20] provides JPEG or FITS cutouts extracted from the FIRST survey at user-specified positions. Here are some statistics about its usage:

- During the last 18 months the FIRST cutout server has delivered on average more than 7,500 image cutouts every day.
- Each image served is equivalent to a three-minute VLA observation (the exposure time required to reach the FIRST depth); thus, our image server issues the equivalent of a 3-minute VLA observation every 12 seconds.
- Every 10 days the FIRST cutout server distributes snapshots with a total exposure time equal to the entire 4000 hours invested in the FIRST survey.

By creating a legacy dataset that covers as much of the sky as possible, we can vastly expand the user community (and scientific productivity) of the VLA. This is the single most important reason to do an all-sky survey.

[20] `http://third.ucllnl.org/cgi-bin/firstcutout`

A.2 NVSS/FIRST publications & citations

Publications and citations are the best objective measures we have of scientific impact. While there are lots of caveats (e.g.,, papers in fashionable fields collect more citations), every other measure of productivity is even less objective and harder to evaluate. In this section we discuss the publication statistics for the FIRST and NVSS surveys. The results strongly support the value of these surveys both in absolute terms and in comparison to other VLA projects.

There are three basic papers that define the FIRST and NVSS survey data products:

- FIRST images: Becker et al. 1995
  - 1311 citations
- FIRST catalogs: White et al. 1997
  - 587 citations
  - 1722 citations combined with Becker et al.
- NVSS images & catalogs: Condon et al. 1998
  - 2675 citations

Combining the FIRST and NVSS papers, there are a total of 3550 citations (3132 refereed citations). These 3 papers are ranked #1, #2, and #11 in citations among all VLA publications.

These papers are highly cited not just among VLA publications, but among all astronomy papers. Of the most-cited papers published since 1995, the NVSS paper is #16 and the Becker et al. paper is #67. Other than WMAP papers, the only other "radio astronomy" papers to crack the top 100 are #29 (Urry & Padovani 1995, "Unified Schemes for Radio-Loud Active Galactic Nuclei") and #63 (Kalberla et al. 2005, "The Leiden/Argentine/Bonn (LAB) Survey of Galactic HI").

There are a few exceptions, but we can generally treat the list of citing papers as an indication of the usage of VLA survey data. The 3522 papers in ADS that cite NVSS and/or FIRST (as of 2014 March 29) have a total of 9086 unique authors. There could be some double-counting here, since some authors publish using more than one version of their name/initials; but even if we compare only last names, there are still 6925 unique authors among these papers. There are 1876 unique first authors on these papers, or 1666 unique first authors using unique last names only. So, if anything, these citation numbers underestimate the usage of the survey data.

The NRAO database includes a total of $\sim$ 6200 users (G. Hunt, private communication). That includes almost everyone who has ever been on a radio proposal. It is clear that the community using NVSS/FIRST data is considerably larger than the community of radio telescope users. By every measure, the impact of FIRST plus NVSS is large compared to other VLA observations. According to the NRAO publications database, there were 192 refereed VLA papers per year over the decade 2000–2009. (We used those years because the VLA publication rate has dropped a little since 2010.) For comparison, over that same period there were 262 refereed publications per year that cited FIRST and/or NVSS. Thus, there is very strong evidence against the argument that the science out of the VLA is negatively impacted when surveys displace regular proposals. Surveys will enhance science at the VLA, just as they have at every other modern observatory. That is why more and more time at all major observatories is being dedicated to large surveys.

A.3 Will VLASS have the same impact as FIRST & NVSS?

Both the publications and data usage provide extremely strong support for the proposition that time invested in VLASS will be repaid many times over. The impact of NVSS and FIRST is demonstrably much greater than the impact of the displaced VLA science proposals. Moreover, after a

few years the time invested in the survey pays for itself by freeing up observing time that would otherwise have been spent on survey-like observations of samples of objects or of small sky areas. And the survey data multiplies the value of other VLA observations by providing ancillary data at a different epoch, frequency, and resolution that can be used in conjunction with new observations. Many current VLA proposals begin with samples that are derived from the existing surveys. From every point of view, the investment of time in VLASS increases the overall scientific productivity of the VLA.

Some have argued that FIRST and NVSS were unique, and that a new VLA sky survey will not have the same impact because it will not have the unique and long-lasting legacy value in the face of the oncoming SKA pathfinders (and the SKA itself). We see two strong counter-argument to this view. First, the resolution of the VLASS is an essential difference that puts VLASS in a class by itself (§5.1.1). WODAN and ASKAP-EMU will surely spawn some great science on radio source properties. However, astronomers attempting to identify radio sources with even moderately deep observations at visible or infrared wavelengths will use the VLASS.

Secondly, we have a clear counter-example to the argument that the survey must be "absolutely unique" compared to any existing or planned future survey. Consider the NVSS and FIRST themselves: They were carried out at the same time, with the same telescope and receivers. They observed at the same frequency. The sky covered by FIRST was also completely covered by NVSS. FIRST is only about 2.5 times deeper than NVSS for point sources, and the sensitivity difference is even less for extended sources. And yet both FIRST and NVSS have thrived, and both have had a demonstrably large impact on radio and multi-wavelength science. How can that be?

The answer is that the higher resolution of FIRST (with a beam 8 times smaller than NVSS) is essential in doing cross-matches to SDSS and other deep imaging observations. Science with NVSS depends on its larger sky coverage and good sensitivity to large-scale emission that come from a low-resolution survey. Even though these surveys were carried out and released essentially simultaneously, and even though they had many characteristics in common, it took only one difference — resolution — to distinguish them and make them both widely used to this day.

While we agree that it is important to consider VLASS in the context of current planned surveys and not to duplicate those surveys, we definitely do not agree that it is necessary to push to the extreme limits of the VLA parameter space (e.g., very high frequencies and the highest possible spatial resolution) in order to distinguish it from coming low-frequency, low-resolution surveys by the SKA pathfinders. NVSS and FIRST have had a huge impact on astronomy, and they have succeeded in vastly expanding the community of users of radio data. VLASS will surely have a comparable impact.

B The "S/N model" of Positional Accuracy

A long-standing notion has been that as the signal-to-noise ratio (S/N) increases, much better positional accuracy is obtained, so that high angular resolution is not needed for effective identification at visible or near-infrared wavelengths. The prediction of what we will call the "S/N model" is that as the flux density increases, the positional error will decrease as $1/S/N$, allowing the optical counterpart to be matched. Specifically, the NVSS description (Condon et al. 1998) gives this formula for the noise in RA or Dec for point sources:

$$\sigma_{1D} = \theta/(S/N\sqrt{2\ln 2}) \quad . \tag{3}$$

Here θ is the resolution FWHM (45″ for NVSS) and S/N is the signal-to-noise ratio. The median NVSS rms noise for these matched sources is 0.47 mJy/beam. Note that this noise equation already has been increased by an emprical factor of $\sqrt{2}$ compared with the theoretical equation "to adjust the errors into agreement with the more accurate FIRST positions" (Condon et al. 1998). This

predicts $\sigma_{1D} \sim 7.6''$at the catalog detection limit ($S/N = 5$) and $\sigma_{1D} \sim 1''$at a flux density of 18 mJy/beam.

The positional scatter in Equation (3) is a 1-dimensional uncertainty, giving the error in either RA or Dec. In a 2-D distribution, many values will scatter outside the 1σ circle. The 90% confidence separation limit σ_{90}, which is typically more appropriate for catalog matching, is a constant factor $\sqrt{2 \ln 10}$ times larger than σ_{1D}:

$$\sigma_{90} = \frac{\theta}{S/N} \sqrt{\frac{\ln 10}{\ln 2}} \quad . \tag{4}$$

With that increase it is necessary for the NVSS flux density to exceed 40 mJy/beam ($S/N = 85$) to reduce the predicted separation error to $1''$.

The above positional accuracy applies to perfect point sources (and perfect data). But how well does it work for real data? Here we assess the accuracy of the S/N model using a comparison of the FIRST and NVSS data. The NVSS resolution is $45''$FWHM. The FIRST resolution is $5.''4$ FWHM. As a large-scale test, we selected a sample of all the FIRST sources that have an SDSS match within $0.''7$ and that have an NVSS match within $100''$. For all these $\sim 135,000$ sources, we computed the distance to the nearest NVSS source. The important thing about this sample is that the FIRST source matches the optical source position. That means that if NVSS is to identify the same counterpart, it needs to have a position close to the FIRST source position. There may be several FIRST source components associated with a single NVSS source, but only the FIRST sources that match optical counterparts are included.

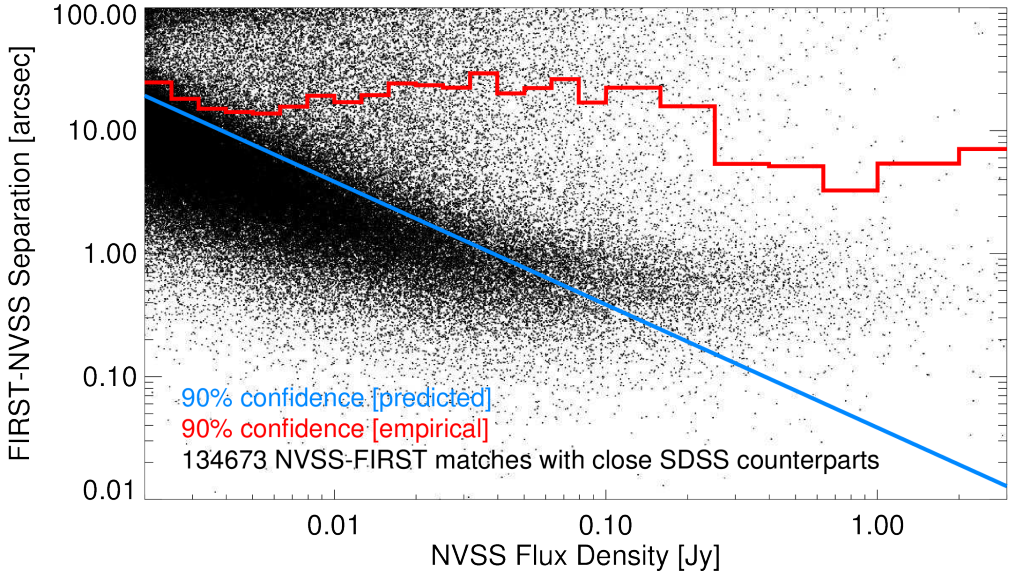

Figure 21: Position difference between NVSS and FIRST positions as a function of NVSS flux density. The sample includes only objects that have a close SDSS counterpart to the FIRST source position (within $0.''7$). *Blue line:* Theoretical 90% confidence separation limit computed using the S/N model. *Red histogram:* Empirical 90% confidence limit, computed by determining the 90th percentile of the actual separations in each bin. Note that this is relatively flat all the way past 100 mJy/beam, and it is much larger than the predicted 90% curve.

How do the positional errors of the S/N model compare with reality? To test this, Figure 21 shows the position distance between the NVSS and FIRST positions as a function of the NVSS flux density. The positional differences do tend to decrease as the flux densities increase. The blue line

shows the 90% confidence separation limit σ_{90} from Equation (4), simply assuming that all objects are point sources with the median NVSS rms value. The red histogram shows the empirical 90% confidence separation as a function of flux density, computed by determining the 90th percentile of the actual separations in each bin. *The actual 90% confidence radius is flat all the way past 100 mJy, and it is much larger than the predicted 90% curve.*

In short, to find 90% of those counterparts using the NVSS positions, it is necessary to use a matching radius of approximately 20″even for sources that are 100 times the rms noise level. The theoretical S/N model predicts that the positions ought to be much more accurate than that ($\sigma_{90} = 0.8''$).

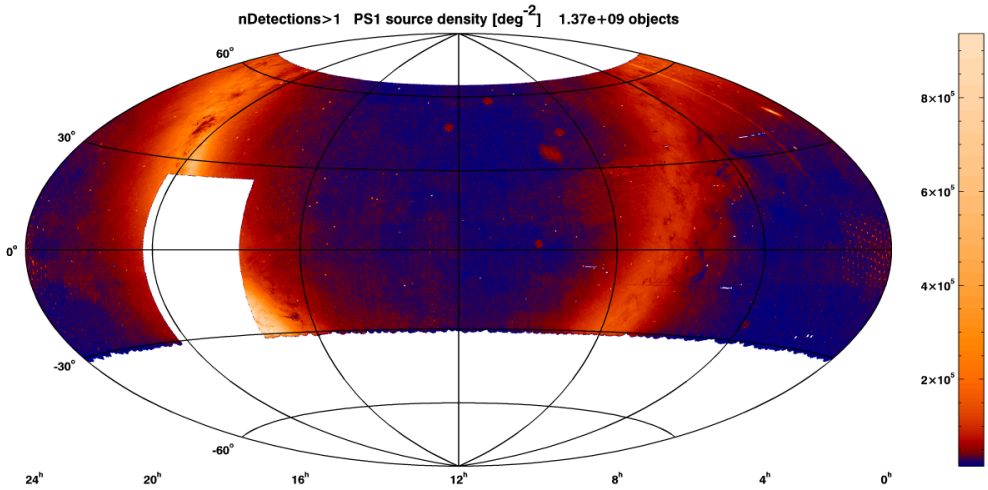

Figure 22: Object density in the Pan-STARRS database. Only confirmed objects with detections in at least two filters or epochs are included. This is based on an early version of the PS1 catalog; the gaps in the Galactic plane and at the north celestial pole will be filled in the next version, so that the whole sky north of -30° will be covered.

Why are the low-resolution positions so inaccurate? — Why are the inaccuracies in the positions so much greater than the S/N model predictions? Real radio sources are not symmetrical objects. They have lobes, jets, cores; star-forming galaxies have spiral arms; and there can be confusion where multiple radio sources get mixed together in the low resolution beam. A low resolution survey does indeed provide a measurement, with high accuracy, of the mean flux-weighted position as the S/N increases. **However, the flux-weighted centroid is often not where the optical counterpart lies.** In many cases, the counterpart is associated with some sharp structure within the radio source, and that structure may be far from the flux-weighted center.

Effect on optical identifications — This analysis shows that matching at the 45″ resolution of NVSS requires a matching radius of 20″ = 40% of the NVSS FWHM resolution. Our experience with the FIRST survey is similar: to get a reasonably complete list of optical identifications we had to use a matching radius of 2″ $\sim$ 40% of the FIRST FWHM resolution. We argue that is a universal requirement for radio sources, at least for sources down to the sub-mJy regime: the matching radius that is required for realistic radio source morphologies is 40% of the FWHM resolution. The resolution for WODAN (which will survey the northern sky accessible to the VLA) is of order $15 \times 17''$, while the resolution for ASKAP-EMU is 10″. WODAN will therefore require an optical matching radius of $6 \times 7''$and ASKAP-EMU will require 4″.

A cross-match between SDSS and FIRST shows that 34% of FIRST sources have a *false* (chance) SDSS counterpart within 6.5″. For comparison, 33% of FIRST sources have a true match within 2″.

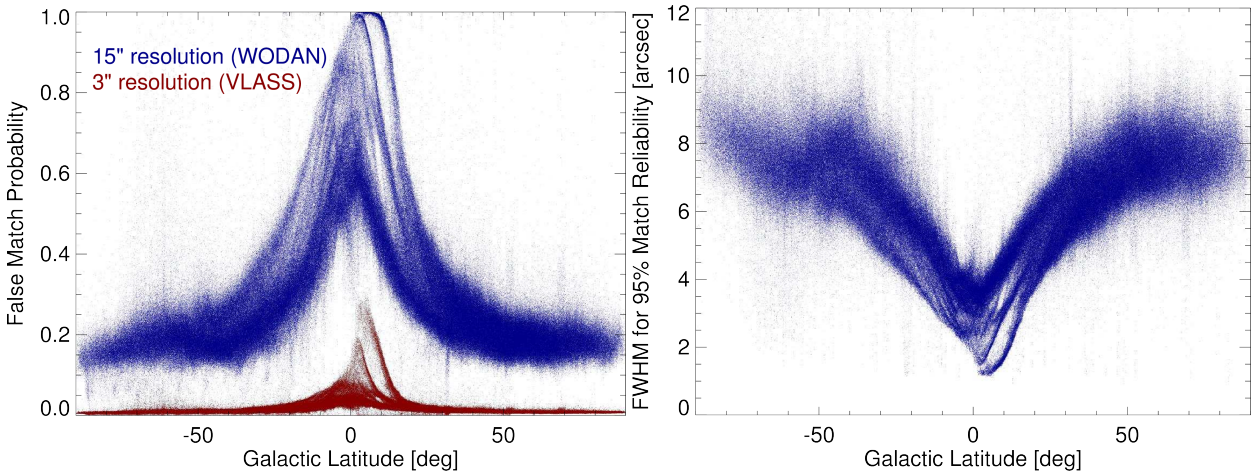

Figure 23: *Left:* Probability of a false match in Pan-STARRS as a function of Galactic latitude. The actual density of PS1 objects (Figure 22) was used to calculate the likelihood of a false counterpart within the 90% confidence radius. The plot shows probabilities both for the WODAN 15″ resolution (blue) and VLASS S-band 3″ resolution (red). Over most of the extragalactic sky 20% of WODAN-PS1 cross-matches will be chance coincidences, compared with 1% of VLASS-PS1 matches. VLASS positions are sufficient for identifications even close to the Galactic plane. *Right:* FWHM resolution required to achieve 95% cross-match reliability in Pan-STARRS as a function of Galactic latitude. In the extragalactic sky ($|\delta| > 30°$) a resolution of 7.2″ is required. This is easily achieved by VLASS S-band survey, but is not met by the SKA-precursor surveys.

The conclusion is that *half* the optical counterparts at SDSS depth will be false matches when using a 6.5″ matching radius.

The number of false matches can be reduced somewhat by doing a careful analysis of the likelihood of association as a function of separation, but when the starting point is contaminated by 50% of false matches, the final list of identifications will not complete or reliable. The false matching problem will only get worse for deeper optical/IR data. For example, Pan-STARRS is about 1 magnitude fainter than SDSS in the red and also goes into the Galactic plane where the source density is much higher, so it demands better resolution. Figure 22 shows the distribution of PS1 sources on the sky. (The gaps will be filled in as data processing is completed.) We have computed the likelihood of false identifications in PS1 as a function of Galactic latitude. The left panel of Figure 23 compares the WODAN and VLASS (S-band B-configuration) surveys. For WODAN, 20% of sources even in the extragalactic sky ($|\delta| > 30°$) will have a spurious counterpart in PS1. For most purposes that is an unacceptable level of contamination. In contrast, VLASS has only a 1% contamination rate in the extragalactic sky, and is usable even quite close to the Galactic plane. The right panel of Figure 23 turns this around and asks what FWHM resolution is required to achieve a 95% reliability ($\sim 2\sigma$) in matches to the PS1 catalog. At $|\delta| > 30°$ a FWHM resolution of 7.2″ is required. That is a higher resolution than either WODAN or ASKAP-EMU will achieve, but is easily satisfied by VLASS. In fact, VLASS with a resolution of 3″ has 95% confident PS1 matches over 96% of the current PS1 catalog area, with only the most crowded areas of the Galactic plane requiring higher resolution.

The next generation of optical/IR surveys will be deeper than Pan-STARRS. Figure 14 shows the resolution required as a function of magnitude using the *r*-band galaxy counts from the CFHTLS-D1 1 deg^2 survey (Jarvis, private communication). Since this does not include stars or redder galaxies, it is more optimistic (and less realistic) at the Pan-STARRS limit, but it shows the res-

olution required for deeper identifications. For 90% reliable identifications, VLASS can be used to $r = 25.8$, ASKAP-EMU to $r = 23.0$, and WODAN to only $r = 22.0$. For 95% reliable identifications, the magnitude limits are 24.9 (VLASS), 22.1 (ASKAP-EMU), and 20.7 (WODAN). The SKA-precursor surveys are barely usable at the depth of SDSS and Pan-STARRS and fall well short of the required resolution at fainter magnitudes. VLASS, by contrast, is useful at least to $r = 25$.

The bottom line is that we need high resolution to get the accurate positions required for optical identifications. Deeper radio imaging is not a substitute for the necessary resolution. VLASS will be the survey of choice for multi-wavelength science, and an all-sky VLASS will have a long and useful life even after the SKA-precursor surveys are complete.